

The Temporal and Spatial Variability of Nitrous Oxide (N₂O) in the Southern Baltic Sea

A master's thesis submitted in partial fulfillment of the requirements for the
award of

M.Sc. Biological Oceanography

in the

Faculty of mathematics and natural sciences,
Christian-Albrechts-University Kiel,

in affiliation with

GEOMAR-Helmholtz Center for Ocean Research Kiel.

Research Division: Marine Biogeochemistry,
Chemical Oceanography.

Submitted by: **Nwafor, Chukwudi Ejikeme**

Matric number: **1142102**

1st examiner: **Prof. Dr. Hermann Bange**

2nd examiner: **Prof. Dr. Anja Engel**

November, 2023

Table of Contents

1.0 Abstract.....	1
2.0 Introduction.....	2
2.1 Nitrous oxide and greenhouse gases.....	2
2.2 Formation of N ₂ O.....	2
2.3 Nitrification.....	3
2.4 Denitrification.....	4
2.5 Distribution of nitrous oxide in marine environment.....	4
2.6 Nitrous oxide in the Baltic Sea.....	6
3.0 Aim and objectives.....	8
4.0 Study sites, Material and Methods.....	9
4.1 Baltic Sea.....	9
4.2 Boknis Eck time series station.....	10
4.3 Sampling and analytical methods.....	12
4.3.1 Dissolved N ₂ O measurements.....	13
4.4 Calibration curve.....	13
4.5 Measurement of N ₂ O from the samples.....	14
4.6 N ₂ O Saturation Calculation.....	16
4.7 N ₂ O Production in the water column.....	16
4.8 Oxygen and Nutrients Measurement.....	17
4.9 Temperature and N ₂ O anomalies.....	18
5.0 Results.....	19
5.1 Nitrous oxide variabilities at Boknis Eck.....	19
5.2 Biogeochemical variation at Boknis Eck.....	23
5.3 Nitrate and nitrite variabilities at Boknis Eck.....	25
5.4 Biogeochemical variation at SEA-EU cruise in relation to N ₂	27
5.5 Biogeochemical variation at SEA-EU cruise in relation to Temperature.....	29

6.0 Discussion.....	33
6.1 Seasonal variability.....	33
6.2 Heatwave impact on N ₂ O.....	36
6.3 N ₂ O distribution pattern.....	38
6.4 N ₂ O saturation.....	39
6.5 N ₂ O production.....	44
7.0 Conclusion.....	46
8.0 Reference.....	47
9.0 Acknowledgment.....	59
10.0 Declaration.....	60
11.0 Appendix.....	61

List of Figures

Figure 1: The sampling stations of the two study areas, Boknis Eck time series and SEA-EU cruise transect.

Figure 2: Plot of a typical calibration curve of standard gases for the calculation of dissolved N_2O . The orange line represents the quadratic fit while the green line represents the linear fit.

Figure 3: The seasonal cycle of nitrous oxide variability in the BE time series site from 2019 to 2023 at six standard depths. The x-axis displays the months of the years, with number representing the month. **Note:** In 2020 data were not collected for all months due to Covid-19 restrictions.

Figure 4: The seasonal cycle of oxygen variability in the BE time series from 2019 to 2023 at six standard depths. The x-axis displays the months of the years, with number representing the month. **Note:** In 2020 data were not collected for all months due to Covid-19 restrictions.

Figure 5: The seasonal cycle of nitrate variability in the BE time series from 2019 to 2023 at six standard depths. The x-axis displays the months of the years, with number representing the month. Note: In 2020 data were not collected for all months due to Covid-19 restrictions.

Figure 6: The seasonal cycle of nitrite variability in the BE time series from 2019 to 2023 at six standard depths. The x-axis displays the months of the years, with number representing the month. **Note:** In 2020 data were not collected for all months due to Covid-19 restrictions.

Figure 7: Temperature variabilities of BE time series from 2019 to 2023. The number on x-axis represent the month of the year. **NOTE:** in 2020 data for all the months were not collected due to Covid-19 restrictions.

Figure 8: Salinity variabilities of BE time series site from 2019 to 2023. The number on x-axis represent the month of the year. **NOTE:** in 2020 data for all the months were not collected due to Covid-19 restrictions.

Figure 9: Distribution pattern of N_2O concentration in relation to O_2 , NO_3^- , NO_2^- , temperature, and salinity during the cruise transect of SEA-EU at Eckernförde Bay and Mecklenburg Bay. **NOTE:** the color dots are represented by the biogeochemical parameters, while the first two data points represents Eckernförde Bay and the last three data points represents Mecklenburg Bay.

Figure 10: Distribution pattern of N_2O concentration in relation to O_2 , NO_3^- , NO_2^- , temperature, and salinity during the cruise transect of SEA-EU at Arkona Basin and Gulf of Gdansk. **NOTE:** the color dots are represented by the biogeochemical parameters, while the first three data points represents Arkona Basin and the last three data points represents Gulf of Gdansk.

Figure 11: Vertical distribution pattern of N_2O and O_2 during during the cruise transect of SEA-EU at Arkona Basin, Gulf of Gdansk, Eckernförde Bay, and Mecklenburg Bay.

Figure 12: Temperature profile against salinity, oxygen NO_3^- , and NO_2^- during cruise transect of SEA-EU at Eckernförde Bay and Mecklenburg Bay. **NOTE:** The color dots represents salinity, oxygen, NO_3^- , and NO_2^- , while the first two dots represents Eckernförde Bay and the last three dots represents Mecklenburg Bay.

Figure 13: Temperature profile against salinity, oxygen, NO_3^- , and NO_2^- during cruise transect of SEA-EU at Arkona Basin and Gulf of Gdansk. **NOTE:** The coloredots represents salinity, oxygen, NO_3^- , and NO_2^- , while the first three dots represents Arkona Basin and the last three dots represents Gulf of Gdansk.

Figure 14: Distribution pattern of N_2O saturation and N_2O concentration during the cruise transect of SEA-EU at Arkona Basin, Gulf of Gdansk, Eckernförde Bay, and Mecklenburg Bay. **NOTE:** More than 90.90% of the observed data are undersaturated.

Figure 15: Correlation between N_2O saturation and temperature at Boknis Eck time series site within year 2019 to 2022 and cruise transect in May 2022.

Figure 16: Correlation between N_2O saturation and salinity at Boknis Eck time series site within year 2019 to 2022 and cruise transect in May 2022.

Figure 17: Monthly anomalies of temperature ($\Delta(\Delta\text{N}_2\text{O})$, blue line right y axis) and (ΔT , red line, right y axis at 1 and 25 m from 2005 to 2023

Figure 18: Relationship between $\Delta\text{-N}_2\text{O}$ and AOU at the Boknis Eck time series between year 2019 to 2022 and cruise transect in May 2022.

List of Tables

Table 1: The different sampling sites and stations along the Baltic Sea

Table 2: Constants for calculating the equilibrium solubility (in $\text{mol L}^{-1} \text{atm}^{-1}$) of N_2O from Weiss and Price (1980)

Table 3: SEA-EU cruise EBG and MBG N_2O , O_2 and NO_3^- mean concentrations and standard deviations. **NOTE:** the first two rows represent Eckernförde Bay and the last three row represent Mecklenburg Bay.

1.0 Abstract

Coastal seas play an important role in the release of nitrous oxide (N_2O) into the atmosphere. Ongoing climate changes have a tremendous impact on ocean biogeochemical processes and are expected to affect the distribution of trace gases such as nitrous oxide in the water column. Here we present our data of N_2O measurements from Eckernförde Bay (Boknis Eck time series station) conducted between the years 2019 and 2023, as well as data from the SEA-EU cruise in May 2022. No studies on the effects of heatwaves on N_2O production in the Boknis Eck time series have been conducted for more than two decades. From our measured N_2O concentration data at the Boknis Eck time series site, it appears that heatwaves do not contribute to N_2O production. However, we did not record very high temperatures between these years.

Other observations such as N_2O saturation and apparent oxygen utilization at Boknis Eck were compared to the SEA-EU cruise transect. N_2O saturation for both measurements was positively correlated, with nearly all data being oversaturated, contrary with previous studies in the Southern Ocean. N_2O concentration showed no significant relationship with temperature and salinity. Excess N_2O ($\Delta\text{N}_2\text{O}$) did not correlate with apparent oxygen utilization at the Boknis Eck time series, but showed a slight correlation during the SEA-EU cruise. Nitrate and nitrite were deficient throughout the water column at both stations.

Finally, this study focuses on the temporal and spatial variability of N_2O in the Baltic Sea from N_2O measurements and on determining the main N_2O production mechanism.

2.0 Introduction

2.1 Nitrous oxide and greenhouse gases

A greenhouse gas, also abbreviated as GHG, is a gas which absorbs and emits radiant energy (energy of electromagnetic and gravitational radiation) at thermal infrared wavelengths that causes the greenhouse effect. Greenhouse gases in the Earth's atmosphere include water vapor (H₂O), carbon dioxide (CO₂), methane (CH₄), nitrous oxide (N₂O) and ozone (O₃). These gases play an important role to maintain Earth surface temperature

(<https://www.britannica.com/science/greenhouse-gas2023>). Without greenhouse gases, the temperature on the Earth's surface would be around -18 °C on average, which corresponds to 0 °F.

N₂O can be found abundant in the atmosphere. The atmospheric mole fraction of N₂O in 2020 reached up to 333 ppb (10⁻⁹, parts per billion) with an increasing rate of about 1 ppb year⁻¹ (Vi, 2021). In the global long-term measurements, the tropospheric N₂O series show an annual growth rate of about 0.25 % year⁻¹ (Weiss, 1981; Prinn et al., 1990; Khalil and Rasmussen, 1992). Due to its low chemical reactivity, N₂O has an atmospheric residence time of about 110-180 years (Cicerone, 1989; Prinn et al., 1990; Ko et al., 1991; Minschwaner et al., 1993).

Nitrous oxide is also known to be one of the major scavenging gases of stratospheric ozone. It is the main source of nitric oxide (NO) radicals which contribute to depletion of ozone (Crutzen and Schmailzl, 1983). This effect of scavenging can be comparable to that of chlorofluorocarbons (CFCs) (Ravishankara, 2009).

The transformations of N compounds such as N₂O have important effects on the balance of marine and global N budgets. Therefore, understanding their formation, distribution and enabling factors is essential to understanding the fate of marine ecosystems and the future Earth system.

2.2 Formation of N₂O

Microorganisms play a major role in the formation of N₂O. Most of the N₂O emitted into the atmosphere either from natural or anthropogenic sources, is produced by microorganisms such as the denitrifying bacteria and

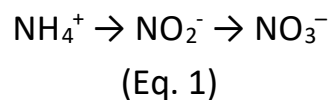
fungi in the ocean or in soils (Sloss, 1992). The world oceans accounts about (35%) and atmospheric chemical reactions contribute (5%) of the N₂O emissions (US Environmental Protection Agency, 2010; Tian et al., 2015)

2.3 Nitrification

Nitrogen is usually the limiting nutrient in the marine environment (Capone et al., 2008) Therefore, nitrogen cycle in the ocean is often a concern. Nitrification is a microbial process by which a reduced nitrogen compound such as ammonia is oxidized to nitrite and nitrate. Ammonia is present in seawater through natural and anthropogenic processes.

Nitrification is a two-step process where in the presence of oxygen NH₄⁺ is oxidized to nitrite (NO₂⁻), (NH₄⁺ loses its electron and its oxidation state is increased). In the subsequent second step nitrite is oxidized to nitrate where nitrite loses its electron and oxidation state is increased. A simplified equation of the nitrification process is given below (Eq. 1).

Nitrification equation:



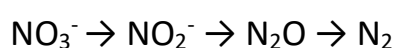
In the marine environment, different microbes are responsible for each step. For example, Nitrosomonas, Nitrospira, and Nitrosococcus are ammonia-oxidizing bacteria (AOB). Ammonia-oxidizing bacteria initiate the nitrification process in the ocean (Martens-Habbena et al., 2009; Zehr & Kudela 2011). However, nitrification is also thought to be vertically decoupled from

primary production. For example, nitrification by ammonia-oxidizing archaea (AOA) does not seem to be inhibited by light, which means that nitrification occurs everywhere in the water column (Zehr & Kudela 2011). In the oceans, this information is not well understood. In some studies, (Beman et al., 2013; Sun et al., 2019; Zehr & Kudela 2011) it was reported that the bacteria Nitrospina and Nitrobacter are known to carry out this step in the ocean.

2.4 Denitrification

Likewise, nitrification, the denitrification is also a microbial process. The NO_3^- is further reduced to NO_2^- and nitric oxide (NO). Then NO is further converted into gaseous N_2O , which is finally converted into molecular N_2 . This process takes place through enzymes of certain microbes. Denitrification process is completed by facultative anaerobic bacteria. These bacteria respire and reduce oxidized forms of nitrogen in response to the oxidation of electron donors such as organic material. Heterotrophic denitrifying microbes need low oxygen concentration of less than 10 % as well as organic carbon for energy (Pajares & Ramos 2019). That's why the N_2O production is high in low-oxygen (O_2) environments (e.g., Goreau et al., 1980; Löscher et al., 2012). This production usually accounts for the majority of N_2O formation in the ocean (Walter et al., 2006). A simplified equation of the denitrification process is given below (Eq. 2).

Denitrification equation:



(Eq. 2)

2.5 Distribution of nitrous oxide in the marine environment

Distribution of N_2O in the marine environment varies greatly depending on the environmental conditions and geographical location. In 1963 Craig and Gordon were the first to published on oceanic N_2O in the South Pacific Ocean. They observed the concentration of N_2O was lower than expected from its solubility equilibrium with atmospheric mole fractions previously reported in the continental atmosphere. This study suggested that N_2O should be an essential trace gas for

atmospheric studies. Later Junge and Hahn in 1971 and 1974 were the first to quantify and publish N_2O in the North Atlantic Ocean (Junge and Hahn, 1971; Hahn, 1974). A study by Yoshinari in 1976 reported the N_2O profiles in the Caribbean and Sargasso Seas. His investigation showed an inverse relationship between N_2O and O_2 concentrations in the water column (Yoshinari, 1976). According to his study nitrification is the major N_2O formation in the ocean that is the process of microbial oxidation of NH_4^+ to NO_3^- .

Another report by Cohen and Gordon (1978) describes the first study of the process of denitrification, in which N_2O is lost through microbial processes by converting N_2O to atmospheric N_2 in surface waters and the tropical Pacific Ocean. This study also provides information on the process of denitrification in the anoxic waters of the Saanich Inlet Basin off Vancouver Island.

The temporal and spatial distribution of N_2O in the world ocean is fairly well known. The highest N_2O levels in the open ocean are found in upwelling regions (Arévalo-Martinez et al., 2015) and production rates can be as high as 120 nM per day (Frey et al., 2020). The highly elevated N_2O concentrations may be located near regions where some of the lowest O_2 concentrations have been measured, usually in the O_2 minimum zone. Due to upward advection of N_2O enriched-waters, N_2O becomes more saturated in the surface waters of equatorial upwelling regions (Arévalo-Martinez et al., 2017). While in the Arctic Ocean shows low net N_2O emissions. Certain regions serving as net N_2O sinks and others as sources (Fenwick et al., 2017; Zhang et al., 2015).

Various physical, chemical and biological parameters such as temperature, salinity, dissolved oxygen, apparent oxygen utilization (AOU), nutrients, and microbial community (composition and abundance) influence net N_2O emissions from the ocean. Among that just three of these variables i.e. chlorophyll, O_2 , and AOU, contribute about 60% of the observed variability in the N_2O concentration in the ocean (Yang et al., 2020), suggesting the importance of N_2O in productive upwelling areas. The importance of N_2O in productive upwelling areas (Stein and Yung, 2003). The correlations between N_2O and environmental parameters provide information about the conditions that influence the distribution of N_2O , but do not tell us anything about the microbes or metabolic processes involved in the activity.

2.6 Nitrous Oxide in the Baltic Sea

The Baltic Sea is the extension of the Atlantic Ocean and is bounded on its northern edge at 60° North latitude by land and the Gulf of Bothnia, on its north-eastern edge by the Gulf of Finland, on its eastern edge by the Gulf of Riga, and on the west by the Swedish part of the southern Scandinavian peninsula. The border around the Baltic Sea thus makes it an almost closed basin with only a limited connection to the North Atlantic/North Sea. For this reason, water exchange with the North Sea is limited. Massive anthropogenic activities such as industrial production, agriculture and the input of waste water occur (Force, 2019). This has led to high inputs of nutrients into the Baltic Sea. As a result, the deeper parts of the central Baltic Sea are affected by oxygen-depleted zones that are becoming more widespread (Carstensen et al, 2014).

Nitrous oxide emissions from coastal regions strongly rely on nitrogen inputs (Seitzinger and Kroeze, 1998; Zhang et al., 2010). The growing input of nitrogen causes eutrophication that has become a global downside in coastal waters resulting in increased productivity and intense O₂ depletion. Such scenario causes increased degradation of organic matter (Breitburg et al., 2018; Rabalais et al., 2014). The oxygen minimum zones (OMZ), whether in coastal waters or in the deeper ocean, could lead to favorable conditions of N₂O production (Codispoti et al., 2001; Nevison et al., 2003). However, it has also been suggested that N₂O production and emissions are very likely to increase in the near future, particularly in shallow anoxic or suboxic coastal systems (Naqvi et al., 2000; Bange, 2006). Therefore, monitoring the N₂O production in the sea is important to predict the future scenarios.

Regular measuring intervals and long-term observations can both be effective methods for tracking seasonal and inter-annual variations and identifying short and long-term trends of an ecosystem, which are necessary to predict how the ecosystem will grow in the future (e.g., see Ducklow et al., 2009).

However, in the light of current global environmental changes different factors are responsible for the formation and consumption of oceanic N₂O. For example, eutrophication, temperature rise, heatwaves, oxygen depletion in coastal and oceanic regions are some of the necessary factors to be considered. In order to achieve the knowledge gap of N₂O with different factors, time-series in different locations would be helpful. Time-series measurements enable us to identify short and long-term trends of different chemical and physical parameters.

Here we try to understand the temporal and spatial distributions of dissolved N_2O from open and coastal Baltic Sea waters observations. We conducted monthly measurements of N_2O and other biogeochemical parameters such as nutrients, temperature, salinity and O_2 in the Eckernförde Bay (Baltic Sea) at the Boknis Eck time-series station site from 2019 to 2023. These data were complemented with N_2O measurements from the SEA-EU cruise to the southern Baltic Sea in May 2022. The data were collected and compared including targeted expeditions, repeated hydrographic surveys and time series station. All of which will contribute decisively to the development of our current knowledge.

The aim and objective of this study is to understand the temporal and spatial variability of the N_2O distribution in the southern Baltic Sea and decipher various factor responsible in the distribution of N_2O . The objectives of this study are given below.

3.0 Aim and objectives

- To decipher the temporal and spatial variability of the N₂O distribution in the southern Baltic Sea.
- To identify the potential effect of heatwaves on N₂O in the time-series measurements of Boknis Eck time series in Eckernförde Bay.
- To identify the major N₂O production and consumption pathways and their major drivers in the southern Baltic Sea.

4.0 Study sites, Material and Methods

4.1 Baltic Sea

Data were collected and analyzed from a research cruise in the Baltic Sea as part of an EU project (SEA-EU, European University of the Seas: <https://sea-eu.org>). The expedition took place from May 24, 2022 to July 3, 2022 onboard the Polish research vessel Oceanograf (**figure 1**). The different sampling sites and stations along the Baltic Sea are listed in Table 1.

One of the largest brackish water areas in the world, the epicontinental and enclosed Baltic Sea (located between roughly 10°- 30° E and 54°- 66° N) has a surface area of 42,105 km² and a volume of 22,103 km³, which correspond to 0.1% and 0.002% of the world's oceans, respectively. With a mean depth of 60 meters and a maximum depth of 460 meters, the Baltic Sea is quite shallow. It was created following the last glacier, around 10,000–15,000 years ago, and has experienced extraordinary changes in its fundamental physicochemical properties within such a geologically brief period of time. The Baltic Sea's "ecological age" now is roughly 8,000 years old (Lass and Matthäus, 2008). The Baltic Sea is located in the changing parts of Atlantic marine and Eurasian continental climate systems, which control the hydro climatic conditions of the sea. Salinity and temperature, which both have substantial gradients and decrease from the southwest to the northeast, are the most crucial. The quantity and frequency of saline water inflows (with high oxygen content) from the North Sea through the Danish Straits and riverine (freshwater) inflows, which are regulated by precipitation are the two main event that define the salinity regime of the Baltic Sea (Lass and Matthäus, 2008). Since the late 1970s, substantial inflows have happened less frequently. This has resulted significant stagnation in the Baltic Sea. The average annual influx of freshwater into the Baltic Sea, which is 481 km³, that is roughly equal to the volume of saline water entering from the North Sea. The major source of freshwater inflow to the Baltic Sea comes via the Gulf of Bothnia, Gulf of Finland, and the Gulf of Riga. A permanent halocline that is situated between depths of roughly 70 and 100 meters divides the upper water layer from the deeper, more saline layer. In the shallower parts of the northeastern Baltic Sea, there is no halocline. Strong permanent haloclines and seasonal thermoclines throughout the summer significantly reduce vertical mixing of the water column. This leads to the formation of oxygen-depleted zones in a number of places, primarily in the central Baltic Sea's deep regions. The freezing temperatures of winter have a significant impact on the water temperature regime. The Bothnian Bay normally experiences the first sea ice formation in November to mid-May. Ice coverage's duration reduces from north

to south (Heino et al., 2008). In some coastal regions, during the summer, the water temperature could exceed to 25°C. The Baltic Sea water has a residence time of 25–35 year (Lass and Matthäus, 2008).

Sampling site	Station code	Sampling depth (m)	Latitude	Longitude
Gulf of Gdansk	MET1_BH	0-87	54°34.4955' N	19°08.1473' E
	MET1_MP	0-77	54°34.2883' N	19°09.8997' E
	MET1_REF	0-77	54°34.41122' N	19°09.08298' E
Arkona Basin	AB_G_1	0-34	54°43.8642' N	13°29.5440' E
	AB_G_2	0-34	54°43.9154' N	13°29.7419' E
	AB_NG	0-18	54°39.3617' N	12°38.2914' E
Mecklenburg Bay	MB_G_1	0-21	54°15.89585' N	11°26.06539' E
	MB_G_2	0-21	54°15.81542' N	11°25.5909' E
	MB_NG	0-19	54°31.46071' N	10°40.0482' E
Eckernförde Bay	EB_G1	0-22	54°28.74616' N	09°54.32495' E
	EB_G2	0-22	54°29.3467' N	09°56.3498' E

Table 1: The different sampling sites and stations at SEA-EU cruise along the Baltic Sea

4.2 Boknis Eck time series station

Data from two study areas were used for this study. Monthly measurements were done at the time series station site of Boknis Eck in the Eckernförde Bay in Schleswig-Holstein, Germany (**figure 1**). Samples were collected once a month from March 2019 to June 2023 from the research vessel Littorina, provided by GEOMAR-Helmholtz Centre for Ocean Research Kiel, Germany.

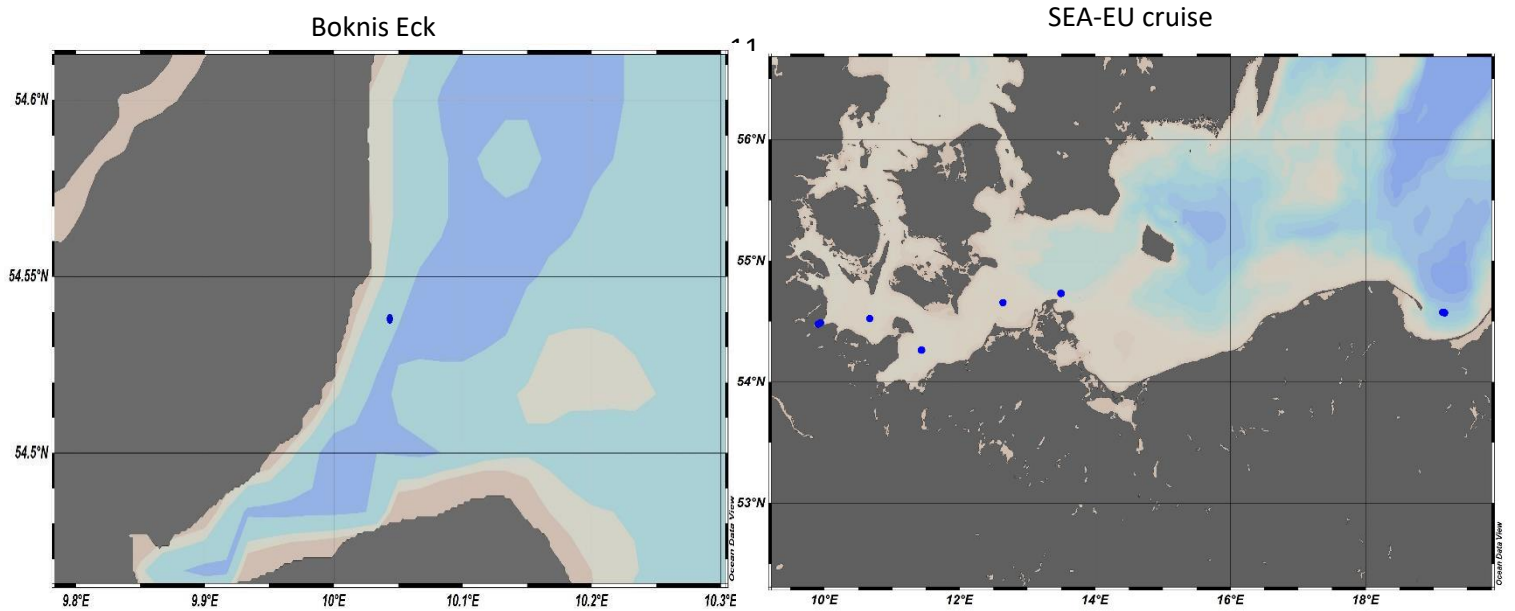


Figure1: The sampling stations of the two study areas, Boknis Eck time series and SEA EU cruise.

The Boknis Eck time series station is one amongst the oldest unendingly conducted marine time series stations within the world. The first samples were taken in 1957 and sampling has been conducted on a monthly base with solely minor interruptions since then (Lennartz et al., 2014). It's located in Eckernförde Bay ($54^{\circ} 310' N$, $10^{\circ} 020' E$;) in the southwestern (SW) Baltic Sea, with a depth of roughly 28 m (Fig. 1). The sediments in the Eckernförde Bay are characterized by high organic matter load and sedimentation rates (Orsi et al., 1996; Whiticar, 2002), that are closely related to the spring and season algae blooms (Smetacek, 1985).

The monitoring of various physical, chemical, and biological parameters was started by Johannes Krey (Institut für Meereskunde, Kiel) in 1957 (Krey et al., 1980), and it has been carried out every month ever since with only two significant breaks in 1975-1979 and 1983-1985, during which no data are available. Starting with measurements of Secchi depth, temperature, salinity and oxygen with CTD on 30 April 1957, the number of parameters has increased almost continuously. Chlorophyll a (since 1960) and nutrients like nitrate, ammonium (1979), nitrite (1986) and phosphate (1957–1966, since 1979) are now part of the monthly routine. Monthly samples have been taken from research vessels during half-day trips, the sampling usually starting around 10:00 to 11:00 in the morning. Seawater has been sampled at six standard depths (1, 5, 10, 15, 20, 25m) using Niskin bottles or the like during several casts, prepared onboard and cooled until further analysis. Analysis was usually carried out in the days following the cruise. The time series of BE provides a highly valuable data set for three main reasons. Firstly, provides continuous information on changes in the time span of decades. Secondly, there have only been minor changes in the methods used for determining the parameters, and careful calibration avoided shifts or inaccuracies in the data. This consistency strongly enhances the quality of the data, as shifts in the data signals through different methods of analysis can be excluded. Thirdly, the location of Boknis Eck was initially chosen because it reflects the hydrographic setting of the Kiel Bight (Krey et al., 1980). As there are no major rivers discharging into the Eckernförde Bay, riverine inputs of nutrients, for example, can be neglected; however, influences by direct runoff from land cannot be excluded.

4.3 Sampling and analytical methods

The seawater samples were collected with 10 L Niskin bottles installed on a rosette water sampler. Subsamples of 20 mL, in triplicate, were taken into opaque glass vials with butyl rubber stoppers and aluminum caps to prevent air – water exchange. Then the samples in the 20 mL vials were poisoned by injecting 0.05 mL of a saturated mercuric chloride solution ($\text{HgCl}_2(\text{aq.})$). Mercuric chloride was used in order to inhibit any form of biological activity. Then the two solutions were homogenized by shaking the vials. This step has been shown by Wilson et al., (2018) to be effective in completely inhibiting microbial activities in water samples. Thereafter, the samples were packed upright to prevent the formation of air bubbles due to temperature and pressure fluctuations.

4.3.1 Dissolved N₂O measurements

4.4 Calibration curve

We used two-point calibration procedure by using standard gas mixtures with 311.8 ± 0.2 ppb and 346.5 ± 0.2 ppb N₂O in synthetic air (Deuste Steining GmbH, Mühlhausen Germany). The standard gas mixtures were calibrated against the NOAA standard scale, in the laboratories of the Air Chemistry Department of the Max Planck Institute for Chemistry in Mainz, Germany. The standard gases used were calibrated against the NOAA-PMEL primary standards, therefore the mole fractions of these standard gases are very accurate. For each measuring day, the gas chromatography was calibrated with two standard gases identified as Standard 5B and 14 with mole fractions of 1044.597 ppb and 355.775 ppb respectively. To obtain diluted gases, 3 mL of helium was added to 6 mL of the standard 5B, while 5 mL of helium was added to 4 mL of the standard 14. Therefore, translating to the dilution factors of 0.67 and 0.44 respectively. The standard gases were injected either as pure gas or mixed with helium with the aid of a gas mouse at varying proportions. An exemplary plot of a typical calibration curve was made for the measurement of N₂O in our sample (figure 2).

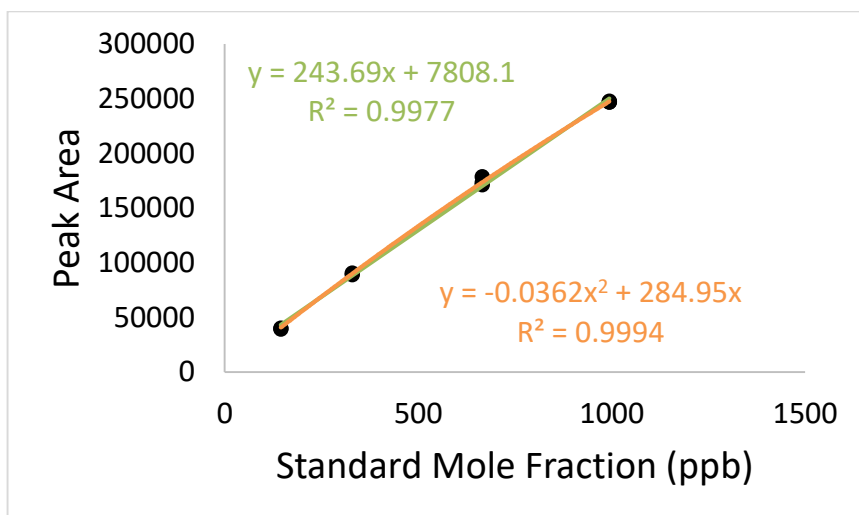


Figure 2: Plot of a typical calibration curve of standard gases for the calculation of dissolved N₂O. The orange line represents the quadratic fit while the green line represents the linear fit.

4.5 Measurement of N₂O from the samples

Dissolved N₂O in the seawater samples were measured in the Chemical Oceanography department at GEOMAR, Kiel, by using the static headspace method. The analytical method applied was a modification of the method described by Bange et al. (2001). Each of the vials was equipped with an air-tight syringe (VICI Precision Sampling, Baton Rouge, USA). This was used to manually inject 10 mL of high-purity helium (99.99%, Air Liquide, Düsseldorf, Germany). Then 10 mL of the sample was replaced with a helium headspace for each vial. The sample was then shaken with a vortex mixer (G560E, Scientific Industries Inc., NY, USA) for about 20 seconds and then left for at least 2 hours to achieve N₂O equilibrium between the air and water phases. After that, the samples were equilibrated at room temperature by continuously recording the temperature. A 9mL subsample from the headspace was used to flush a 2mL sample loop after passing through a moisture trap (filled with Sicapent, Merck Germany). Detection of N₂O was performed at 190°C on a packed molecular sieve column (6 ft×1/800 SS, 5 A, mesh size 80/100, Alltech GmbH, Germany) by Gas chromatographic connected with electron capture detector (GC-ECD). A mixture of argon and methane of ration 95:5 (by volume) was used as carrier gas with a flow of 21 mL min⁻¹.

Helium and head spaced samples, of 9 mL each, were injected into GC-ECD simultaneously, this step was important so as to flush the gas chromatograph of any impurities and/or leftover samples from previous measurements. Right after taking a 9 mL headspace sample from the vials and having injected it into the GC-ECD, the corresponding ambient temperature was recorded and this step was repeated for each measurement. After measurements, the chromatograms were processed using the ChromStar 6.3 desktop software. Each chromatogram comprises of several peaks recorded during the measurements, and each peak was evaluated individually through integration processes. The integration procedure allows for the adjustment of the baseline such that all the peaks in a chromatogram would be annotated and take note of the peak areas. The adjusted peaks were eventually transformed into gas molar fractions and the data was transferred into excel spreadsheets where further calculations were carried out. The mole fraction of N₂O measured in the headspace was calculated from the peak area using the quadratic fit. It is presented in equation(3).

$$X_{N_2O_{quadratic}} = -\frac{b}{2a} \pm \sqrt{\left(\frac{b}{2a}\right)^2 + \frac{PA}{a}} \quad (3)$$

The final concentration of dissolved N₂O in the samples was determined using equation (4) below, and the N₂O is given in nmol L⁻¹.

$$C_{gas}[\text{nmol L}^{-1}] = \left(\frac{\beta x P V_{WP} + \frac{xP}{RT} V_{hs}}{V_{WP}} \right) \quad (4)$$

Where β is the Bunsen solubility (in mol L⁻¹ atm⁻¹), and was calculated using the solubility equation by Weiss and Price, (1980) at equilibration temperature and in situ salinity.

x is the dry gas mole fraction of N₂O (in nmol mol⁻¹).

P is the atmospheric pressure (atm).

V_{wp} and V_{hs} are the volume of water and volume of headspace, respectively, both in milliliter (mL).

R is the gas constant (0.08205746 L atm K⁻¹ mol⁻¹).

T is the equilibration temperature (K).

The Bunsen solubility of N₂O (C_{N_2O} in mol L⁻¹) in seawater in equilibrium with moist air at $P = 1$ atm can be calculated with the polynomial given by Weiss and Price (1980). Where β is the Bunsen solubility (in mol L⁻¹ atm⁻¹), T is for temperature in K, S stands for salinity and the values of the constants: A_1 , A_2 , A_3 , A_4 , B_1 , B_2 and B_3 are presented in the table 2 below.

$$\beta = \exp \left(A_1 + A_2 \left(\frac{100}{T} \right) + A_3 \ln \left(\left(\frac{T}{100} \right) + A_4 \left(\frac{T}{100} \right)^2 + S \left(B_1 + B_2 \left(\frac{T}{100} \right) + B_3 \left(\frac{T}{100} \right)^2 \right) \right) \right) \quad (5)$$

A1	-165.8806
A2	222.8743
A3	92.07292
A4	-1.4843
B1	-0.0562
B2	0.0316
B3	-0.0048

Table 2: Constants for calculating the equilibrium solubility (in mol L⁻¹ atm⁻¹) of N₂O from Weiss and Price (1980).

4.6 N₂O Saturation Calculation

N₂O saturation was calculated with the following formula:

$$S = (N_2O_m / N_2O_{atm}) \times 100$$

Where N₂O_m represents measured N₂O concentration, and N₂O_{atm} is the N₂O theoretical equilibrium concentration that depends on temperature, salinity, ambient air pressure and the atmospheric N₂O mole fraction at the time of sampling. Atmospheric N₂O data from NOAA Mace Head (MHD), County Galway, Ireland, were used for the calculation, matching the month and year of N₂O_m sampling. The data were collected from NOAA website: (https://gml.noaa.gov/aftp/data/trace_gases/n2o/flask/surface/txt/n2o_mhd_surface-flask_1_ccgg_month.txt).

The N₂O_{atm} data updated on the website stopped in December 2021, subsequent years were not updated, and the data show an annual atmospheric increase of approximately (1.09 ppb) for each year. Therefore, N₂O_{atm} values for 2022 and 2023 were estimated by adding (1.09 ppb yr⁻¹) to the previous year.

4.7 N₂O Production in the water column

The relationship between N₂O excess (ΔN_2O) and apparent oxygen utilization (AOU) is an important indicator for determining N₂O production in the water column. The formula used to calculate (ΔN_2O) is shown in the equation below and is calculated by subtracting the equilibrium concentration of N₂O from the

measured N₂O concentration.

$$(\Delta N_2O) = N_2O_m - N_2O_{atm}$$

Where N₂O_m is the measured N₂O concentration, and N₂O_{atm} is the N₂O equilibrium concentration.

The difference between the oxygen equilibrium value or solubility value and the measured concentration is called apparent oxygen utilization (AOU) and its calculated using the equation below.

$$AOU = [O_2]_{eq} - [O_2]_{meas}$$

Where [O₂]_{eq} is the equilibrium concentration at the temperature and the salinity of the water sample according to Garcia and Gordon (1992) and [O₂]_{meas} is the measured oxygen concentration of the sample.

AOU indicates the amount of oxygen consumed, considering that the oxygen concentration was in equilibrium with the atmosphere when the water was at the surface. Due to the influences of atmospheric pressure, which in water production zones frequently lowers the degree of saturation, and bubble processes, which raise the degree of saturation, the surface water was probably not completely saturated (Stanley et al., 2012).

4.8 Oxygen and Nutrient Measurements

During both cruises CTD rosette was equipped with SBE oxygen sensor (Sea-Bird Electronics, Bellevue, WA, USA), was used to obtain dissolved oxygen profile. Additionally, oxygen was measured by Winkler titration method. Temperature, salinity, depth and pressure sensors were also mounted on the CTD rosette. Nitrate, nitrite and phosphate samples from the rosette were analyzed at GEOMAR chemistry laboratory by applying the methods described by Hansen et al. (1999).

4.9 Temperature and N₂O anomalies

The measurements at the Boknis Eck time series station conducted during this study allows us to determine the effect of the European heatwave in 2018 in the monthly time-series measurements of water temperature and dissolved N₂O at Boknis Eck (Lennartz et al., 2014; Ma et al., 2020). To this end, we computed the anomalies of water temperature and ΔN_2O at 1 and 25 m depth for the period of July 2005 to June 2023. The anomalies were defined as

$$\Delta T = T - T_{i, avg} \text{ and}$$

$$\Delta(\Delta N_2O) = (\Delta N_2O) - (\Delta N_2O)_{i, avg}$$

Where T is the measured monthly water temperature in the period of July 2005 to June 2023 at 1 and 25 m depth at Boknis Eck (Lennartz et al., 2014). $T_{i, avg}$ is the mean water temperature at 1 and 25 m depth of the respective month over this period at Boknis Eck. The resulting ΔT is the anomaly of the water temperature which is cleaned from seasonal differences throughout each year. $\Delta(\Delta N_2O)$ is calculated similarly to ΔT in the same time period using ΔN_2O ; which is the monthly excess N₂O at 1 and 25 m depth. $(\Delta N_2O)_{i, avg}$ is the mean excess N₂O at 1 and 25 m depth of the respective month over this period at Boknis Eck. ΔN_2O was computed as the difference of the monthly measurements of dissolved N₂O at 1 and 25 m water depth (Ma et al., 2020).

5.0 Results

The results from Boknis Eck time series between 2019 to 2023 and the SEA-EU cruise in May 2022 were analyzed and compared to understand the temporal and spatial distributions of dissolved N_2O in the open and coastal waters of the southern Baltic Sea. The monthly measurements of nitrous oxide and other biogeochemical parameters at Boknis Eck are presented below.

5.1 Nitrous oxide variabilities at Boknis Eck

The annual distribution of N_2O varied from season to season of the year. In 2019 January to March were higher in N_2O than the rest of the year. Similarly, this pattern was observed in 2020, 2021, 2022 in (figure 3) except in 2023 January and April where N_2O were higher than the rest of the months. We observed similar concentrations from surface to the depth of 25 meters. However, in 2022 the results showed higher concentrations of N_2O in all months of the year, which was more or less uniform from surface to depth.

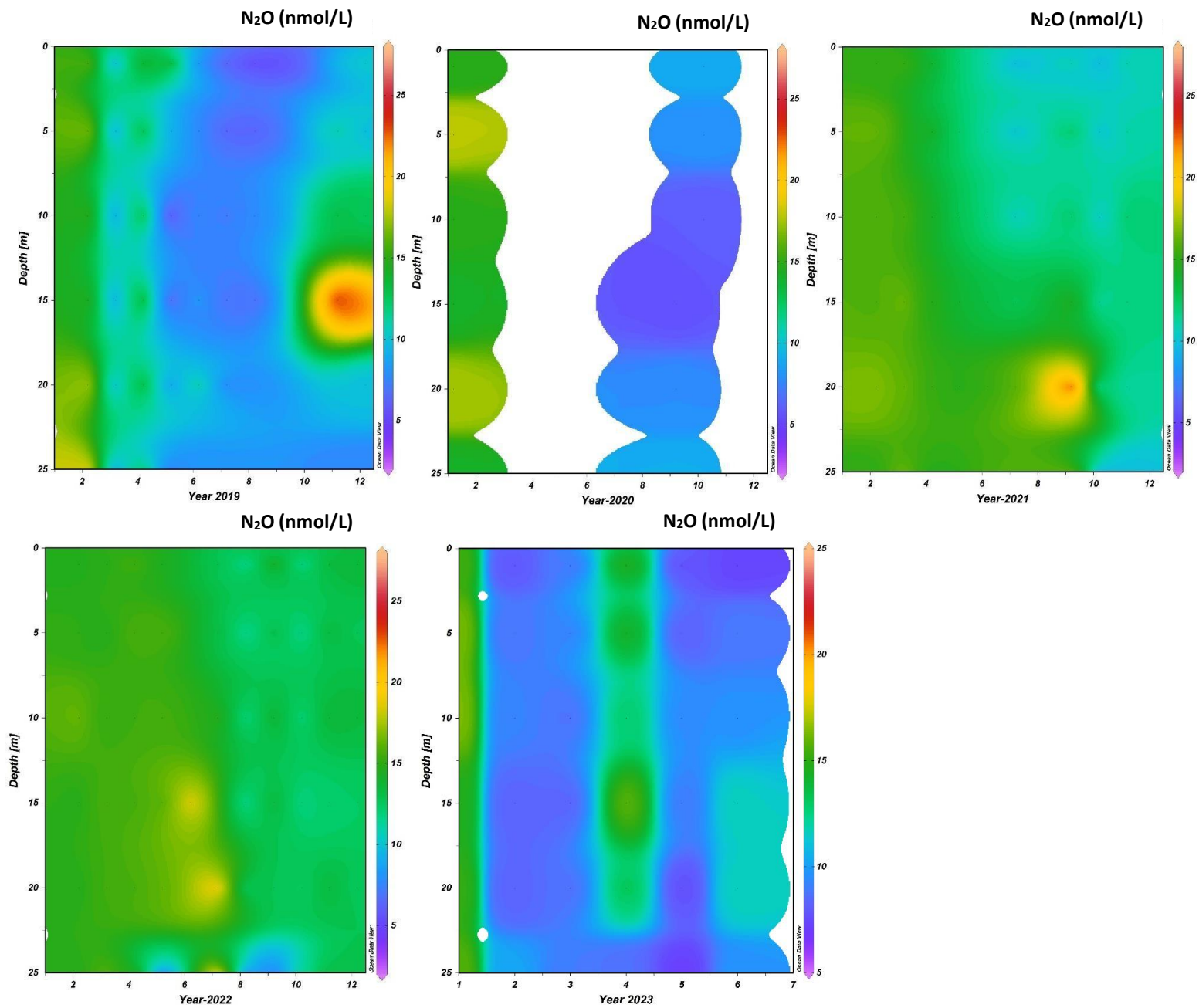


Figure 3: The seasonal cycle of nitrous oxide variability in the BE time series site from 2019 to 2023 at six standard depths. The x-axis displays the months of the years, with number representing the month. **Note:** In 2020 data were not collected for all months due to Covid-19 restrictions.

The concentration of N₂O was observed to be low from April to October of the year 2019 and 2020. However, the data of year 2020 does not include all months of the year. Only the samples of February, October and November were measured and analyzed, and the results showed high to low concentrations from the surface to the water column. In 2021 the surface (1-10 m) N₂O concentration in summer was lower than the deeper water (15-25 m). Nevertheless, the concentration of N₂O in the year 2021 was higher compared to the previous years. However, the concentration of N₂O was observed to be low in February, March, May and June of the year 2023.

The oxygen resulted to be higher in concentrations at surface waters in January to March of 2019, 2020 and 2022, (figure 4) although in 2023 the higher oxygen concentration extended to May. It decreased at the depth during the spring to the summer months. The lowest oxygen concentration was recorded at a depth of 20-25 m. In 2021 from January to March the oxygen concentrations is homogeneous. The average oxygen concentration for all years, both at the surface and at depth, was 311 $\mu\text{mol L}^{-1}$ at 1 m depth and 184 $\mu\text{mol L}^{-1}$ at 25 m depth. Overall result showed lowest O₂ concentrations at the depth of 20-25m during the August to December which can be as a result of decomposition of organic particles.

The oxygen data was compared to the N₂O concentrations to see if oxygen deficiencies had any influence on them. It showed that O₂ concentrations at the surface and depth had no relationship with N₂O concentrations.

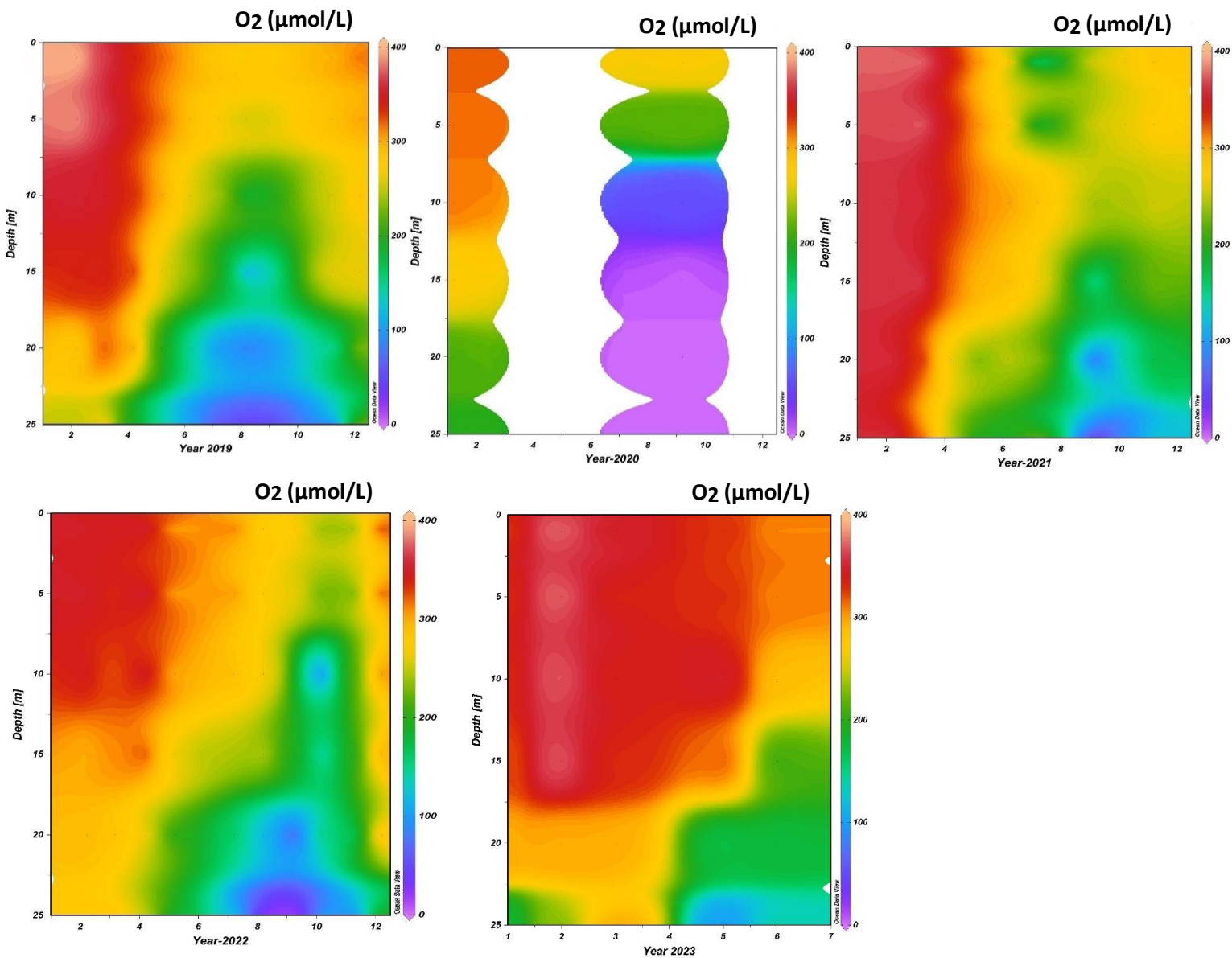


Figure 4: The seasonal cycle of oxygen variability in the BE time series from 2019 to 2023 at six standard depths. The x-axis displays the months of theyears, with number representing the month. **Note:** In 2020 data were not collected for all months due to Covid-19 restrictions.

5.2 Biogeochemical variation at Boknis Eck

Surface temperature was highest during the summer from July to October from 2019 to 2022. However, the high surface temperature in 2023 was found in May and June, and our data ended in June. In 2021, the summer was longer, and the water temperature remained high until December.

The results from 2022 shows to be warmer compared to the other years (figure 5). The temperature remained warm at the depth of 20 meters. However, in 2022, summer was short but warm, with average of 15 °C. During the winter months, the temperature was low from the surface to 25 m depth. During winter such as from January to March the water column temperature remains low and uniform.

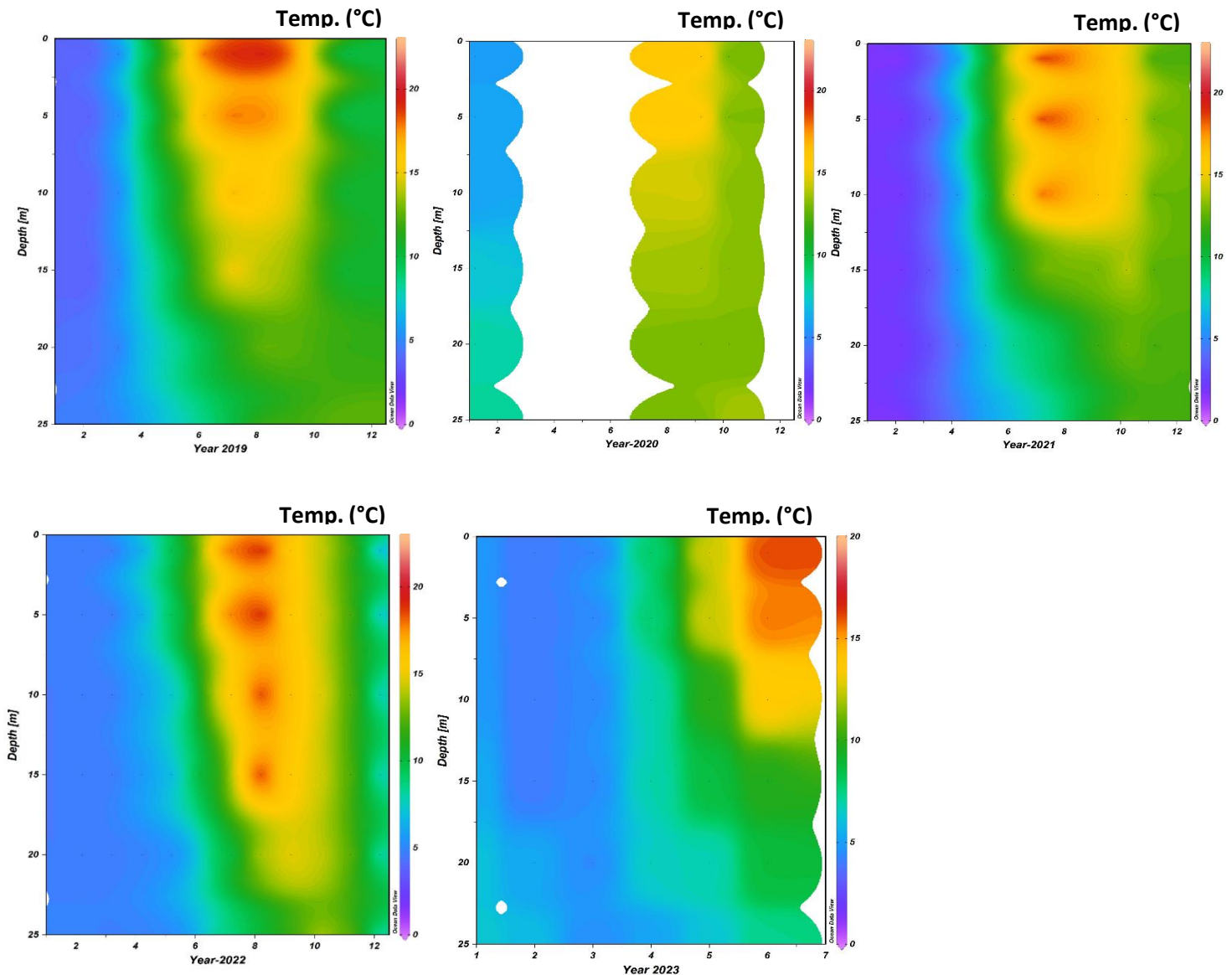


Figure 5: Temperature variabilities of BE time series from 2019 to 2023. The number on x-axis represent the month of the year. **NOTE:** in 2020 data for all the months were not collected due to Covid-19 restrictions.

The salinity was lower at the surface and increased with the depth. Our results (figure 6) show that salinity being highest during the winter seasons and remained higher at the depth of 20-25 meters. In the summer the surface water salinity was observed to be lower except for 2020 due to lack of data.

In 2021, the salinity was higher than the previous year, being high from May to December at the depth. In November and December, the salinity remains more or less uniform from surface to depth. The lowest salinity in all years was observed in the summer months.

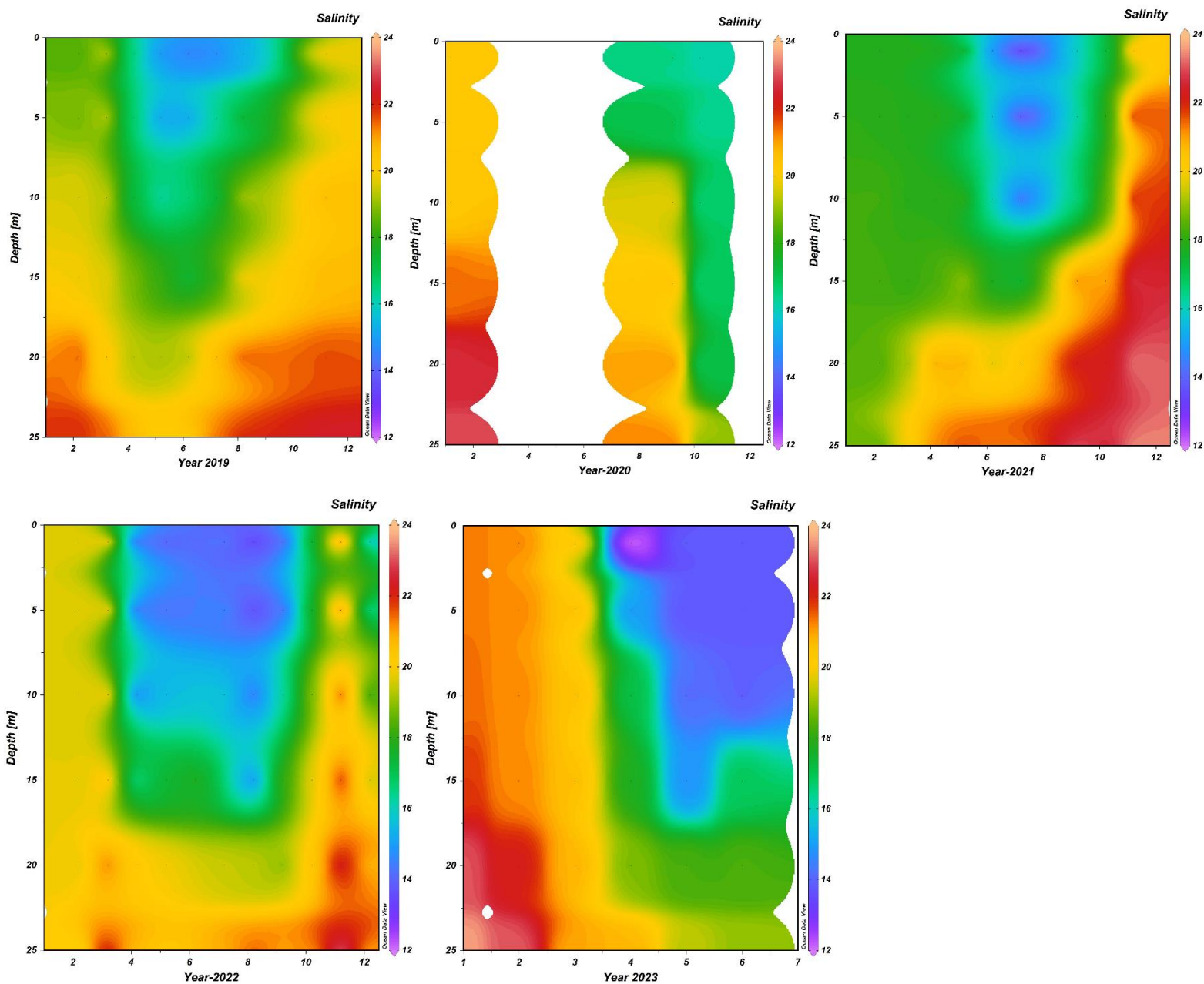


Figure 6: Salinity variabilities of BE time series from 2019 to 2023. The number on x-axis represent the month of the year. **NOTE:** in 2020 data for all the months were not collected due to Covid-19 restrictions.

5.3 Nitrate and nitrite variabilities at Boknis Eck

The seasonal distribution of NO_3^- and NO_2^- from 2019 to 2023 is low to high from surface to the depth (figures 7 & 8). During the winter of 2020 to 2023 show higher concentration of the NO_3^- and NO_2^- respectively from surface to the depth. During summer the NO_3^- and NO_2^- concentrations were observed to be lowest at the surface water column. While the year 2019 observed to have lowest level of NO_3^- and NO_2^- at the surface waters throughout the year of 2019. The low concentration of NO_3^- and NO_2^- was same for the all observation except for the January and February.

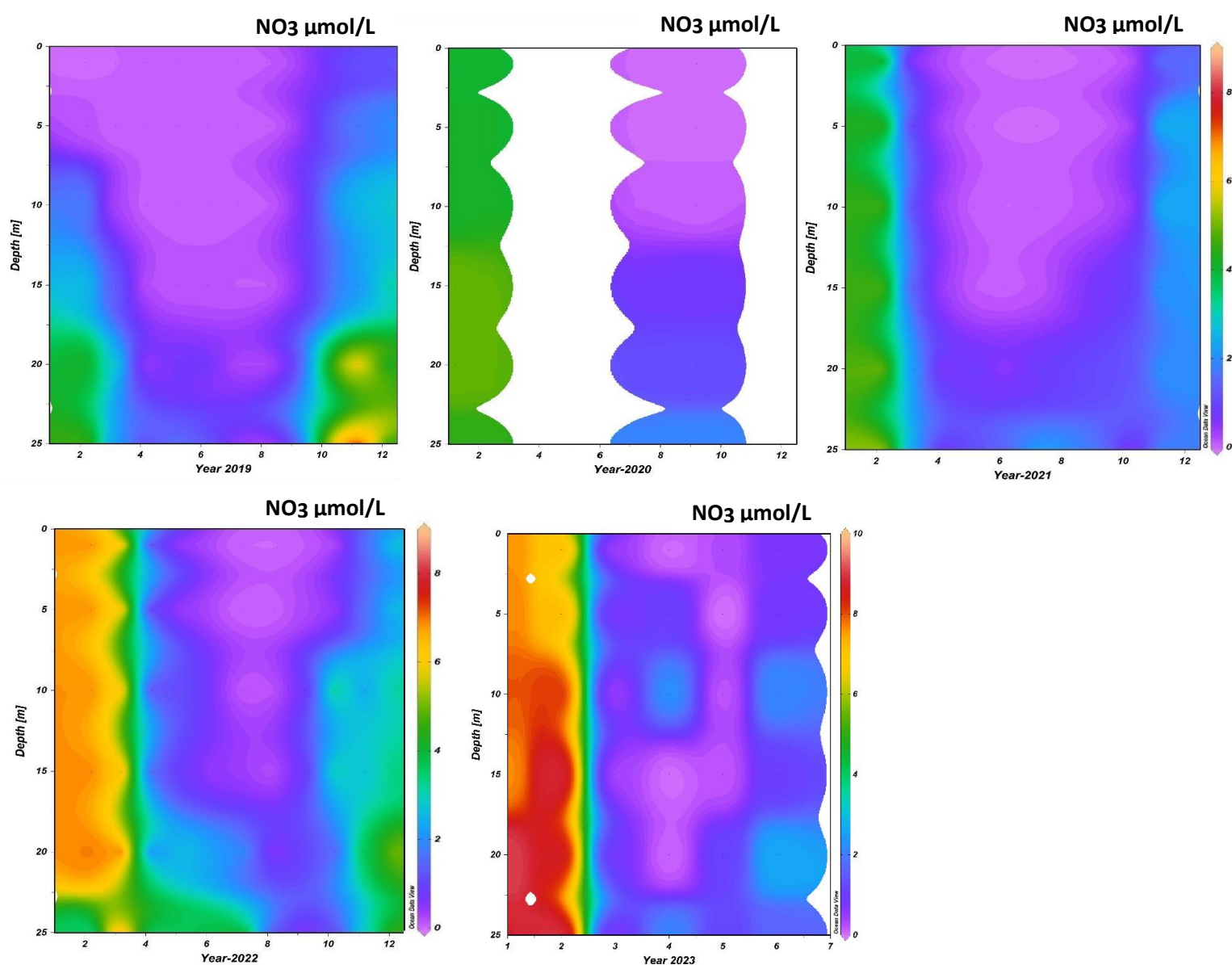


Figure 7: The seasonal cycle of nitrate variability in the BE time series from 2019 to 2023 at six standard depths. The x-axis displays the months of the years, with number representing the month. **Note:** In 2020 data were not collected for all months due to Covid-19 restrictions.

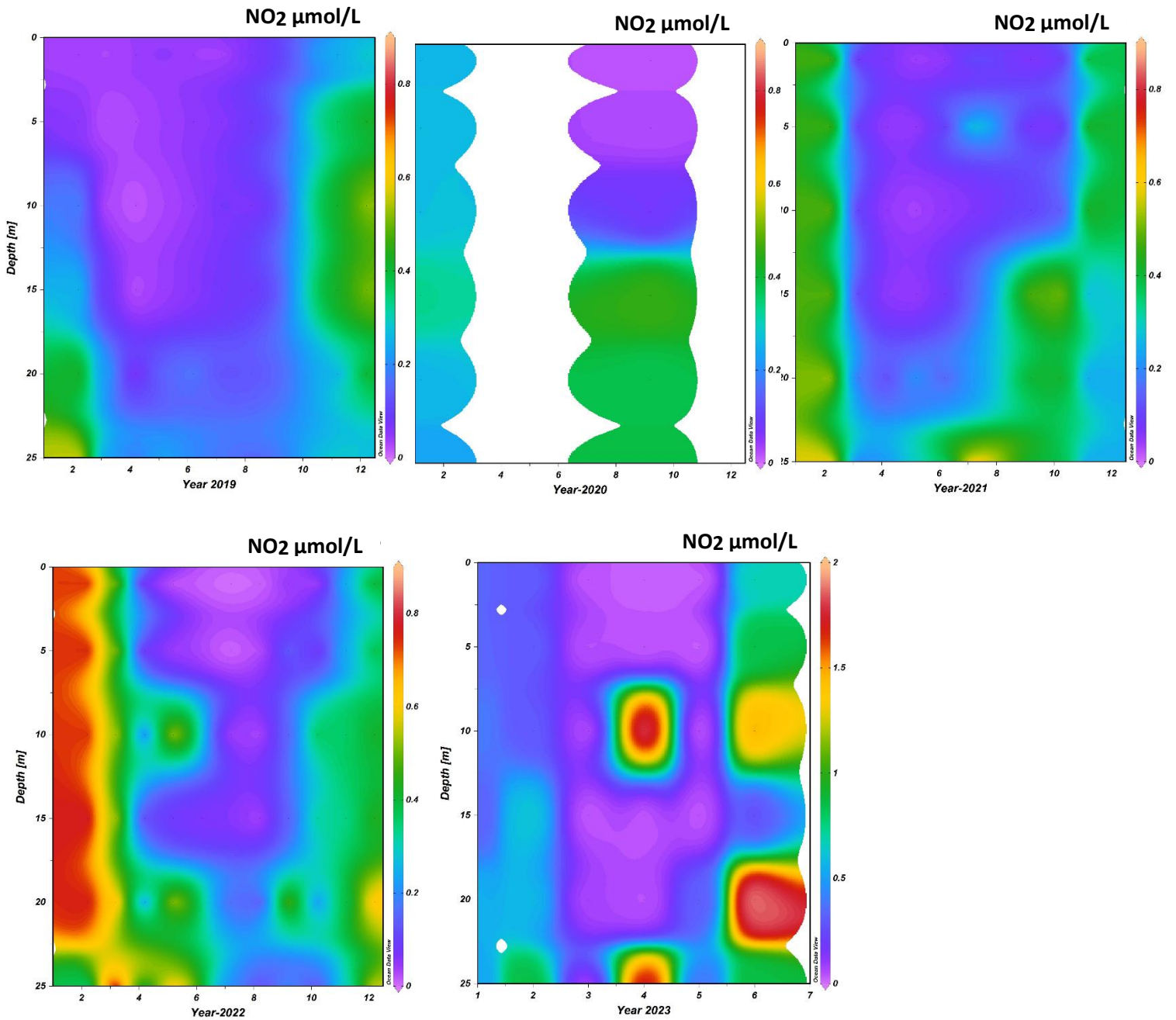


Figure 8: The seasonal cycle of nitrite variability in the BE time series from 2019 to 2023 at six standard depths. The x-axis displays the months of the years, with number representing the month. **Note:** In 2020 data were not collected for all months due to Covid-19 restrictions.

5.4 Biogeochemical variation during the SEA-EU cruise in relation to N_2O

Dissolved N_2O was sampled in four different sites along the cruise transect and they were further grouped into two sites (Eckernförde Bay and Mecklenburg Bay) and (Arkona Basin and Gulf of Gdansk) due to their different depth.

Here we present the biogeochemical parameters (figures 9 & 10; NO_2^- , NO_3^- , temperature, salinity, and oxygen) as a function of depth on the y-axis and N_2O on the x-axis on the Eckernförde Bay and Mecklenburg Bay cruise track at six water depths (1-22 meters).

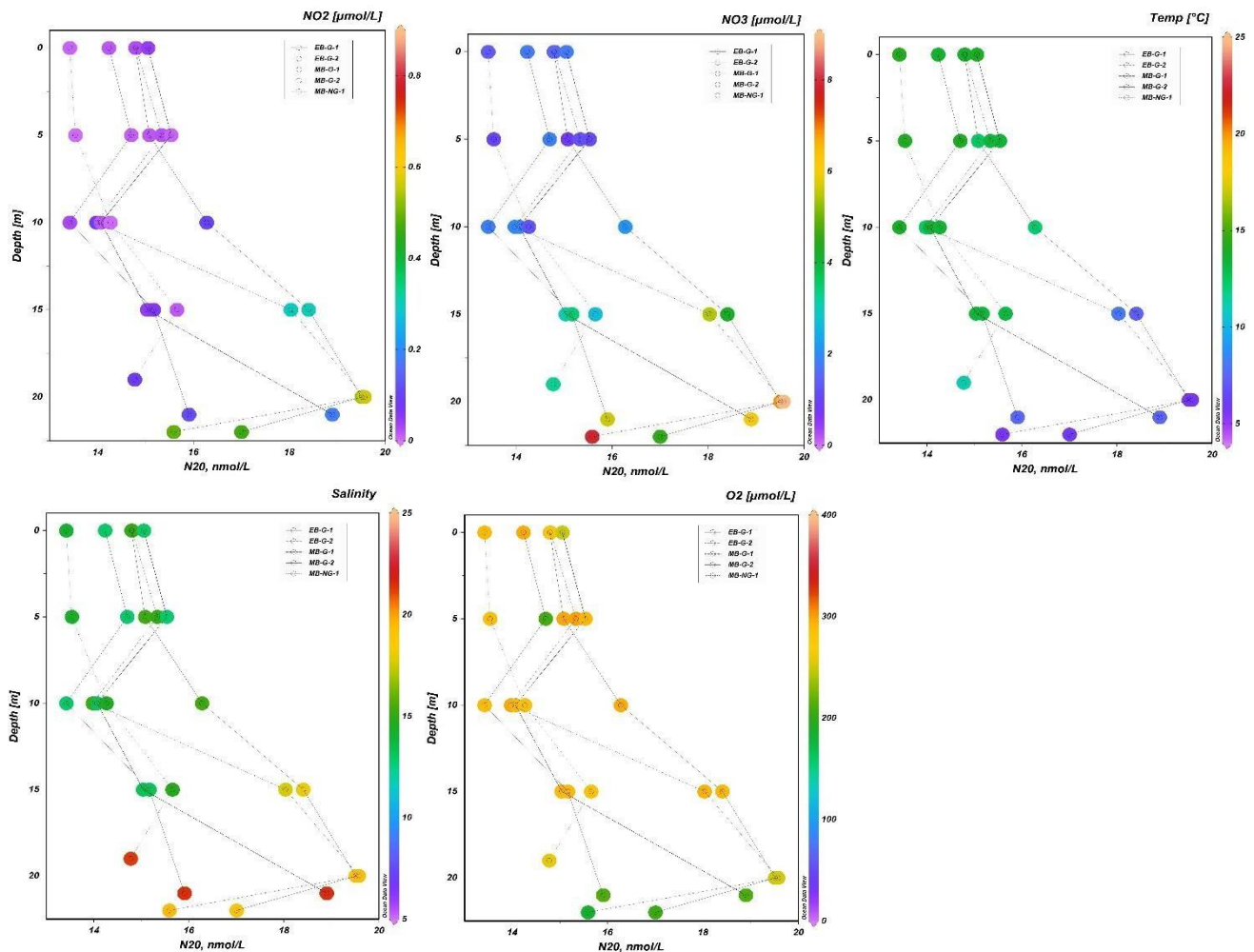


Figure 9: Distribution pattern of N_2O concentration in relation to O_2 , NO_3^- , NO_2^- , temperature, and salinity during the cruise transect of SEA-EU at Eckernförde Bay and Mecklenburg Bay. **NOTE:** the color dots are represented by the biogeochemical parameters, while the first two data points represents Eckernförde Bay and the last three data points represents Mecklenburg Bay.

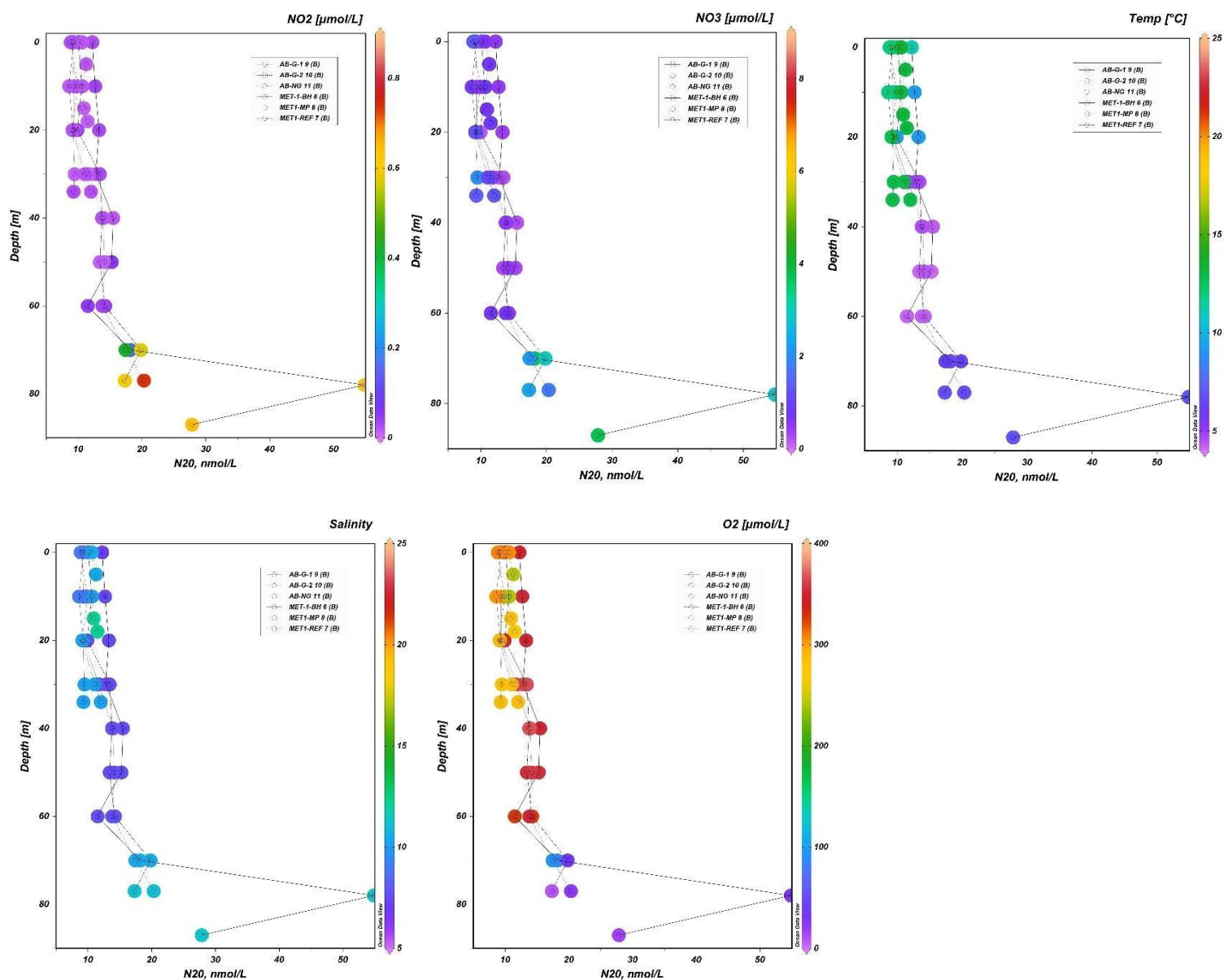


Figure 10: Distribution pattern of N_2O concentration in relation to O_2 , NO_3^- , NO_2^- , temperature, and salinity during the cruise transect of SEA-EU at Arkona Basin and Gulf of Gdansk. **NOTE:** the color dots are represented by the biogeochemical parameters, while the first three data points represents Arkona Basin and the last three data points represents Gulf of Gdansk.

The NO_2^- and NO_3^- distribution from the cruise transect was very low in the surface water close to zero with the lowest values of $0.01 \mu\text{mol L}^{-1}$ and $0.14 \mu\text{mol L}^{-1}$. As the water column depth increases, the concentrations of NO_2^- and NO_3^- slightly increased with values of $0.64 \mu\text{mol L}^{-1}$ and $8.89 \mu\text{mol L}^{-1}$ and N_2O concentrations partially increased from the water surface to the depth. The concentration of NO_2^- was almost low from the surface to the water column.

Temperature and oxygen were relatively high at the water surface between 1-15m and decreased at depth 20-22 m except oxygen concentrations that only changes at 22 m depth, while N_2O concentration changes from the surface to the water column (low-high). There is a relationship between N_2O concentration at water depth, temperature, and oxygen content. At the surface, the water is warmer, more oxygenated, and has a low N_2O concentration.

The salinity result shows high salinity at greater depth between 15-22 m, and low salinity at the surface. Salinity increases with depth due to factors such as evaporation and mixing of water masses, while N_2O concentration is lower at the surface and increases in the water column.

5.5 Biogeochemical variation during the SEA-EU cruise in relation to temperature

Here we present the biogeochemical parameters (figures 11 & 12; NO_2^- , NO_3^- , salinity, and oxygen) as a function of depth on the y-axis and temperature on the x-axis on the Eckernförde Bay and Mecklenburg Bay cruise track at six water depths (1-22 meters).

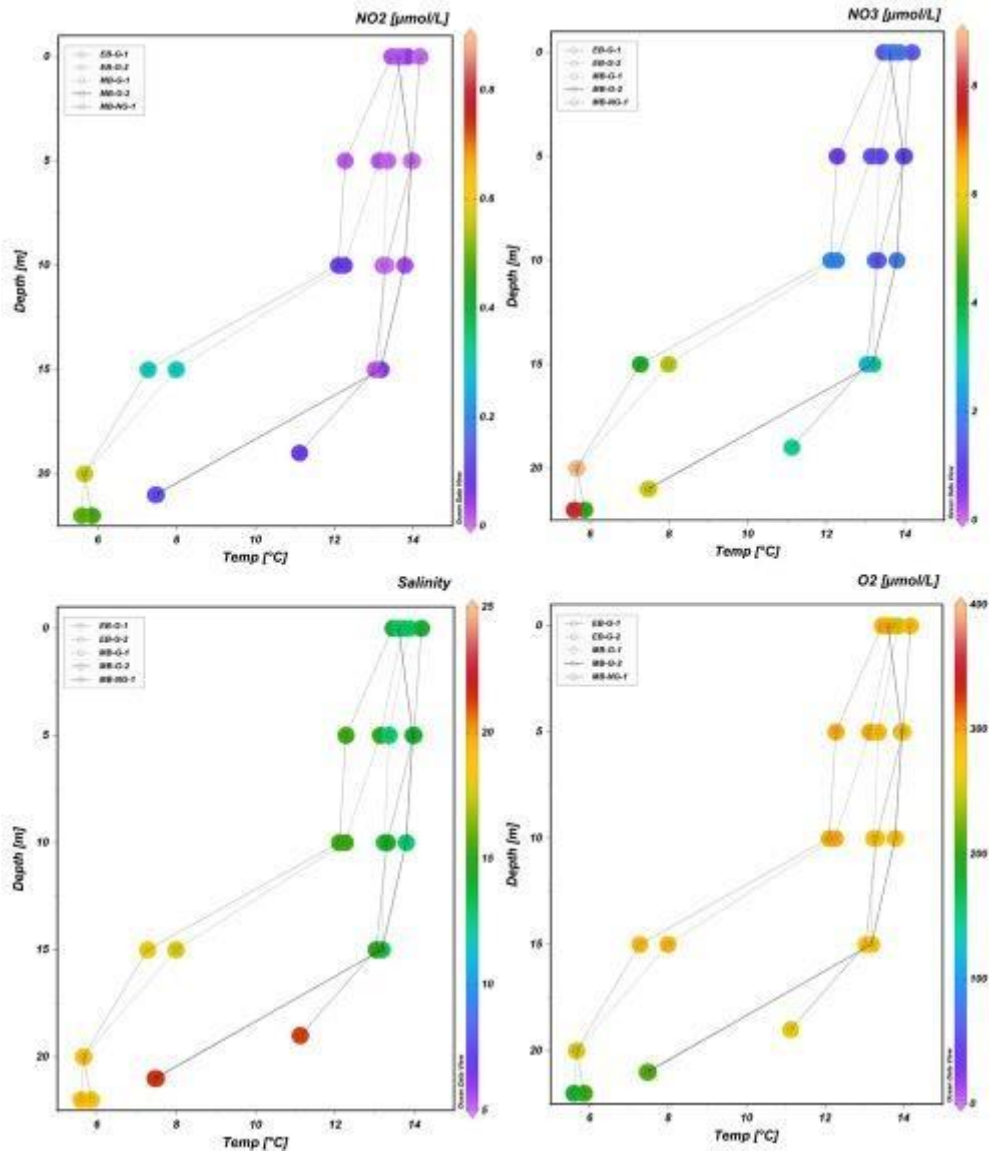


Figure 11: Temperature profile against salinity, oxygen, NO_3^- , and NO_2^- during cruise transect of SEA-EU at Eckernförde Bay and Mecklenburg Bay. **NOTE:** The color dots represents salinity, oxygen, NO_2^- , and NO_3^- , while the first two dots represents Eckernförde Bay and the last three dots represents Mecklenburg Bay.

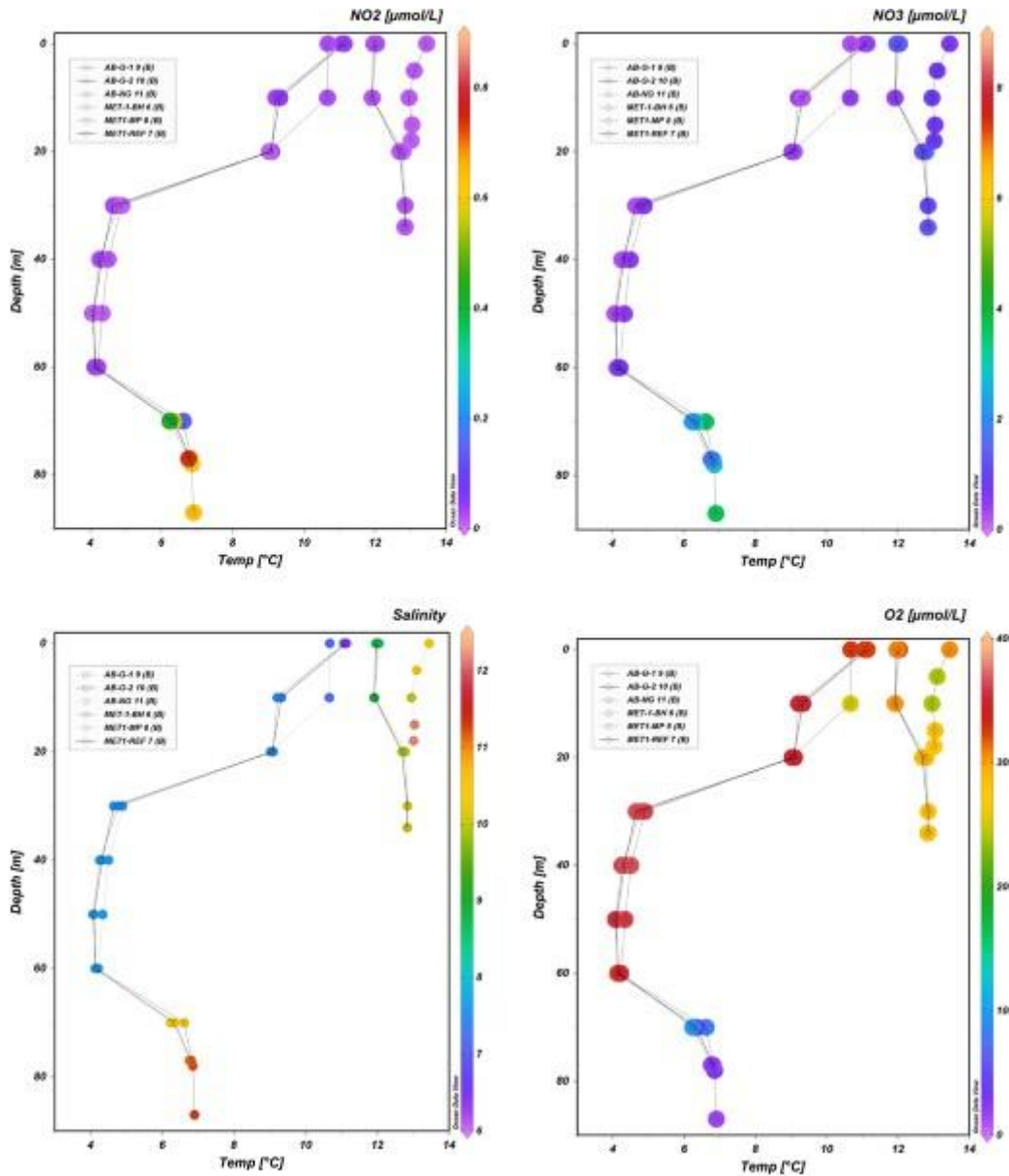


Figure 12: Temperature profile against salinity, oxygen, NO_3^- , and NO_2^- during cruise transect of SEA-EU at Arkona Basin and Gulf of Gdansk. **NOTE:** The color dots represents salinity, oxygen, NO_3^- , and NO_2^- , while the first three dots represents Arkona Basin and the last three dots represents Gulf of Gdansk.

The nitrite and nitrate concentrations were slightly higher at the depth and lower at the surface. As the water column depth increases, the concentration of NO_2^- and NO_3^- increased, and the temperature concentration decreased from the water surface to the depth. This shows that surface water was warmer and associated with exposure to sunlight.

The salinity result showed high salinity at higher depth and low at the surface. Salinity increased with depth due to factors such as evaporation and mixing of water masses, while temperature concentration was higher at the surface and decreased in the water column.

Oxygen concentration was higher at the water surface and decreased in the watercolumn, and surface water was warmer, indicating high temperature at the surfaceand lower temperature at depth.

6.0 Discussion

We conducted measurements of dissolved N_2O in two different regions of the southern Baltic Sea, (1) in the Eckernförde Bay (Boknis Eck time series site) and (2) during a cruise with a Polish research vessel at four stations in the Gulf of Gdansk, Arkona Basin, Mecklenburg Bay, and Eckernförde Bay. In this chapter, we discuss the results of measurements during both the Littorina cruises from 2019 to June 2023 to Boknis Eck time series site and the SEA-EU cruise in May 2022 in the context of seasonal variability, distribution pattern, and heatwave effects (at Boknis Eck).

6.1 Seasonal variability

The annual distribution of N_2O from year 2019 to 2023, between January to March N_2O concentration was higher in 2019 to 2022 from the surface to the depth (figure 3) although in 2023 N_2O concentration was higher in January and April from surface to depth. However, in 2022 the result shows higher concentrations of N_2O in all months of the year, which is almost homogenous from surface to depth. The concentration of N_2O was low from April to October in the year 2019 and 2020, in 2023 it was low in February, March, May and June. In 2021 the surface (1-10 m) N_2O concentration in summer was lower than deeper water (15-25 m). Nevertheless, the concentration of N_2O in the year 2021 was higher compared to the previous years.

From 2005 to 2017, there were remarkable depth and time-dependent variations in N₂O concentrations at the BE time-series station. With a range of 1.2 to 37.8 nmol L⁻¹, the average N₂O concentration was 13.9 nmol L⁻¹ (Ma et al., 2019). Although our N₂O concentrations data at Boknis Eck time series station from 2019 to 2023 range from 3.93-27.42 nmol L⁻¹ and the average N₂O concentration was 12.36 nmol L⁻¹ which almost similar with paper published by Ma et al., (2019). Given the low anthropogenic influence in the North Pacific Subtropical Gyre, this value was higher than results from surface water at the ALOHA station (5.9-7.4 nmol L⁻¹, average 6.5 ± 0.3 nmol L⁻¹; Wilson et al., 2017). Past N₂O concentrations at the BE were significantly below those at the time-series station in the nearshore upwelling region off Chile (2.9-492 nmol L⁻¹, averaging 39.4 ± 29.2 nmol L⁻¹ in the oxyclines and 37.6 ± 23.3 nmol L⁻¹ in bottom waters; Farías et al., 2015) and a quasi-time-series station off Goa (Naqvi et al., 2010), where significant N₂O depletion in deep waters during anoxic events was observed in both areas. Here, primary production in summer exerts a strong influence on biogeochemical cycles, and nitrification is thought to be inhibited by light in the well-lit surface water (Grundle and Juniper 2011). However, our N₂O data in some months were almost in agreement to the time series station from Saanchi Inlet (~0.5–37.4 nmol L⁻¹, average 14.7 nmol L⁻¹; Capelle et al., 2018) that showed significant temporal and depth dependent variability in the course of their time series. Our observed N₂O concentration in some months are in agreement with data of Wilson et al., (2017) which from 7.7 to 12.7 nmol L⁻¹. The oxygen data showed higher concentration at the surface water between January to March in 2019 to 2022, and it extended to April in 2023 (figure 4). It decreased at depth during spring and summer months. At depth of 20-25 m lowest oxygen concentration was recorded. In 2021 from January to March the oxygen concentration was homogeneous from surface through the water column. In general oxygen concentration is lowest at depth of 20-25 m during August to December. However, the study conducted by (Lennartz et al., 2014) showed a steady decline in oxygen concentration and oxygen saturation at a depth of 25 meters, the major oxygen decline occurred from April to September in range of 0.5 μmol L⁻¹ yr⁻¹ and 0.8 μmol L⁻¹ yr⁻¹ for summer months and trends that indicate potential environmental changes and challenges to oxygen concentrations in the aquatic environment. The spread of hypoxic and even anoxic zones in marine coastal ecosystems is known worldwide and is often linked to eutrophication (Diaz and Rosenberg, 2008). The Baltic Sea is affected by a large-scale oxygen decline (HELCOM, 2009), which has been observed since 2001.

Surface temperature was highest during the summer from July to October from 2019 to 2022, and in 2023 the surface temperature was highest from May to June (figure 7). In 2021, the summer was longer, and the water temperature

remained high until December. However, the temperature patterns at BE were well in line with the patterns in other Baltic Sea regions. The trend is positive and is 0.2 degrees Celsius every decade (Feistel et al., 2008) which is within the spectrum of earlier detected patterns. At the same time, the temperature in the bottom water did not rise as quickly as at the surface, which led to a significant overall increase in the density gradient in spring (Lennartz et al., 2014). Stratification therefore begins earlier in the year, which in turn can lead to less oxygenation.

The salinity was lower at the surface and increased with the depth. Our results show that salinity being highest during the winter seasons and remained higher at the depth of 20-25 meters' (figure 8). Hence, the results of the BACC team of authors (BACC, 2008). They reported no significant changes in salinity in the 20th century at numerous measuring stations (BACC, 2008). Salinity fluctuates in the short term between years due to large-scale advection (Lehmann et al., 2013).

The seasonal distribution of NO_3^- and NO_2^- from 2019 to 2023 is low to high from surface to the depth (figures 5 & 6). During the winter of 2020 to 2023 show higher concentration of the NO_3^- and NO_2^- respectively from surface to the depth. During summer the NO_3^- and NO_2^- concentrations were observed to be lowest at the surface water column. However, since the mid-1980s, major nutrient declines have been reported at the BE time-series station, but bottom O_2 concentrations have continued to decline over the past 60 years, according to Lennartz et al. (2014). According to Meier et al. (2018) and Lennartz et al. (2014), the extended stratification period at the BE time-series station and temperature-driven depletion of O_2 in bottom waters are two factors leading to the continued decline in oxygen.

The highly elevated N_2O concentrations may be located near regions where some of the lowest O_2 concentrations have been measured, usually the O_2 minimum zone. Oxygen being a major contributor to N_2O production, our result of measured N_2O concentrations at Boknis Eck between year 2019 to 2023 does not show clear significant of changing oxygen conditions so much (figures 3 & 4). In winter season between January to March of the all years' oxygen concentration was almost homogeneous from 1-20 m depth except in the year 2021 where oxygen concentration is homogeneous from surface to depth (figure 4). The N_2O concentrations at winter season were almost homogeneous and show no clear relationship with oxygen.

The detected N_2O concentrations in the surface waters of the shallow stations and in the harmonic water bodies were close to equilibrium, which can be attributed to the exchange with the surrounding atmosphere. N_2O

concentrations in winter waters were also close to equilibrium, although with higher absolute values than in the surface layer. Here, hydrographic factors were mainly responsible for the observed N_2O distribution. When N_2O concentrations were in equilibrium with the atmosphere during winter convection, this water mass was generated, and this signal was maintained during summer stratification of the uppermost layer (Walter et al., 2006).

6.2 Heatwave impact on N_2O

Figure 17 shows the anomalies of T and $\Delta\text{N}_2\text{O}$ at 1 and 25 m water depths from July 2005 to June 2023. A pronounced temperature anomaly is slightly visible at 1m depth in the year 2018, 2019 and 2021, which also reflects the heatwave that occurred in northwestern Europe in August 2018 (Kueh and Lin, 2020). The maximum $\Delta\text{N}_2\text{O}$ anomaly at 1 and 25 m depths is visible in November 2017 and thus not related to the heatwave signal of the temperature anomaly at either depth. The maximum temperature anomaly is found at 1 m water depth in 2018, 2019 and 2021. Also, the 2018, 2019 and 2021 heatwave signal is not visible in the $\Delta\text{N}_2\text{O}$ anomalies. However, our data show no significant relationship between water temperature anomalies and $\Delta\text{N}_2\text{O}$ at 1 and 25 m water depths in relation to the heatwave in higher N_2O production that is temperature dependent. As marine autotrophic and heterotrophic processes display sensitivities to temperature, ocean warming might result in changes of the bacterial community structure and hence in the changes of N_2O production. Changes in ocean temperature also affect the solubility of N_2O (Freing et al., 2012). Thus, the signal of the heatwave is not visible in the anomalies of $\Delta\text{N}_2\text{O}$. Generally, there is no relationship between the water temperature anomalies and $\Delta\text{N}_2\text{O}$ anomalies at both 1 and 25m depths. High temperature can facilitate microbial activities responsible for N_2O production. Increased temperature can accelerate the rates of denitrification and nitrification, resulting to higher N_2O production rates in certain oceanic regions (Poh et al., 2015). However, our data are not in agreement with a heatwave-induced increase in N_2O concentrations at Boknis Eck (Eckernförde Bay). Hence, our measurement of dissolved N_2O was conducted in a euphotic zone 1-25 m depth which is oxic water and has a clear relationship regarding N_2O production via nitrification.



Figure 17: Monthly anomalies of temperature ($\Delta(\Delta N_2O)$, blue line right y axis) and (ΔT , red line, left y axis) at 1 and 25 m from 2005 to 2023.

6.3 N₂O distribution pattern

We discuss vertical distribution of N₂O in the SEA-EU cruise conducted in May 2022. In order to identify the N₂O concentration in this transect, we group the sites into two groups due to their difference in depth. Eckernförde Bay and Mecklenburg Bay are plotted together which have bottom depths of up to 33 m, while Arkona Basin and Gulf of Gdansk are plotted together which have bottom depths up to 87 m. The N₂O concentration in the Eckernförde Bay and Mecklenburg Bay in the surface and water column were homogeneously distributed. The average dissolved N₂O concentrations in the surface water was approximately 14 nmol L⁻¹ and water column it was approximately 15 nmol L⁻¹ (figure 9). The N₂O concentrations in the Arkona Basin and Gulf of Gdansk were relatively homogeneous at the surface water and changes in the water column. The average dissolved N₂O concentrations in the surface water and the water column were approximately 9 nmol L⁻¹ and 18 nmol L⁻¹, respectively. Though the highest concentration of dissolved N₂O observed was between 27 and 54 nmol L⁻¹ in Gulf of Gdansk at a depth of 70-80 m (figure 10). However, the high concentration of dissolved N₂O at great depth where oxygen concentration declines could be as a result of stratification, sinking of organic particles. The sinking and decomposition of these particles were as a result of phytoplankton bloom and N₂O production below chlorophyll-rich layer, which coincided with the layer of minimum oxygen (Boontanon et al., 2010).

These vertical N₂O distributions are in agreement with the earlier studies of N₂O profiles from the central Baltic Sea (Rönner, 1983; Rönner and Sörensson, 1985; Brettar and Rheinheimer, 1992). However, they conducted their work both in oxic and anoxic conditions in the deep central Baltic Sea. When oxic conditions prevailed between August and September 1977, Rönner (1983) collected N₂O profiles in the central Baltic Sea immediately following a significant inflow event in 1976-1977 (Schinke and Matthäus, 1998). Moreover, these N₂O profiles are similar to our profiles, measured in the well oxygenated areas of the cruise transect in May 2022.

In the Baltic Sea, nitrification and denitrification are two biological processes that have been investigated in previous studies, both of which showed the presence of N₂O producing bacteria (Bauer, 2003; Brettar and Höfle, 1993; Brettar et al., 2001). Relationships between N₂O and oxygen or nitrate are commonly used to determine both processes (Yoshinari, 1976; Yoshida et al., 1989; Cohen and Gordon, 1978; Butler et al., 1989).

Our data in the SEA-EU cruise (table 3) showed slight significant relationship between N₂O and oxygen or nitrate that N₂O production could be as a result of denitrification and sinking of organic particles at the sediment.

Depth (m)	Mean N ₂ O (nmol L ⁻¹)	Std dev (nmol L ⁻¹)	Mean O ₂ (umol L ⁻¹)	Std dev (umol L ⁻¹)	NO ₃ ⁻ umol L ⁻¹
0	14.79	0.55	295.12	2.51	1.18
5	15.08	0.24	296.76	0.07	0.81
10	16.28	0.10	295.75	0.18	2.08
15	18.41	0.81	289.44	1.26	4.20
20	19.51	0.72	247.90	2.03	6.82
22	17.00	1.39	204.59	1.17	4.51
0	14.80	1.37	279.79	0.59	1.48
5	15.33	0.26	299.73	0.40	1.21
10	13.97	5.24	296.71	0.17	1.91
15	18.03	0.20	292.09	1.00	5.43
20	19.57	0.68	251.33	1.93	8.89
22	15.59	1.61	182.49	2.02	7.88
0	15.05	1.05	247.53	0.59	1.76
5	15.53	0.68	289.56	0.40	1.12
10	14.07	2.08	289.56	0.18	1.91
15	15.04	1.04	288.31	0.11	3.01
21	18.90	1.43	211.32	3.59	5.95
0	14.24	1.32	295.43	1.55	1.76
5	14.70	1.24	208.63	0.41	1.82
10	13.42	0.91	287.68	0.72	1.80
15	15.17	0.56	288.28	0.07	3.42
21	15.90	0.51	212.01	2.95	5.61
0	13.42	0.63	288.45	1.03	1.35
5	13.53	0.40	284.67	0.50	1.03
10	14.27	0.33	283.31	0.18	1.25
15	15.65	0.33	281.79	0.10	2.69
19	14.78	0.32	257.66	0.23	3.21

Table 3: SEA-EU cruise EBG and MBG N₂O, O₂ and NO₃⁻ mean concentrations and standard deviations. **NOTE:** the first two rows represent Eckernförde Bay and the last three rows represent Mecklenburg Bay.

6.4 N₂O saturation

Dissolved N₂O can be either saturated, undersaturated, or supersaturated in the study area. The N₂O saturation data recorded in this study area (Boknis Eck and the SEA-EU cruise) provide information on possible sources, accumulation, and sinks of N₂O. Saturation data are considered to be in equilibrium when the value in seawater is 100%, while undersaturation has a value less than 100% and supersaturation has a value greater than 100%. More than 99.90% of the

recorded data for the two measurements campaigns (Boknis Eck and SEA-EU cruise) are oversaturated in line with N_2O concentrations, and the saturation increases with increasing measured N_2O concentration. N_2O saturation at Boknis Eck is highly oversaturated with highest value of 355% (figure 14), with few data points being undersaturated with lowest value of 50% and mean value of 155%, while N_2O saturation during the cruise transect were highly oversaturated with highest value of 594% (figure 14), with three data points being undersaturated with values of 94 and 97% and mean value of 166% which is contrary with some past studies that have found undersaturation of N_2O in surface waters of the Southern Ocean (Zahn et al., 2015; Chen et al., 2014; Rees et al., 1997), although (Zahn et al., 2017) found supersaturation in surface waters. However, Zahn et al., (2015) stated that undersaturation of water at the surface led to dilution of N_2O by melting sea ice, while Zhan and Chen (2009) linked it to the influence of stratification brought on by sea ice melting. We observed highest N_2O saturation at latitude $54.6^\circ S$ between 78-87m, while the lowest was observed at latitude $54.7^\circ S$ between 18-34m. In addition, stratification in the Southern Ocean has been seen to impede the circulation of gases between surface and deep waters throughout the summer (Chen et al., 2014; Gibson and Trull, 1999; Smith and Dong, 1984). Our data for both surface to water column measurements for N_2O saturation were plotted against temperature and salinity as shown in (figures 15 & 16), although previous studies have recorded significant relationships between N_2O saturation, temperature and salinity in the Antarctic ocean as a result of melting sea ice in the summer season (Zhan et al., 2015b; Zhan and Chen 2009). However, we recorded r^2 values 0.1436 and 0.0689 and there is no relationship between N_2O saturation and temperature for the both cruises. The relationship between N_2O saturation and salinity were almost similar to temperature (figure 16), although the correlation decreased in the Boknis Eck time series station and increased in the SEA EU cruise ($r^2= 0.0364$ and 0.1799) respectively. Therefore, temperature and salinity have no significant effect on the N_2O saturation in these study areas.

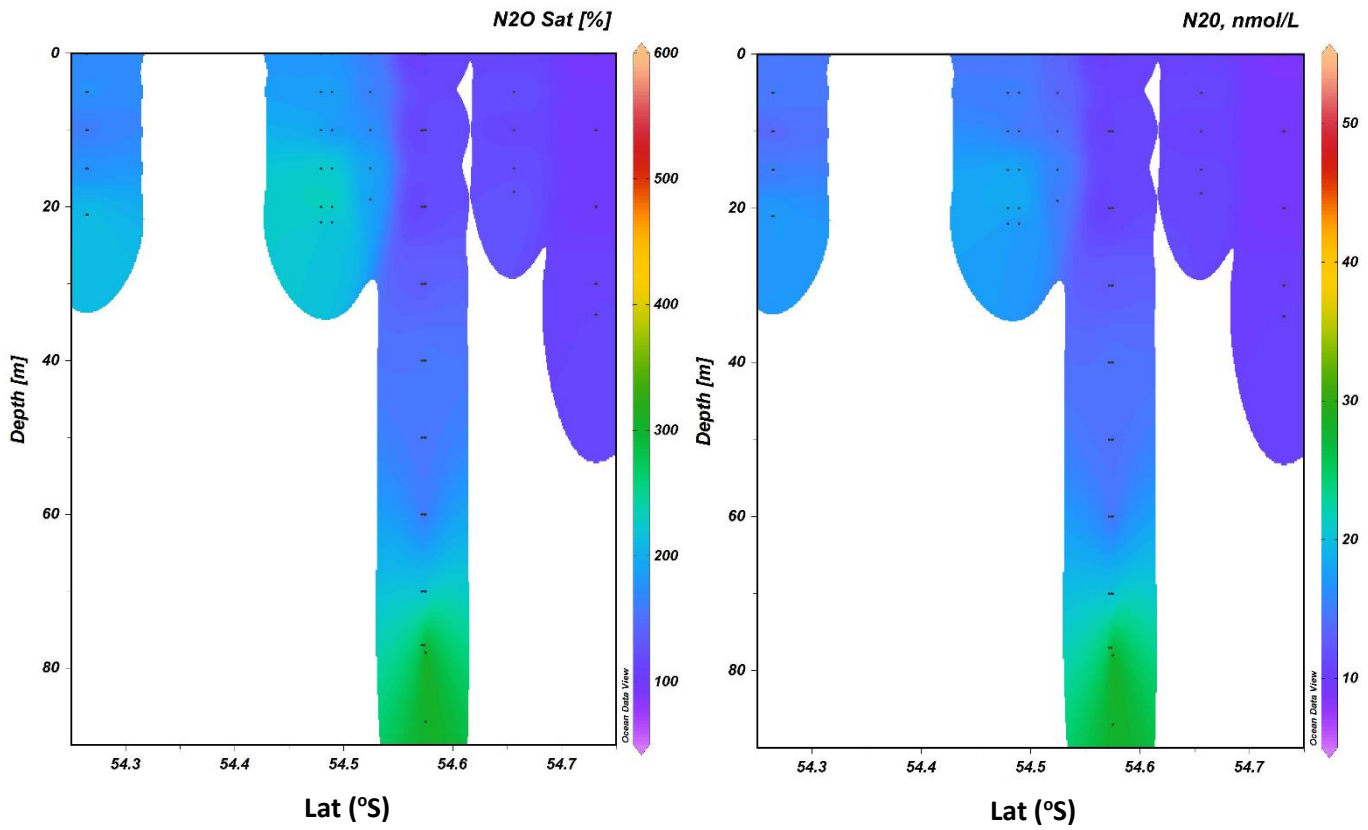
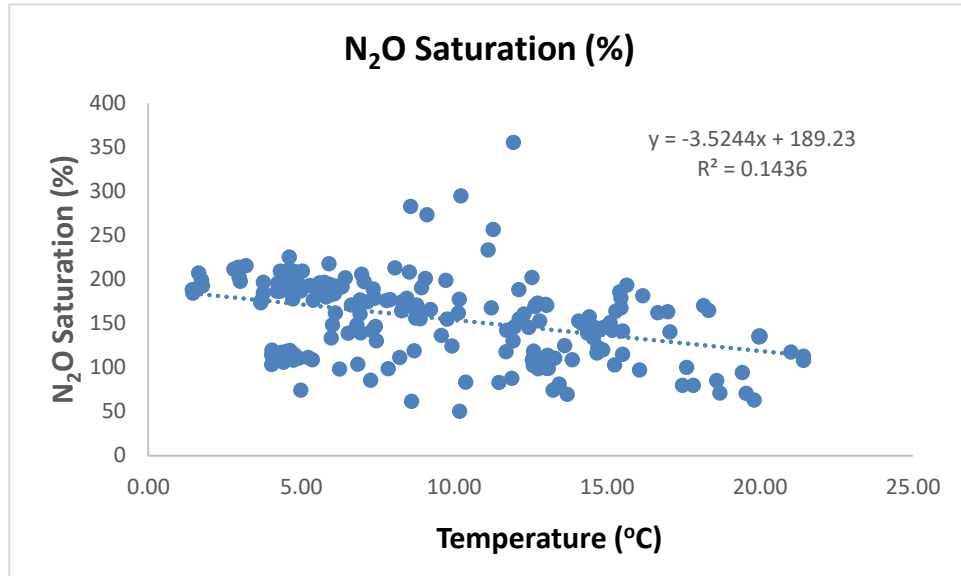


Figure 14: Distribution pattern of N₂O saturation and N₂O concentration during the cruise transect of SEA-EU at Arkona Basin, Gulf of Gdansk, Eckernförde Bay, and Mecklenburg Bay. **NOTE:** More than 90.90% of the observed data are undersaturated.

Boknis Eck



SEA-EU cruise

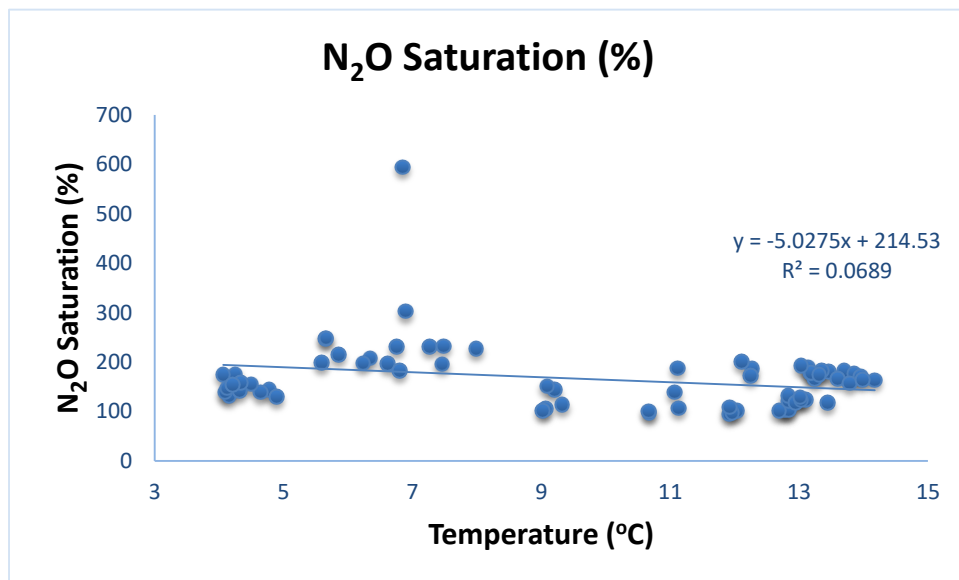


Figure 15: Correlation between N₂O saturation and temperature at Boknis Eck time series within year 2019 to 2022 and cruise transect in May 2022.

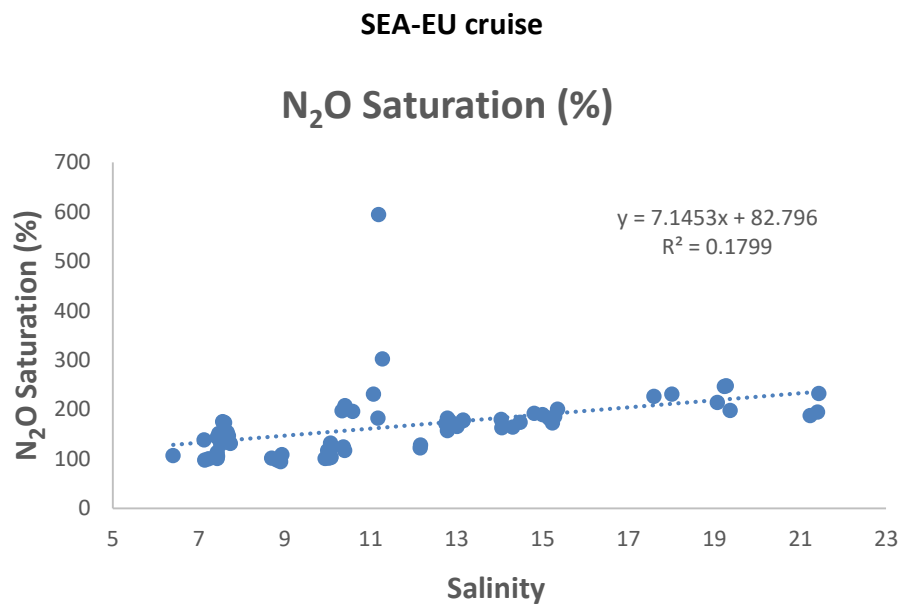
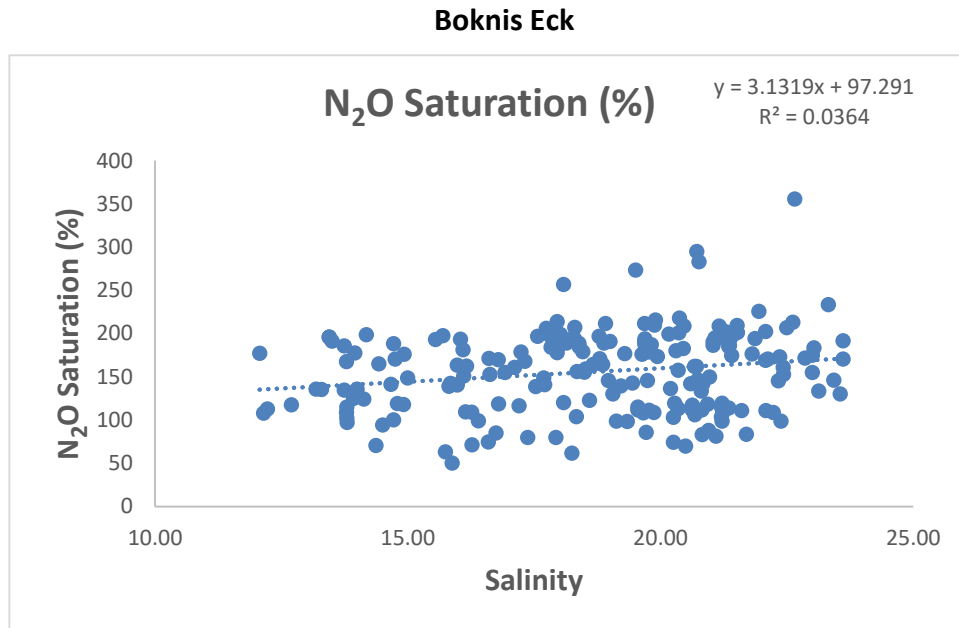


Figure 16: Correlation between N₂O saturation and salinity at Boknis Eck time series within year 2019 to 2022 and cruise transect in May 2022.

6.5 N₂O production

Due to the strong assumption that denitrification is inhibited by high ambient dissolved oxygen (DO) concentrations and nitrification is inhibited by light (Horrigan et al., 1981; Olson, 1981), research on biological N₂O formation in the area known as euphotic has been less significant. However, recent reports of active nitrification and N₂O generation in sunlit oceans around the world (Ji and Ward, 2017; Shiozaki et al., 2016; Wan et al., 2018) highlight the need to examine the source of N₂O in the euphotic zone.

The source of N₂O in the ocean is frequently investigated using a linear regression analysis between N₂O, AOU, and NO₃⁻ (Wan et al., 2022). According to numerous studies (Cohen and Gordon, 1979; de la Paz et al., 2017; De Wilde and Helder, 1997; Freing et al., 2009; Nevison et al., 1995, 2003; Tseng et al., 2016; Walter et al., 2006; Yoshinari, 1976), there is a significant positive linear correlation between N₂O and AOU away from oxygen minimum zones. This correlation is typically seen as proof that N₂O is produced through nitrification, an essential aerobic process that changes NH₄⁺ to NO₃⁻ (Wan et al., 2022). However, regarding with these studies, significant correlation was not observed in our study between $\Delta N_2O / AOU$ in the Eckernförde Bay and the correlation increases in the cruise transect and the r^2 values of 0.008 and 0.3948 for the both cruises (figure 18), although not totally in agreement with the paper published by Rees et al., (1997) where they recorded a significant relationship between $\Delta N_2O / AOU$ in the Southern Ocean whereas our data in Eckernförde Bay are not in agreement with the paper published by Rees et al., (1997). Therefore, we suggest that nitrification may not be major N₂O production mechanism in Eckernförde Bay though our data in the cruise transect show that nitrification contributed in the N₂O production. However, the main N₂O production mechanism is either nitrification or denitrification process, although our data were collected not in a very deep water. The maximum depth in our study is 87 m at the Gulf of Gdansk and these studies shows results beyond 100m.

The horizontal and vertical variations in $\Delta N_2O / AOU$ have been explained by a number of theories, including variations in N₂O production mechanisms (De Wilde and Helder, 1997; Law and Owens, 1990), the effects of mixing and circulation (de la Paz et al., 2017; Nevison et al., 2003), changing N₂O results during nitrification at various ambient dissolved oxygen (DO) concentrations (Capelle et al., 2018; Nevison et al., 2003) and the possible impact of pressure and temperature on N₂O emission (Freing et al., 2009; Walter et al., 2006). Most microbial metabolisms accelerate with temperature, therefore both N₂O

formation and O_2 utilization are temperature-dependent (Nevison et al., 2003). However, it is questionable how temperature affects ΔN_2O /AOU overall. It is suggested that the overall reduction in temperature with depth causes a decrease in N_2O production and O_2 utilization however not for the ΔN_2O /AOU ratio considering both of these processes are influenced by the aerobic organic remineralization process when the ambient DO is adequate (Freing et al., 2009; Walter et al., 2006).

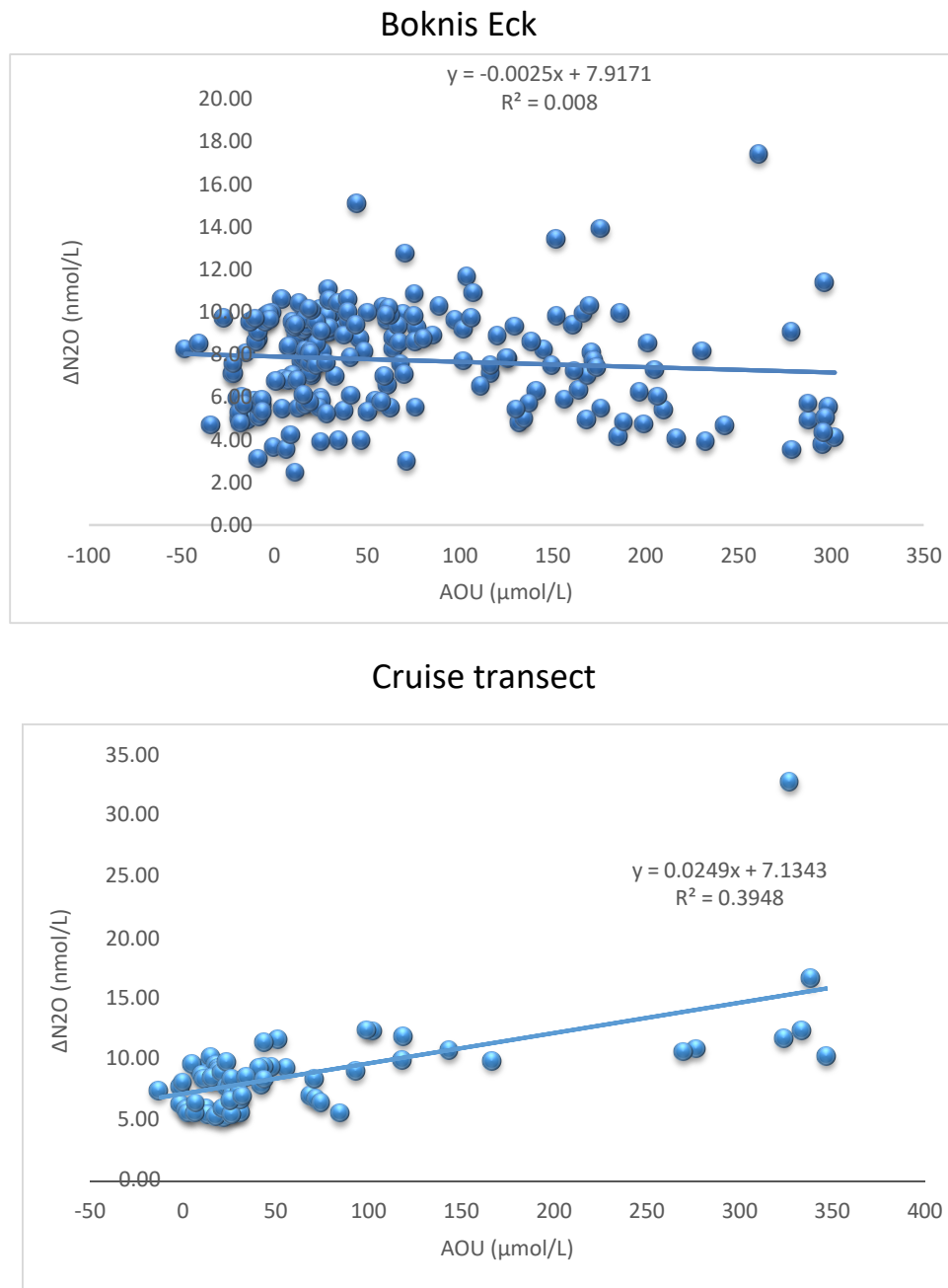


Figure 18: Relationship between ΔN_2O and AOU at Boknis Eck time series between year 2019 to 2022 and the SEA-EU cruise transect in May 2022.

7.0 Conclusion

In order to determine temporal and spatial variability of dissolved N_2O . N_2O concentrations were measured with the static head- space method for the both cruises (Boknis Eck time series and SEA-EU cruise transect) between year 2019 to 2023 for the Boknis Eck time series and May 2022 for SEA-EU cruise transect. Our measurements showed almost homogeneous N_2O concentrations at winter period throughout the water column for all the years and in summer the concentration changed at surface with lower N_2O concentrations and higher concentrations at the bottom at Boknis Eck time series this could be as a result of stratification of the water column.

In 2018, there was a pronounced heatwave that increased water temperature in the Baltic and North Seas. This was assumed to improve the N_2O production through denitrification by sinking of organic particles. However, we found no significant relationship between water temperature and excess N_2O in both surface and water column at Boknis Eck.

The N_2O saturation for the both cruises were oversaturated in the surface layer and in the water column. We found no significant relationship between temperature, salinity and N_2O saturation.

There is no clear relationship between excess N_2O and apparent oxygen utilization at Boknis Eck time series, though we found slight relationship between excess N_2O and apparent oxygen utilization at SEA-EU cruise transect which is in partial agreement with the paper published by Rees et al., (1997) in Southern Ocean.

Therefore, we suggest that nitrification may not be a major N_2O production mechanism in Eckernförde Bay though our data in the cruise transect show that nitrification contributed in the N_2O production. However, the main N_2O production mechanism could be nitrification or denitrification process.

8.0 References

- Arévalo-Martínez, D. L., Kock, A., Steinhoff, T., Brandt, P., Dengler, M., Fischer, T., ... & Bange, H. W. (2017). Nitrous oxide during the onset of the Atlantic cold tongue. *Journal of Geophysical Research: Oceans*, *122*(1), 171-184.
- BACC: Assessment of Climate Change for the Baltic Sea Basin, Springer, 2008.
- Bange, H. W., Dahlke, S., Ramesh, R., Meyer-Reil, L. A., Rapsomanikis, S., & Andreae, M. O. (1998). Seasonal study of methane and nitrous oxide in the coastal waters of the southern Baltic Sea. *Estuarine, Coastal and Shelf Science*, *47*(6), 807-817.
- Bange, H. W., & Andreae, M. O. (1999). Nitrous oxide in the deep waters of the world's oceans. *Global biogeochemical cycles*, *13*(4), 1127-1135.
- Bange, H. W., Rapsomanikis, S., & Andreae, M. O. (2001). Nitrous oxide cycling in the Arabian Sea. *Journal of Geophysical Research: Oceans*, *106*(C1), 1053-1065.
- Bange, H. W. (2006). Nitrous oxide and methane in European coastal waters. *Estuarine, Coastal and Shelf Science*, *70*(3), 361-374.
- Bauer, S. (2003). *Structure and function of nitrifying bacterial communities in the eastern Gotland basin (central Baltic Sea)*.
- Beman, J. M., Leilei Shih, J., & Popp, B. N. (2013). Nitrite oxidation in the upper water column and oxygen minimum zone of the eastern tropical North Pacific Ocean. *The ISME journal*, *7*(11), 2192-2205.
- Boontanon, N., Watanabe, S., Odate, T., & Yoshida, N. (2010). Production and consumption mechanisms of N₂O in the Southern Ocean revealed from its isotopomer ratios. *Biogeosciences Discussions*, *7*(5), 7821-7848.
- Breitburg, D., Levin, L. A., Oschlies, A., Grégoire, M., Chavez, F. P., Conley, D. J., ... & Zhang, J. (2018). Declining oxygen in the global ocean and coastal waters. *Science*, *359*(6371), eaam7240.

Brettar, I., & Höfle, M. G. (1993). Nitrous oxide producing heterotrophic bacteria from the water column of the central Baltic: abundance and molecular identification. *Marine Ecology Progress Series*, 253-265.

Brettar, I., Moore, E. R. B., & Höfle, M. G. (2001). Phylogeny and abundance of novel denitrifying bacteria isolated from the water column of the central Baltic Sea. *Microbial ecology*, 42, 295-305.

Butler, J.H., J.W. Elkins, T.M. Thompson, and K.B. Egan, Tropospheric and dissolved N₂O of the west Pacific and east Indian Oceans during the E1 Nifio Southern Oscillation Event of 1987, d. *Geophys. Res.*, 94, 14,865-14,877, 1989.

Butler, J. H., & Montzka, S. A. (2016). The NOAA annual greenhouse gas index (AGGI). *NOAA Earth System Research Laboratory*, 58, 55-75.

Capelle, D. W., Hawley, A. K., Hallam, S. J., and Tortell, P. D.: A multi-year time-series of N₂O dynamics in a seasonally anoxic fjord: Saanich Inlet, British Columbia, *Limnol. Oceanogr.*, 63, 524–539, <https://doi.org/10.1002/lno.10645>, 2018.

Capone, D. G., Bronk, D. A., Mulholland, M. R., & Carpenter, E. J. (Eds.). (2008). *Nitrogen in the marine environment*. Elsevier.

Carstensen, J., Andersen, J. H., Gustafsson, B. G., & Conley, D. J. (2014). Deoxygenation of the Baltic Sea during the last century. *Proceedings of the National Academy of Sciences*, 111(15), 5628-5633.

Chen, L., Zhang, J., Zhan, L., Li, Y., & Sun, H. (2014). Differences in nitrous oxide distribution patterns between the Bering Sea basin and Indian Sector of the Southern Ocean. *Acta Oceanologica Sinica*, 33, 9-19. Chiriaco, M., Bastin, S., Yiou, P., Haeffelin, M., Dupont, J. C., & Stéfanon,

M. (2014). European heatwave in July 2006: Observations and modeling showing how local processes amplify conducive large-scale conditions. *Geophysical Research Letters*, 41(15), 5644-5652.

- Cicerone, R. J. (1989). Analysis of sources and sinks of atmospheric nitrous oxide (N_2O). *Journal of Geophysical Research: Atmospheres*, 94(D15), 18265-18271.
- Codispoti, L. A., Yoshinari, T., and Devol, A. H.: Suboxic respiration in the oceanic water column, in: *Respiration in aquatic ecosystems*, edited by: del Giorgio, P. A. and Williams, P. J., Oxford Univ. Press, New York, 225–247, 2005.
- Codispoti, L. A., Elkins, J. W., Yoshinari, T., Fredrich, G., Sakamoto, C., and Packard, T.: On the nitrous oxide flux from productive regions that contain low oxygen waters, in: *Oceanography of the Indian Ocean*, edited by: Desai, B. N., Oxford Univ. Press, New York, 271–284, 1992.
- Codispoti, L. A., Brandes, J., Christensen, J. P., Devol, A. H., Naqvi, S. W.A., Paerl, H., & Yoshinari, T. (2001). The oceanic fixed nitrogen and nitrousoxide budgets: Moving targets as we enter the anthropocene?. *Scientia Marina*, 65(S2), 85-105.
- Cohen, Y., & Gordon, L. I. (1978). Nitrous oxide in the oxygen minimum of the eastern tropical North Pacific: Evidence for its consumption during denitrification and possible mechanisms for its production. *Deep Sea Research*, 25(6), 509-524
- Cohen, Y., & Gordon, L. I. (1979). Nitrous oxide production in the ocean. *Journal of Geophysical Research: Oceans*, 84(C1), 347-353.
- Cornejo, M., Murillo, A. A., & Farías, L. (2015). An unaccounted for N_2O sink in the surface water of the eastern subtropical South Pacific: Physical versus biological mechanisms. *Progress in Oceanography*, 137, 12-23.
- Craig, H., & Gordon, L. I. (1963). Nitrous oxide in the ocean and the marine atmosphere. *Geochimica et Cosmochimica Acta*, 27(9), 949-955.
- Crutzen, P. J., & Schmailzl, U. (1983). Chemical budgets of the stratosphere. *Planetary and Space Science*, 31(9), 1009-1032.
- de la Paz, M., García-Ibáñez, M. I., Steinfeldt, R., Ríos, A. F., & Pérez, F. F. (2017). Ventilation versus biology: What is the controlling mechanism of nitrous oxide distribution in the North Atlantic?. *Global Biogeochemical Cycles*, 31(4), 745-760.
- De Wilde, H. P., & Helder, W. (1997). Nitrous oxide in the Somali Basin: the role

of upwelling. *Deep Sea Research Part II: Topical Studies in Oceanography*, 44(6-7), 1319-1340.

Diaz, R. J., & Rosenberg, R. (2008). Spreading dead zones and consequences for marine ecosystems. *science*, 321(5891), 926-929.

Ducklow, H. W., Doney, S. C., & Steinberg, D. K. (2009). Contributions of long-term research and time-series observations to marine ecology and biogeochemistry. *Annual Review of Marine Science*, 1, 279-302.

Etheridge, D. M., Steele, L. P., Langenfelds, R. L., Francey, R. J., Barnola, J. M., & Morgan, V. I. (1996). Natural and anthropogenic changes in atmospheric CO₂ over the last 1000 years from air in Antarctic ice and firn. *Journal of Geophysical Research: Atmospheres*, 101(D2), 4115- 4128.

Farías, L., Faúndez, J., Fernández, C., Cornejo, M., Sanhueza, S., and Carrasco, C.: Biological N₂O fixation in the Eastern South Pacific Ocean and marine cyanobacterial cultures, *Plos One*, 8, e63956, <https://doi.org/10.1371/journal.pone.0063956>, 2013.

Farías, L., Besoain, V., and García-Loyola, S.: Presence of nitrous oxide hotspots in the coastal upwelling area off central Chile: an analysis of temporal variability based on ten years of a biogeochemical time series, *Environ. Res. Lett.*, 10, 044017, <https://doi.org/10.1088/1748-9326/10/4/044017>, 2015.

Fenwick, L., Capelle, D., Damm, E., Zimmermann, S., Williams, W. J., Vagle, S., & Tortell, P. D. (2017). Methane and nitrous oxide distributions across the North American Arctic Ocean during summer, 2015. *Journal of Geophysical Research: Oceans*, 122(1), 390-412.

Force, A. (2019). Baltic Sea. *General relativity*.

Freing, A., Wallace, D. W., Tanhua, T., Walter, S., & Bange, H. W. (2009). North Atlantic production of nitrous oxide in the context of changing atmospheric levels. *Global biogeochemical cycles*, 23(4).

Freing, A., Wallace, D. W., & Bange, H. W. (2012). Global oceanic production of nitrous oxide. *Philosophical Transactions of the Royal Society B: Biological*

Sciences, 367(1593), 1245-1255.

Frey, C., Bange, H. W., Achterberg, E. P., Jayakumar, A., Löscher, C. R., Arévalo-Martínez, D. L., León-Palmero, E., Sun, M., Sun, X., Xie, R. C., Oleynik, S., and Ward, B. B (2020). Regulation of nitrous oxide production in low-oxygen waters off the coast of Peru. *Biogeosciences*, 17(8), 2263-2287.

Gibson, J. A., & Trull, T. W. (1999). Annual cycle of fCO₂ under sea-ice and in open water in Prydz Bay, East Antarctica. *Marine Chemistry*, 66(3-4), 187-200.

Gindorf, S., Bange, H. W., Booge, D., & Kock, A. (2022). Seasonal study of the small-scale variability in dissolved methane in the western Kiel Bight (Baltic Sea) during the European heatwave in 2018. *Biogeosciences*, 19(20), 4993-5006.

Goreau, T. J., Kaplan, W. A., Wofsy, S. C., McElroy, M. B., Valois, F. W., and Watson, S. W.: Production of and N₂O by nitrifying bacteria at reduced concentrations of oxygen, *Appl. Environ. Microb.*, 40,526–532, 1980.

Grundle, D. S., & Juniper, S. K. (2011). Nitrification from the lower euphotic zone to the sub-oxic waters of a highly productive British Columbia fjord. *Marine Chemistry*, 126(1-4), 173-181.

Hahn, J. (1974). The North Atlantic Ocean as a source of atmospheric N₂O. *Tellus*, 26(1-2), 160-168.

Heino, M., & Dieckmann, U. (2008). Detecting fisheries-induced life-history evolution: an overview of the reaction-norm approach. *Bulletin of Marine Science*, 83(1), 69-93.

HELCOM: Eutrophication in the Baltic Sea – an integrated assessment of the effects of nutrient enrichment in the Baltic Sea region, *Baltic Sea Environ. Proc.*, 115, 1–145, 2009.

Horrigan, S.G., Carlucci, A. F., & Williams, P. M. (1981). Light inhibition of nitrification in sea-surface films.

Jain, A. K., Briegleb, B. P., Minschwaner, K., & Wuebbles, D. J. (2000). Radiative forcing and global warming potentials of 39 greenhouse gases. *Journal of Geophysical Research: Atmospheres*, *105*(D16), 20773-20790.

Ji, Q., & Ward, B. B. (2017). Nitrous oxide production in surface waters of the mid-latitude North Atlantic Ocean. *Journal of Geophysical Research: Oceans*, *122*(3), 2612-2621.

Junge, C., & Hahn, J. (1971). N₂O measurements in the North Atlantic. *Journal of Geophysical Research*, *76*(33), 8143-8146.

Khalil, M. A. K., & Rasmussen, R. A. (1992). The global sources of nitrous oxide. *Journal of geophysical research: atmospheres*, *97*(D13), 14651- 14660.

Ko, M. K., Sze, N. D., & Weisenstein, D.K. (1991). Use of satellite data to constrain the model-calculated atmospheric lifetime for N₂O: Implications for other trace gases. *Journal of Geophysical Research: Atmospheres*, *96*(D4), 7547-7552.

Kueh, M. T., & Lin, C.Y. (2020). The 2018 summer heatwaves over northwestern Europe and its extended-range prediction. *Scientific reports*, *10*(1), 19283.

Matthäus, W., Nehring, D., Feistel, R., Nausch, G., Mohrholz, V., & Lass, H. U. (2008). The inflow of highly saline water into the Baltic Sea. *State and Evolution of the Baltic Sea, 1952–2005: A Detailed 50-Year Survey of Meteorology and Climate, Physics, Chemistry, Biology, and Marine Environment*, 265-309.

Law, C.S., and N.J.P. Owens, Significant flux of atmospheric nitrous oxide from the northwest Indian Ocean, *Nature*, *346*, 826-828, 1990.

Lennartz, S. T., Lehmann, A., Herrford, J., Malien, F., Hansen, H. P., Biester, H., and Bange, H. W.: Long-term trends at the Boknis Eck time series station (Baltic Sea), 1957–2013: does climate change counteract the decline in eutrophication?, *Biogeosciences*, *11*, 6323–6339, <https://doi.org/10.5194/bg-11-6323-2014>, 2014.

Lilley, M.D., M.A. de Angelis, and L.I. Gordon, CH₄, H₂, CO, N₂O in submarine

hydrothermal vent waters, *Nature*, 300, 48-50, 1982.

Löscher, C. R., Kock, A., Könneke, M., LaRoche, J., Bange, H. W., & Schmitz, R. A. (2012). Production of oceanic nitrous oxide by ammonia-oxidizing archaea. *Biogeosciences*, 9(7), 2419-2429.

Ma, X., Lennartz, S. T., & Bange, H. W. (2019). A multi-year observation of nitrous oxide at the Boknis Eck Time Series Station in the Eckernförde Bay (southwestern Baltic Sea). *Biogeosciences*, 16(20), 4097-4111.

Ma, X. (2020). From coastal waters to the open ocean: the variability and emissions of methane and nitrous oxide (Doctoral dissertation, Christian-Albrechts-Universität zu Kiel).

Martens-Habbena, W., Berube, P. M., Urakawa, H., de La Torre, J. R., & Stahl, D.A. (2009). Ammonia oxidation kinetics determine niche separation of nitrifying Archaea and Bacteria. *Nature*, 461(7266), 976- 979.

Meier, H.M., Väli, G., Naumann, M., Eilola, K., and Frauen, C.: Recently accelerated oxygen consumption rates amplify deoxygenation in the Baltic Sea, *J. Geophys. Res.-Ocean.*, 123, 3227–3240, <https://doi.org/10.1029/2017JC013686>, 2018.

Minschwaner, K. (1993). Absorption of solar radiation by O₂: Implications for O₃ and lifetimes of N₂O, CFC13, and CF₂C12. *Journal of Geophysical Research*, 98(10), 543.

Myhre, G., Shindell, D., Bréon, F. M., Collins, W., Fuglestedt, J., Huang, J., ... & Midgley, P. (2013). The Physical Science Basis. Contribution of Working Group I to the Fifth Assessment Report of the Intergovernmental Panel on Climate Change: Anthropogenic and Natural Radiative Forcing. *Climate Change. Cambridge University Press, Cambridge, United Kingdom and New York*, 659-740.

Naqvi, S.W.A., and R.J. Noronha, Nitrous oxide in the Arabian Sea, *Deep Sea Res., Part A*, 38, 871-890, 1991.

Naqvi, S. W. A., Jayakumar, D. A., Narvekar, P. V., Naik, H., Sarma, V. V.

S. S., D'souza, W., ... & George, M. D. (2000). Increased marine production of N₂O

due to intensifying anoxia on the Indian continental shelf. *Nature*, 408(6810), 346-349.

Nevison, C. D., Weiss, R. F., & Erickson III, D. J. (1995). Global oceanic emissions of nitrous oxide. *Journal of Geophysical Research: Oceans*, 100(C8), 15809-15820.

Nevison, C., Butler, J. H., & Elkins, J. W. (2003). Global distribution of N₂O and the Δ N₂O-AOU yield in the subsurface ocean. *Global Biogeochemical Cycles*, 17(4).

Olson, R. J. (1981). Differential photo inhibition of marine nitrifying bacteria: a possible mechanism for the formation of the primary nitrite maximum.

Orsi, T. H., Werner, F., Milkert, D., Anderson, A. L., & Bryant, W. R. (1996). Environmental overview of Eckernförde bay, northern Germany. *Geo-Marine Letters*, 16, 140-147.

Pajares, S., & Ramos, R. (2019). Processes and microorganisms involved in the marine nitrogen cycle: knowledge and gaps. *Frontiers in Marine Science*, 6, 739.

Poh, L. S., Jiang, X., Zhang, Z., Liu, Y., Ng, W. J., & Zhou, Y. (2015). N₂O accumulation from denitrification under different temperatures. *Applied microbiology and biotechnology*, 99, 9215-9226.

Prinn, R., Cunnold, D., Rasmussen, R., Simmonds, P., Alyea, F., Crawford, A., ... & Rosen, R. (1990). Atmospheric emissions and trends of nitrous oxide deduced from 10 years of ALE-GAGE data. *Journal of Geophysical Research: Atmospheres*, 95(D11), 18369-18385.

Rabalais, N. N., Cai, W. J., Carstensen, J., Conley, D. J., Fry, B., Hu, X., ... & Zhang, J. (2014). Eutrophication-driven deoxygenation in the coastal ocean. *Oceanography*, 27(1), 172-183.

Ravishankara, A. R., Daniel, J. S., & Portmann, R. W. (2009). Nitrous oxide (N₂O): the dominant ozone-depleting substance emitted in the 21st century. *science*, 326(5949), 123-125.

Rees, A. P., Owens, N. J. P., & Upstill-Goddard, R. C. (1997). Nitrous oxide in the Bellingshausen sea and drake passage. *Journal of Geophysical Research: Oceans*, *102*(C2), 3383-3391.

Rönner, U. (1983). Distribution, production and consumption of nitrous oxide in the Baltic Sea. *Geochimica et Cosmochimica Acta*, *47*(12), 2179-2188.

Schinke, H., & Matthäus, W. (1998). On the causes of major Baltic inflows—an analysis of long time series. *Continental Shelf Research*, *18*(1), 67-97.

Seitzinger, S.P., Denitrification in aquatic sediments, in Denitrification in Soil and Sediment, edited by N.P. Revsbech and J. S6rensen, pp. 301-321, Plenum, New York, 1990.

Seitzinger, S. P., & Kroeze, C. (1998). Global distribution of nitrous oxide production and N inputs in freshwater and coastal marine ecosystems. *Global biogeochemical cycles*, *12*(1), 93-113.

Shiozaki, T., Ijichi, M., Isobe, K., Hashihama, F., Nakamura, K. I., Ehama, M., ... & Furuya, K. (2016). Nitrification and its influence on biogeochemical cycles from the equatorial Pacific to the Arctic Ocean. *The ISME journal*, *10*(9), 2184-2197.

Sloss, L L, Hjalmarsson, A -K, Soud, H N, Campbell, L M, Stone, D K, Shareef, G S, Emmel, T, Maibodi, M, Livengood, C D, and Markussen, J. (1992). Nitrogen oxides control technology fact book. United States: N. p., 1992. Web.

Smetacek, V., von Bodungen, B., von Brockel, K., Knoppers, B., Martens, P., Peinert, R., ... & Zeitzschel, B. (1987). Seasonality of plankton growth and sedimentation. *Seawater—Sediment Interactions in Coastal Waters*. Springer, Berlin, 34-56.

Smith, N. R., Zhaoqian, D., Kerry, K. R., & Wright, S. (1984). Water masses and circulation in the region of Prydz Bay, Antarctica. *Deep Sea Research Part A. Oceanographic Research Papers*, *31*(9), 1121-1147.

Sohm, J. A., Webb, E. A., & Capone, D. G. (2011). Emerging patterns of marine nitrogen fixation. *Nature Reviews Microbiology*, *9*(7), 499-508.

Stanley, R. H., Doney, S. C., Jenkins, W. J., & Lott III, D. E. (2012). Apparent oxygen utilization rates calculated from tritium and helium-3 profiles at the Bermuda Atlantic Time-series Study site. *Biogeosciences*, 9(6), 1969-1983.

Stein, L. Y. and Yung, Y. L.: Production, isotopic composition, and atmospheric fate of biologically produced nitrous oxide, *Annu. Rev. Earth Planet. Sci.*, 31, 329–356, 2003.

Stocker, T. (Ed.). (2014). *Climate change 2013: the physical science basis: Working Group I contribution to the Fifth assessment report of the Intergovernmental Panel on Climate Change*. Cambridge university press.

Sun, X., Kop, L. F., Lau, M. C., Frank, J., Jayakumar, A., Lücker, S., & Ward, B. B. (2019). Uncultured Nitrospina-like species are major nitrite oxidizing bacteria in oxygen minimum zones. *The ISME Journal*, 13(10), 2391-2402.

Tarendash, Albert S. (2001). *Let's review: chemistry, the physical setting* (3rd ed.). Barron's Educational Series. p. 44. ISBN 978-0-7641-1664-3.

Tian, H., Chen, G., Lu, C., Xu, X., Ren, W., Zhang, B., ... & Wofsy, S. (2015). Global methane and nitrous oxide emissions from terrestrial ecosystems due to multiple environmental changes. *Ecosystem Health and Sustainability*, 1(1), 1-20.

Tiedje, J. M.: Ecology of denitrification and dissimilatory nitrate reduction to ammonium, in: *Environmental Microbiology of Anaerobes*, edited by: Zehnder, A. J. B., John Wiley & Sons, NY, 179–244, 1988.

Tseng, H. C., Chen, C. T. A., Borges, A. V., DelValls, T. A., Lai, C. M., & Chen, T. Y. (2016). Distributions and sea-to-air fluxes of nitrous oxide in the South China Sea and the West Philippines Sea. *Deep Sea Research Part I: Oceanographic Research Papers*, 115, 131-144.

U.S. Environmental Protection Agency (2010), "Methane and Nitrous Oxide Emissions from Natural Sources. Report EPA 430-R-10-001.

Usui, T., I. Koike, and N. Ogura, Vertical profiles of nitrous oxide and dissolved

oxygen in marine sediments, *Mar. Chem.*, 59, 253- 270, 1998.

Usui, T., Koike, I., & Ogura, N. (2001). N₂O production, nitrification and denitrification in an estuarine sediment. *Estuarine, Coastal and Shelf Science*, 52(6), 769-781.

Vi, K. C. (2021). *Plantain mixed pasture: seasonality of herbage accumulation and potential for mitigating nitrous oxide emissions from cow urine patches: a thesis presented in partial fulfilment of the requirements for the degree of Master in Horticulture Science at Massey University, Manawatū, New Zealand* (Doctoral dissertation, Massey University).

Walter, S., Breitenbach, U., Bange, H. W., Nausch, G., and Wallace, D. W.: Distribution of N₂O in the Baltic Sea during transition from anoxic to oxic conditions, *Biogeosciences*, 3, 557–570, <https://doi.org/10.5194/bg-3-557-2006>, 2006.

Wan, X. S., Sheng, H. X., Dai, M., Zhang, Y., Shi, D., Trull, T. W., ... & Kao, S. J. (2018). Ambient nitrate switches the ammonium consumption pathway in the euphotic ocean. *Nature Communications*, 9(1), 915.

Wan, X. S., Lin, H., Ward, B. B., Kao, S. J., & Dai, M. (2022). Significant Seasonal N₂O Dynamics Revealed by Multi-Year Observations in the Northern South China Sea. *Global Biogeochemical Cycles*, 36(10), e2022GB007333.

Wedderburn-Bisshop, G., Longmire, A., & Rickards, L. (2015). Neglected transformational responses: implications of excluding short lived emissions and near term projections in greenhouse gas accounting. *International Journal of Climate Change: Impacts & Responses*, 7(3).

Weiss, R. F. (1981). The temporal and spatial distribution of tropospheric nitrous oxide. *Journal of Geophysical Research: Oceans*, 86(C8), 7185- 7195.

Whiticar, M. J. (2002). Diagenetic relationships of methanogenesis, nutrients, acoustic turbidity, pockmarks and freshwater seepages in Eckernförde Bay. *Marine Geology*, 182(1-2), 29-53.

Wilson, S. T., Ferrón, S., and Karl, D. M.: Interannual variability of methane and

nitrous oxide in the North Pacific Subtropical Gyre, *Geophys. Res. Lett.*, *44*, 9885–9892.

Wolgast, D.M., A.F. Carlucci, and J.E. Bauer, Nitrate respiration associated with detrital aggregates in aerobic bottom waters of the abyssal NE Pacific, *Deep Sea Res., Part II*, *45*, 881-892, 1998.<https://doi.org/10.1002/2017GL074458>, 2017.

Yang, S., Chang, B. X., Warner, M. J., Weber, T. S., Bourbonnais, A. M., Santoro, A. E., ... & Bianchi, D. (2020). Global reconstruction reduces the uncertainty of oceanic nitrous oxide emissions and reveals a vigorous seasonal cycle. *Proceedings of the National Academy of Sciences*, *117*(22), 11954-11960.

Yoshinari, T., Nitrous oxide in the sea, *Mar. Chem.*, *4*, 189-202, 1976.

Yoshinari, T. (1976). Nitrous oxide in the sea. *Marine Chemistry*, *4*(2), 189-202.

Yoshida, N., Morimoto, H., Hirano, M., Koike, I., Matsuo, S., Wada, E., ... & Hattori, A. (1989). Nitrification rates and ^{15}N abundances of N_2O and NO_3^- in the western North Pacific. *Nature*, *342*(6252), 895-897.

Zehr, J. P., & Kudela, R. M. (2011). Nitrogen cycle of the open ocean: from genes to ecosystems. *Annual review of marine science*, *3*, 197-225.

Zhan, L., Chen, L., Zhang, J., Yan, J., Li, Y., Wu, M., ... & Zhao, J. (2015).

Austral summer N_2O sink and source characteristics and their impact factors in Prydz Bay, Antarctica. *Journal of Geophysical Research: Oceans*, *120*(8), 5836-5849.

Zhan, L., Wu, M., Chen, L., Zhang, J., Li, Y., & Liu, J. (2017). The air-sea nitrous oxide flux along cruise tracks to the Arctic Ocean and Southern Ocean. *Atmosphere*, *8*(11), 216.

9.0 Acknowledgement

I would like to thank Prof. Dr. Hermann Bange for his tireless support from the beginning of this work until its completion. My appreciation goes to all team members who helped me in one way or another during the difficult times of this work.

10.0 Declaration

I, Nwafor Chukwudi Ejikeme, hereby declare that I have written this thesis solely on the advice of my supervisor and that I have fully acknowledged all sources and aids used. The submitted written version of this thesis corresponds to the one on the electronic storage medium. I furthermore assure that neither this nor a similar thesis has already been submitted elsewhere for the purpose of obtaining a Master's degree.

Kiel,

Signature.....

11.0 Appendix

Cruise No	Depth (m)	Latitude	Longitude	Date	Time	Mean N ₂ O[nmol/L-1]	Temp (°C)	Salinty	Oxygen (μmol L ⁻¹)	NO ₂ ⁻ (μmol L ⁻¹)	NO ₃ ⁻ (μmol L ⁻¹)	AOU (μmol L ⁻¹)	ΔN ₂ O (nmol L ⁻¹)	N ₂ O Sat (%)
372	1	54°31.77 N	10°02.36 E	28.07.2005	08:58	9.494252218	18.19	13.72	281.4	0.01	0.09			
372	5	54°31.77 N	10°02.36 E	28.07.2005	08:58	9.180039244	17.98	14.14	285.1	0.01	0.04			
372	10	54°31.77 N	10°02.36 E	28.07.2005	08:58	10.52925082	17.38	16.63	231.2	0.02	0.05			
372	15	54°31.77 N	10°02.36 E	28.07.2005	08:58	14.24864399	10.6	21.78	130	0.3	2.32			
372	20	54°31.77 N	10°02.36 E	28.07.2005	08:58	15.77936652	8.41	24.49	85.1	0.21	6.5			
372	25	54°31.77 N	10°02.36 E	28.07.2005	08:58	18.51136897	7.7	24.72	31.5	0.14	10.77			
373	1	54°31.77 N	10°02.36 E	11.08.2005	08:42	9.539075248	16.71	15.47	274	0	0.75			
373	5	54°31.77 N	10°02.36 E	11.08.2005	08:42	9.475144542	16.7	15.48	275.1	0	0.24			
373	10	54°31.77 N	10°02.36 E	11.08.2005	08:42	9.859040041	16.81	16.51	259	0.04	0.08			
373	15	54°31.77 N	10°02.36 E	11.08.2005	08:42	12.60217162	13.34	21.28	151	0.01	0.02			
373	20	54°31.77 N	10°02.36 E	11.08.2005	08:42	16.95021409	9.44	23.67	56.7	0.27	5.7			
373	25	54°31.77 N	10°02.36 E	11.08.2005	08:42	18.10535082	8.13	24.54	16.3	0.21	12.2			
374	1	54°31.77 N	10°02.36 E	14.09.2005	10:38	10.09047869	17.22	14.97	284.2	0.03	0.06			
374	5	54°31.77 N	10°02.36 E	14.09.2005	10:38	10.17762305	17.32	15.27	281	0.02	0.01			

374	10	54°31.77 N	10°02.36 E	14.09.200 5	10:38	10.18501968	17.68	16.51	273.6	0.02	0
374	15	54°31.77 N	10°02.36 E	14.09.200 5	10:38	9.812620781	16.9	17.97	214.5	0.03	0.06
374	20	54°31.77 N	10°02.36 E	14.09.200 5	10:38	9.98544085	14.22	20.92	86.1	0.06	0.09
374	25	54°31.77 N	10°02.36 E	14.09.200 5	10:38	1.743822729	10.95	23.25	0	0.17	0.17
375	1	54°31.77 N	10°02.36 E	26.10.200 5	08:52	10.83624151	13.38	16.7	268.2	0.03	0.07
375	5	54°31.77 N	10°02.36 E	26.10.200 5	08:52	10.74295731	13.38	16.72	269.3	0.03	0.02
375	10	54°31.77 N	10°02.36 E	26.10.200 5	08:52	10.69516606	13.9	17.4	254.8	0.02	0.05
375	15	54°31.77 N	10°02.36 E	26.10.200 5	08:52	9.296025063	14.38	18.13	158.4	0.02	0.06
375	20	54°31.77 N	10°02.36 E	26.10.200 5	08:52	7.0486763	14.39	19.73	70	0.06	0.12
375	25	54°31.77 N	10°02.36 E	26.10.200 5	08:52	1.198048132	12.43	22.32	0	0.52	0.53
376	1	54°31.77 N	10°02.36 E	15.11.200 5	09:57	17.07351997	11.7	20.08	234.4	0.25	2.65
376	5	54°31.77 N	10°02.36 E	15.11.200 5	09:57	16.44709709	11.69	20.22	237.1	0.25	2.63
376	10	54°31.77 N	10°02.36 E	15.11.200 5	09:57	18.13677285	11.91	21.21	220.5	0.24	2.9
376	15	54°31.77 N	10°02.36 E	15.11.200 5	09:57	19.38578864	12.21	22.36	180.2	0.25	3.51
376	20	54°31.77 N	10°02.36 E	15.11.200 5	09:57	19.5720606	12.24	23.7	163.2	0.26	3.9
376	25	54°31.77 N	10°02.36 E	15.11.200 5	09:57	18.50418005	12.15	24.34	178.2	0.3	5.19
377	1	54°31.77 N	10°02.36 E	13.12.200 5	10:41	13.46629639	5.68	17.91	349.6	0.14	1.06
377	5	54°31.77 N	10°02.36 E	13.12.200 5	10:41	13.5264712	6.17	19.51	345.9	0.1	1.07
377	10	54°31.77 N	10°02.36 E	13.12.200 5	10:41	13.01183522	6.73	20.64	328.7	0.11	1.8

377	15	N	54°31.77	10°02.36	13.12.200	5	E	10:41	13.17499367	6.84	20.91	324.6	0.13	2.06
377	20	N	54°31.77	10°02.36	13.12.200	5	E	10:41	12.70767633	7.67	22.22	274	0.23	2.96
377	25	N	54°31.77	10°02.36	13.12.200	5	E	10:41	11.74672244	9.87	25.03	146.1	0.57	3.16
378	1	N	54°31.77	10°02.36	17.01.200	6	E	10:27	15.27896988	2.41	19.89	367	0.49	4.12
378	5	N	54°31.77	10°02.36	17.01.200	6	E	10:27	14.38965144	2.42	19.91	368.5	0.27	3.62
378	10	N	54°31.77	10°02.36	17.01.200	6	E	10:27	14.55291329	2.7	20	356.9	0.2	3.15
378	15	N	54°31.77	10°02.36	17.01.200	6	E	10:27	15.01496875	3.73	20.59	336.9	0.18	2.87
378	20	N	54°31.77	10°02.36	17.01.200	6	E	10:27	14.83245064	4.48	21.1	284.3	0.17	2.76
378	25	N	54°31.77	10°02.36	17.01.200	6	E	10:27	14.80079667	6.65	22.05	195.2	0.17	2.85
379	1	N	54°31.77	10°02.36	14.02.200	6	E	10:31	16.18607811	1.12	16.53	436.2	0.09	0.03
379	5	N	54°31.77	10°02.36	14.02.200	6	E	10:31	16.36247471	1.42	16.72	431	0.08	0.11
379	10	N	54°31.77	10°02.36	14.02.200	6	E	10:31	15.76700862	1.56	17.25	402.5	0.17	1.55
379	15	N	54°31.77	10°02.36	14.02.200	6	E	10:31	16.01300952	1.79	18.4	376.6	0.32	3.41
379	20	N	54°31.77	10°02.36	14.02.200	6	E	10:31	16.18945787	2.2	19.28	341	0.35	3.92
379	25	N	54°31.77	10°02.36	14.02.200	6	E	10:31	16.17732474	2.57	19.79	293.3	0.49	4.32
380	1	N	54°31.77	10°02.36	14.03.200	6	E	11:17	15.47476315	1.07	17.29	397.7	0.03	0.1
380	5	N	54°31.77	10°02.36	14.03.200	6	E	11:17	15.9835144	1.1	17.36	399.3	0.02	0.05
380	10	N	54°31.77	10°02.36	14.03.200	6	E	11:17	15.82231899	1.32	17.72	386.1	0.02	0.07

380	15	54°31.77 N	10°02.36 E	14.03.200 6	11:17	16.0087845	1.36	17.83	382	0.03	0.08
380	20	54°31.77 N	10°02.36 E	14.03.200 6	11:17	16.03272507	1.23	17.85	360.5	0.04	0.11
380	25	54°31.77 N	10°02.36 E	14.03.200 6	11:17	16.02073938	2.22	19.02	276	0.14	1.69
381	1	54°31.77 N	10°02.36 E	21.04.200 6	11:02	14.7864616	5.56	16.57	375.3	0.02	0.06
381	5	54°31.77 N	10°02.36 E	21.04.200 6	11:02	14.22854821	4.82	16.97	372.5	0.03	0.02
381	10	54°31.77 N	10°02.36 E	21.04.200 6	11:02	14.1167887	3.42	19.84	315.7	0.1	0.97
381	15	54°31.77 N	10°02.36 E	21.04.200 6	11:02	14.93382853	4.1	22.2	315.1	0.05	1.25
381	20	54°31.77 N	10°02.36 E	21.04.200 6	11:02	12.91070342	4.41	24.05	296.8	0.05	2.02
381	25	54°31.77 N	10°02.36 E	21.04.200 6	11:02	12.31005833	4.15	25.9	212.7	0.12	3.07
382	1	54°31.77 N	10°02.36 E	17.05.200 6	10:26	12.36454144	12.15	12.65	325.4	0.06	0.06
382	5	54°31.77 N	10°02.36 E	17.05.200 6	10:26	12.64491736	11.76	14.19	331	0.06	0.04
382	10	54°31.77 N	10°02.36 E	17.05.200 6	10:26	13.01238589	10.31	16.96	353.6	0.05	0.02
382	15	54°31.77 N	10°02.36 E	17.05.200 6	10:26	13.07541063	9.15	17.16	335.4	0.03	0.05
382	20	54°31.77 N	10°02.36 E	17.05.200 6	10:26	14.67779231	5.89	20.27	237.6	0.19	1.8
382	25	54°31.77 N	10°02.36 E	17.05.200 6	10:26	10.11170759	4.32	25.44	73.5	0.16	1.84
383	1	54°31.77 N	10°02.36 E	21.06.200 6	11:19		17.19	16.36	299.7	0.07	0.02
383	5	54°31.77 N	10°02.36 E	21.06.200 6	11:19	11.15315754	17.18	16.38	301	0.07	0.02
383	10	54°31.77 N	10°02.36 E	21.06.200 6	11:19	11.13800384	13.52	17.95	299.1	0.07	0.02
383	15	54°31.77 N	10°02.36 E	21.06.200 6	11:19	12.91267362	10.53	21.33	313.2	0.04	0

383	20	54°31.77 N	10°02.36 E	21.06.200 6	11:19	12.88608374	6.12	23.87	165.5	0.12	0
383	25	54°31.77 N	10°02.36 E	21.06.200 6	11:19	14.14857975	7.4	25.44	154.9	0.22	0.63
384	1	54°31.77 N	10°02.36 E	27.07.200 6	11:19		23.2	12.5	282.2	0.04	0.02
384	5	54°31.77 N	10°02.36 E	27.07.200 6	11:19	12.85766345	22.9	12.6	289.5	0.11	0.06
384	10	54°31.77 N	10°02.36 E	27.07.200 6	11:19	15.27866443	16.5	17.6	274.2	0.44	0.38
384	15	54°31.77 N	10°02.36 E	27.07.200 6	11:19	17.78939957	10.2	21.8	199.6	0.27	0.21
384	20	54°31.77 N	10°02.36 E	27.07.200 6	11:19	20.28328856	8	24	142	0.55	1.18
384	25	54°31.77 N	10°02.36 E	27.07.200 6	11:19	21.5208856	8	24	94	0.24	3.31
385	1	54°31.77 N	10°02.36 E	17.08.200 6	08:59	12.93401758	17.9	16.85	257	0.11	0.13
385	5	54°31.77 N	10°02.36 E	17.08.200 6	08:59	13.68994295	17.8	17.05	267.8	0.07	0.02
385	10	54°31.77 N	10°02.36 E	17.08.200 6	08:59	15.47575611	16.11	18.78	194.8	0.1	0.08
385	15	54°31.77 N	10°02.36 E	17.08.200 6	08:59	17.24244356	13.05	21.34	143.5	0.16	0.36
385	20	54°31.77 N	10°02.36 E	17.08.200 6	08:59	17.08507651	9.93	23.82	128.7	0.16	0.48
385	25	54°31.77 N	10°02.36 E	17.08.200 6	08:59	20.88532373	9.05	24.3	63.6	0.62	2.53
386	1	54°31.77 N	10°02.36 E	20.09.200 6			16.81	20.08	259.1	0.05	0.08
386	5	54°31.77 N	10°02.36 E	20.09.200 6			16.74	20.6	254.2	0.05	0.07
386	10	54°31.77 N	10°02.36 E	20.09.200 6			16.52	21.26	246.5	0.04	0.01
386	15	54°31.77 N	10°02.36 E	20.09.200 6		9.846644493	16.31	21.65	234.2	0.04	0.02
386	20	54°31.77 N	10°02.36 E	20.09.200 6		4.578681618	11.46	24.47	21.8	0.11	0.03

386	25	54°31.77 N	10°02.36 E	20.09.200 6		4.578138936	11.05	24.88	6	0.27	0.17
387	1	54°31.77 N	10°02.36 E	11.10.200 6	09:11		15.63	20.14			
387	5	54°31.77 N	10°02.36 E	11.10.200 6	09:11		15.6	20.13			
387	10	54°31.77 N	10°02.36 E	11.10.200 6	09:11		15.61	20.26			
387	15	54°31.77 N	10°02.36 E	11.10.200 6	09:11		15.41	21.05			
387	20	54°31.77 N	10°02.36 E	11.10.200 6	09:11		13.87	23.17			
387	25	54°31.77 N	10°02.36 E	11.10.200 6	09:11		12.38	23.81			
388	1	54°31.77 N	10°02.36 E	14.11.200 6	10:14	15.25931337	10.57	20.51	305.1	0.76	2.05
388	5	54°31.77 N	10°02.36 E	14.11.200 6	10:14	15.83545923	10.58	20.53	305	0.75	2
388	10	54°31.77 N	10°02.36 E	14.11.200 6	10:14	15.13903879	10.58	20.53	292.1	0.75	2.04
388	15	54°31.77 N	10°02.36 E	14.11.200 6	10:14	15.82413649	10.6	20.55	296.4	0.76	2.01
388	20	54°31.77 N	10°02.36 E	14.11.200 6	10:14		11.03	21.06	228.2	0.67	3.84
388	25	54°31.77 N	10°02.36 E	14.11.200 6	10:14	15.19482773	13	22.73	57	0.56	13.76
389	1	54°31.77 N	10°02.36 E	12.12.200 6	08:28	18.26228714	8.49	22.46	303.3	0.44	3.36
389	5	54°31.77 N	10°02.36 E	12.12.200 6	08:28	17.48486605	8.49	22.47	307	0.41	3.24
389	10	54°31.77 N	10°02.36 E	12.12.200 6	08:28	18.06880261	8.59	22.59	300.9	0.57	4.06
389	15	54°31.77 N	10°02.36 E	12.12.200 6	08:28	17.67983299	8.64	22.64	297.9	0.61	4.36
389	20	54°31.77 N	10°02.36 E	12.12.200 6	08:28	18	8.91	22.91	293.3	0.75	5.13

389	25	N	54°31.77	E	10°02.36	12.12.200	08:28	17.0953936	8.98	23	284.5	0.82	5.47
390	1	N	54°31.77	E	10°02.36	22.02.200		16.31838949	3.93	18.42		0.75	9.64
390	5	N	54°31.77	E	10°02.36	22.02.200		17.09221723	3.86	19.59		0.79	9.63
390	10	N	54°31.77	E	10°02.36	22.02.200		17.50470614	3.83	19.81		0.81	10.2
390	15	N	54°31.77	E	10°02.36	22.02.200		17.03622287	3.83	20.85		0.85	11.42
390	20	N	54°31.77	E	10°02.36	22.02.200		16.94548613	3.9	21.27		0.88	11.68
390	25	N	54°31.77	E	10°02.36	22.02.200			3.92	21.36		0.9	11.34
391	1	N	54°31.77	E	10°02.36	15.03.200	10:31	18.42502276	5.19	13.16	445.6	0.09	0.01
391	5	N	54°31.77	E	10°02.36	15.03.200	10:31	17.80896984	5.16	13.31	452.5	0.07	0.01
391	10	N	54°31.77	E	10°02.36	15.03.200	10:31	17.32377074	4.41	15	395	0.34	4.23
391	15	N	54°31.77	E	10°02.36	15.03.200	10:31	17.79833849	3.97	16.43	362.5	0.63	8.08
391	20	N	54°31.77	E	10°02.36	15.03.200	10:31	17.41699861	3.78	18.02	342.7	0.94	10.85
391	25	N	54°31.77	E	10°02.36	15.03.200	10:31	17.28655104	3.89	19.08	293.6	1.05	12.3
392	1	N	54°31.77	E	10°02.36	05.04.200	10:23	15.83604483	6.8	15.5	343.5	0.05	0.32
392	5	N	54°31.77	E	10°02.36	05.04.200	10:23	16.04270856	6.81	15.56	343.1	0.04	0.27
392	10	N	54°31.77	E	10°02.36	05.04.200	10:23	16.65681763	6.78	15.51	342.5	0.04	0.19
392	15	N	54°31.77	E	10°02.36	05.04.200	10:23	16.12896281	6.65	15.56	342.4	0.04	0.12
392	20	N	54°31.77	E	10°02.36	05.04.200	10:23	17.92129735	4.74	19.73	300	0.27	6.97

392	25	54°31.77 N	10°02.36 E	05.04.200 7	10:23	22.59599996	4.97	21.06	291	0.17	4.54
393	1	54°31.77 N	10°02.36 E	04.05.200 7		14.90714954	10.86	15.61	304.7	0.02	0.01
393	5	54°31.77 N	10°02.36 E	04.05.200 7		17.0843744	10.85	15.62	300.8	0.02	0.02
393	10	54°31.77 N	10°02.36 E	04.05.200 7		18.46549089	10.05	15.94	216.7	0.04	0.19
393	15	54°31.77 N	10°02.36 E	04.05.200 7		17.85860838	7.76	17.32	137.5	0.12	2.11
393	20	54°31.77 N	10°02.36 E	04.05.200 7		21.02513026	5.81	19.56	90.3	0.16	6.19
393	25	54°31.77 N	10°02.36 E	04.05.200 7		18.53142369	5.32	20.31	87	0.16	6.25
395	1	54°31.77 N	10°02.36 E	14.06.200 7	11:10	17.00096234	18.36	15.28	290.2	0.13	0.1
395	5	54°31.77 N	10°02.36 E	14.06.200 7	11:10	17.37611963	18.3	15.26	288.8	0.17	0.03
395	10	54°31.77 N	10°02.36 E	14.06.200 7	11:10	15.220553	15.55	15.29	314.4	0.01	0.03
395	15	54°31.77 N	10°02.36 E	14.06.200 7	11:10	17.45448352	13.91	16.06	277.2	0.03	0.09
395	20	54°31.77 N	10°02.36 E	14.06.200 7	11:10	16.43049164	9.14	17.41	154.3	0.29	0.57
395	25	54°31.77 N	10°02.36 E	14.06.200 7	11:10	21.34585532	5.87	19.66	21.4	0.26	3.1
396	1	54°31.77 N	10°02.36 E	12.07.200 7				14.4	316.5	0.12	0.11
396	5	54°31.77 N	10°02.36 E	12.07.200 7				14.5	306.7	0.12	0.02
396	10	54°31.77 N	10°02.36 E	12.07.200 7				16.3	199.8	0.13	0.33
396	15	54°31.77 N	10°02.36 E	12.07.200 7				18.3	150.9	0.25	4.42
396	20	54°31.77 N	10°02.36 E	12.07.200 7				19.5	133.5	0.57	7.26
396	25	54°31.77 N	10°02.36 E	12.07.200 7				19.7	87.6	0.21	7.74

397	1	N	54°31.77	E	10°02.36	16.08.200	7	10:43	14.30111632	17.8	16.78	242	0.07	0.06
397	5	N	54°31.77	E	10°02.36	16.08.200	7	10:43	14.3	17.39	17.1	237	0.07	0.01
397	10	N	54°31.77	E	10°02.36	16.08.200	7	10:43		14.26	19.76	134	0.16	0.34
397	15	N	54°31.77	E	10°02.36	16.08.200	7	10:43	14.3	13.43	20.62	109.1	0.26	2.01
397	20	N	54°31.77	E	10°02.36	16.08.200	7	10:43	15.54	13.16	21.12	84.7	0.28	4.44
397	25	N	54°31.77	E	10°02.36	16.08.200	7	10:43	15.8	12.78	21.41	62.8	0.21	6.44
398	1	N	54°31.77	E	10°02.36	12.09.200	7	08:53		16.04	15.66	279.1	0.09	0.03
398	5	N	54°31.77	E	10°02.36	12.09.200	7	08:53		16.04	15.72	286.2	0.08	0.01
398	10	N	54°31.77	E	10°02.36	12.09.200	7	08:53		16.02	15.79	277.1	0.09	0.08
398	15	N	54°31.77	E	10°02.36	12.09.200	7	08:53		16	16.01	264	0.07	0.14
398	20	N	54°31.77	E	10°02.36	12.09.200	7	08:53		13.77	19.92	13.7	0.08	0.24
398	25	N	54°31.77	E	10°02.36	12.09.200	7	08:53		12.49	20.98	0	0.13	0.51
399	1	N	54°31.77	E	10°02.36	16.10.200	7	08:48	11.54255334	13.12	17.78	281.9	0.01	0.31
399	5	N	54°31.77	E	10°02.36	16.10.200	7	08:48	12.0064652	13.12	17.81	285.2	0.01	0.11
399	10	N	54°31.77	E	10°02.36	16.10.200	7	08:48	14.5401846	13.13	17.84	281.5	0.01	0.05
399	15	N	54°31.77	E	10°02.36	16.10.200	7	08:48	13.56183627	13.68	18.63	234.4	0.06	0.04
399	20	N	54°31.77	E	10°02.36	16.10.200	7	08:48	12.14973018	13.9	19.83	119.8	0.5	3.26
399	25	N	54°31.77	E	10°02.36	16.10.200	7	08:48	13.48214939	13.8	20.55	94.4	0.4	5.39
400	1	N	54°31.77	E	10°02.36	13.11.200	7	09:26	19.94042238	8.86	16.69	317.8	0.08	0.08

400	5	N	54°31.77	E	10°02.36	13.11.200	7	09:26	21.42064733	8.88	16.72	317.3	0.07	0
400	10	N	54°31.77	E	10°02.36	13.11.200	7	09:26	17.90910847	9.19	16.87	311.2	0.1	0.14
400	15	N	54°31.77	E	10°02.36	13.11.200	7	09:26	20.19276951	9.97	17.37	290.3	0.21	0.97
400	20	N	54°31.77	E	10°02.36	13.11.200	7	09:26	15.87519919	10.86	18.02	235	0.18	4.53
400	25	N	54°31.77	E	10°02.36	13.11.200	7	09:26	18.33265491	12.98	19.27	70	0.27	11.71
401	1	N	54°31.77	E	10°02.36	11.12.200	7	09:35	16.65097384	6.82	17.98	323.9	0.81	2.495
401	5	N	54°31.77	E	10°02.36	11.12.200	7	09:35	17.6390138	6.81	18	323.5	0.915	2.475
401	10	N	54°31.77	E	10°02.36	11.12.200	7	09:35	17.53418266	6.84	18.04	323.6	0.94	2.535
401	15	N	54°31.77	E	10°02.36	11.12.200	7	09:35	18.22988105	7	18.24	318.6	0.615	2.755
401	20	N	54°31.77	E	10°02.36	11.12.200	7	09:35	18.44027304	7.21	18.5	298.8	0.76	4.36
401	25	N	54°31.77	E	10°02.36	11.12.200	7	09:35	17.76912871	7.71	18.97	254.1	0.655	4.575
402	1	N	54°31.77	E	10°02.36	17.01.200	8	09:30	21.10437716	4.44	17.85	349	0.565	5.94
402	5	N	54°31.77	E	10°02.36	17.01.200	8	09:30	17.70869478	4.45	17.87	350.4	0.59	5.845
402	10	N	54°31.77	E	10°02.36	17.01.200	8	09:30	18.44440754	4.45	17.9	348.9	0.615	5.665
402	15	N	54°31.77	E	10°02.36	17.01.200	8	09:30	18.29796925	4.44	17.9	349.7	0.635	5.655
402	20	N	54°31.77	E	10°02.36	17.01.200	8	09:30	19.26809304	4.44	17.9	347.6	0.655	5.56
402	25	N	54°31.77	E	10°02.36	17.01.200	8	09:30	19.1	4.44	17.9	348.3	0.685	5.585
403	1	N	54°31.77	E	10°02.36	19.02.200	8	09:25	15.51386802	3.52	17.39	379.9	0.23	2.91

403	5	N	54°31.77	E	10°02.36	19.02.200	8	09:25	14.93472362	3.57	17.59	390.6	0.23	2.995
403	10	N	54°31.77	E	10°02.36	19.02.200	8	09:25	14.26361607	3.77	18.7	388.8	0.25	4.745
403	15	N	54°31.77	E	10°02.36	19.02.200	8	09:25	14.6904554	3.81	18.78	382.8	0.255	3.875
403	20	N	54°31.77	E	10°02.36	19.02.200	8	09:25	15.05728083	5.04	22.76	313.3	0.49	7.015
403	25	N	54°31.77	E	10°02.36	19.02.200	8	09:25	16.3	5.16	23.15	283.9	0.42	7.09
405	1	N	54°31.77	E	10°02.36	16.04.200	8	11:48	16.95260845	6.94	11.34	360.5	0.03	0.1
405	5	N	54°31.77	E	10°02.36	16.04.200	8	11:48	16.54252635	7.22	13.62	358.5	0.03	0.02
405	10	N	54°31.77	E	10°02.36	16.04.200	8	11:48	17.2	6.38	17.15	358	0.05	0.03
405	15	N	54°31.77	E	10°02.36	16.04.200	8	11:48	17.02122093	5.98	18.61	351.7	0.04	0.02
405	20	N	54°31.77	E	10°02.36	16.04.200	8	11:48	17.6	5.36	19.78	339.3	0.04	0.06
405	25	N	54°31.77	E	10°02.36	16.04.200	8	11:48	17.1	5.05	20.69	224.3	0.17	0.97
406	1	N	54°31.77	E	10°02.36	20.05.200	8	10:37	14.62702752	13.74	11.47	317.3	0.01	0.03
406	5	N	54°31.77	E	10°02.36	20.05.200	8	10:37	12.71246535	13.76	11.5	316.8	0.01	0
406	10	N	54°31.77	E	10°02.36	20.05.200	8	10:37		13.59	11.5	318.5	0.01	0.02
406	15	N	54°31.77	E	10°02.36	20.05.200	8	10:37	14.65663895	8.96	13.71	348	0.02	0.04
406	20	N	54°31.77	E	10°02.36	20.05.200	8	10:37		5.88	19.56	246.6	0.25	1.02
406	25	N	54°31.77	E	10°02.36	20.05.200	8	10:37	18.2	5.63	20.2	146.1	0.62	2.04
407	1	N	54°31.77	E	10°02.36	24.06.200	8	10:35	11.60139141	15.42	12.4	292.2	0.07	0.01
407	5	N	54°31.77	E	10°02.36	24.06.200	8	10:35	12.51768084	14.63	13.9	288.2	0.08	0.02

407	10	54°31.77 N	10°02.36 E	24.06.200 8	10:35	14.8	13.48	16.97	273.1	0.07	0.03
407	15	54°31.77 N	10°02.36 E	24.06.200 8	10:35	18.21479174	10.27	18.97	236.4	0.09	0.09
407	20	54°31.77 N	10°02.36 E	24.06.200 8	10:35	21.5	8.41	20.85	183.8	0.2	3.19
407	25	54°31.77 N	10°02.36 E	24.06.200 8	10:35	22	7.57	21.38	148.7	0.19	5.14
408	1	54°31.77 N	10°02.36 E	09.07.200 8	09:35	10.28889506	15.06	17.35	277.3	0.06	0.14
408	5	54°31.77 N	10°02.36 E	09.07.200 8	09:35	11.38075285	14.59	17.75	274	0.07	0.19
408	10	54°31.77 N	10°02.36 E	09.07.200 8	09:35		11.3	20.59	223.5	0.04	0.29
408	15	54°31.77 N	10°02.36 E	09.07.200 8	09:35	14.73407538	11.48	21.75	228.8	0.03	0.31
408	20	54°31.77 N	10°02.36 E	09.07.200 8	09:35		10.38	22.93	174.7	0.03	0.59
408	25	54°31.77 N	10°02.36 E	09.07.200 8	09:35	16.6	9.87	23.64	134.3	0.37	0.97
409	1	54°31.77 N	10°02.36 E	19.08.200 8	15:44	13.54285313	17.74	16.12	278.2	0.05	0.13
409	5	54°31.77 N	10°02.36 E	19.08.200 8	15:44	12.29869792	17.06	17.02	270.6	0.06	0.15
409	10	54°31.77 N	10°02.36 E	19.08.200 8	15:44	16.6	15.37	19.19	227.9	0.07	0.25
409	15	54°31.77 N	10°02.36 E	19.08.200 8	15:44	18.81722854	13.91	20.81	169.2	0.09	0.48
409	20	54°31.77 N	10°02.36 E	19.08.200 8	15:44	17.7	11.47	22.79	98	0.11	0.99
409	25	54°31.77 N	10°02.36 E	19.08.200 8	15:44	14.364007	10.98	23.39	26	0.13	2.32
410	1	54°31.77 N	10°02.36 E	15.09.200 8	15:33		15.3	17.36	288.4	0.01	0.3
410	5	54°31.77 N	10°02.36 E	15.09.200 8	15:33	8.3	15.28	18.2	280.3	0.01	0.33
410	10	54°31.77 N	10°02.36 E	15.09.200 8	15:33		15.61	18.86	269.2	0.02	0.33

410	15	N	54°31.77	10°02.36	15.09.200	8	15:33	10.1	15.48	19.11	269.2	0.05	0.31
410	20	N	54°31.77	10°02.36	15.09.200	8	15:33		15.14	20.65	86.2	0.1	1.9
410	25	N	54°31.77	10°02.36	15.09.200	8	15:33	9.333774	12.14	23.3	3.5	0.15	4.43
414	1	N	54°31.77	10°02.36	27.10.200	8	12:45	11.47268226	12.31	21.23	255	0.51	2
414	5	N	54°31.77	10°02.36	27.10.200	8	12:45	10.4	12.3	21.25	255.1	0.45	1.75
414	10	N	54°31.77	10°02.36	27.10.200	8	12:45	9.8	12.45	21.98	235	0.64	2.58
414	15	N	54°31.77	10°02.36	27.10.200	8	12:45	9.7	12.62	22.41	228.8	0.57	2.57
414	20	N	54°31.77	10°02.36	27.10.200	8	12:45	10.2	12.69	23.6	225	0.22	1.88
414	25	N	54°31.77	10°02.36	27.10.200	8	12:45		12.68	24.04	224.4	0.15	1.73
415	1	N	54°31.77	10°02.36	17.11.200	8	10:14	10.93592991	9.59	20.7	310.7	0.67	2.17
415	5	N	54°31.77	10°02.36	17.11.200	8	10:14	14.2	9.6	20.71	310.2	0.68	2.2
415	10	N	54°31.77	10°02.36	17.11.200	8	10:14	12.5	9.79	20.85	307.4	0.71	2.3
415	15	N	54°31.77	10°02.36	17.11.200	8	10:14	13	11.09	22.69	266.4	1.22	4.93
415	20	N	54°31.77	10°02.36	17.11.200	8	10:14	12.6	11.73	23.87	224.6	1.53	6.69
415	25	N	54°31.77	10°02.36	17.11.200	8	10:14	15.1015277	11.68	23.97	221.3	1.55	7.05
416	1	N	54°31.77	10°02.36	08.12.200	8	10:46		6.56	20.54			
416	5	N	54°31.77	10°02.36	08.12.200	8	10:46		6.56	20.61			
416	10	N	54°31.77	10°02.36	08.12.200	8	10:46		6.58	20.72			
416	15	N	54°31.77	10°02.36	08.12.200	8	10:46		6.76	20.9			

416	20	54°31.77 N	10°02.36 E	08.12.200 8	10:46		8.61	21.84			
416	25	54°31.77 N	10°02.36 E	08.12.200 8	10:46		9.65	22.58			
417	1	54°31.77 N	10°02.36 E	19.01.200 9	10:25	11.46847	4.36	18.66	329.6	0.49	5.72
417	5	54°31.77 N	10°02.36 E	19.01.200 9	10:25	16.9	4.35	18.68	330.9	0.5	6.48
417	10	54°31.77 N	10°02.36 E	19.01.200 9	10:25	21.3	5.04	19.39	311.7	0.5	7.08
417	15	54°31.77 N	10°02.36 E	19.01.200 9	10:25	26.3	5.46	19.93	295.7	0.47	7.79
417	20	54°31.77 N	10°02.36 E	19.01.200 9	10:25	19.6	5.59	20.15	284.7	0.43	8.38
417	25	54°31.77 N	10°02.36 E	19.01.200 9	10:25		5.71	20.33	279.5	0.42	8.53
418	1	54°31.77 N	10°02.36 E	10.02.200 9	10:30	12.4297436	2.54	16.93	375.9	0.26	3.89
418	5	54°31.77 N	10°02.36 E	10.02.200 9	10:30	12.14720221	2.54	16.95	370.6	0.24	4
418	10	54°31.77 N	10°02.36 E	10.02.200 9	10:30		2.54	17.04	376.3	0.22	4.15
418	15	54°31.77 N	10°02.36 E	10.02.200 9	10:30		2.67	17.48	372.3	0.24	4.23
418	20	54°31.77 N	10°02.36 E	10.02.200 9	10:30		2.87	17.77	361.4	0.32	5.23
418	25	54°31.77 N	10°02.36 E	10.02.200 9	10:30		2.96	18.11	347	0.37	5.22
419	1	54°31.77 N	10°02.36 E	02.03.200 9	10:09	15.02022867	2.54	15.55	398.4	0.02	0.09
419	5	54°31.77 N	10°02.36 E	02.03.200 9	10:09	15.19459886	2.51	15.62	379.4	0.01	0.01
419	10	54°31.77 N	10°02.36 E	02.03.200 9	10:09	15.40710688	2.53	15.9	383.5	0.01	0.5
419	15	54°31.77 N	10°02.36 E	02.03.200 9	10:09	15.6739867	2.58	16.93	381.1	0.17	3.25

419	20	54°31.77 N	10°02.36 E	02.03.200 9	10:09	16.0148604	2.66	17.44	333	0.35	5.49
419	25	54°31.77 N	10°02.36 E	02.03.200 9	10:09	16.6536184	2.69	17.51	324.4	0.44	6.15
420	1	54°31.77 N	10°02.36 E	24.04.200 9		13.87555564	9.01	14.99	345	0.03	0.07
420	5	54°31.77 N	10°02.36 E	24.04.200 9		14.1836028	7.99	15.77	348.1	0.05	0.03
420	10	54°31.77 N	10°02.36 E	24.04.200 9		14.0323947	7.74	16.02	349.3	0.07	0.14
420	15	54°31.77 N	10°02.36 E	24.04.200 9		14.07303635	7.89	16.4	343.9	0.1	0.26
420	20	54°31.77 N	10°02.36 E	24.04.200 9		15.42755128	5.47	17.21	314.5	0.22	1.1
420	25	54°31.77 N	10°02.36 E	24.04.200 9		24.57230209	4.24	19.73	213.2	0.15	5.43
421	1	54°31.77 N	10°02.36 E	20.05.200 9		11.61504125	12.24	14.83	285.1	0.05	0.02
421	5	54°31.77 N	10°02.36 E	20.05.200 9		10.48621014	12.16	14.92	287.1	0.05	0.01
421	10	54°31.77 N	10°02.36 E	20.05.200 9		12.20245466	11.37	15.17	317.3	0.06	0.03
421	15	54°31.77 N	10°02.36 E	20.05.200 9		14.04129579	7.67	18.98	266.7	0.48	1.98
421	20	54°31.77 N	10°02.36 E	20.05.200 9		14.70017856	7.6	20.16	239.1	0.46	4.27
421	25	54°31.77 N	10°02.36 E	20.05.200 9		17.81069664	7.11	21.11	196.6	0.32	4.7
422	1	54°31.77 N	10°02.36 E	23.06.200 9	10:00:38	15.48868636	15.16	16.02	301.1	0.05	0.05
422	5	54°31.77 N	10°02.36 E	23.06.200 9	10:00:38	12.34542223	15.17	16.03	275.4	0.05	0.02
422	10	54°31.77 N	10°02.36 E	23.06.200 9	10:00:38	12.77966127	14.3	16.03	303	0.05	0.01
422	15	54°31.77 N	10°02.36 E	23.06.200 9	10:00:38	13.56778148	12.06	19.28	241.4	0.15	0.16
422	20	54°31.77 N	10°02.36 E	23.06.200 9	10:00:38		9.65	20.63	171	0.12	2.62

422	25	N	54°31.77	E	10°02.36	23.06.200	10:00:38		8.63	21.15	135	0.18	4.45
423	1	N	54°31.77	E	10°02.36	14.07.200	10:04:26	8.976259256	17.4	16.45	294.7	0.03	0.05
423	5	N	54°31.77	E	10°02.36	14.07.200	10:04:26	9.113596381	16.97	16.57	295.8	0.02	0
423	10	N	54°31.77	E	10°02.36	14.07.200	10:04:26	9.572776257	15.49	17.02	278.9	0.01	0.01
423	15	N	54°31.77	E	10°02.36	14.07.200	10:04:26	12.78101873	12.61	19.15	226.3	0.09	0.16
423	20	N	54°31.77	E	10°02.36	14.07.200	10:04:26	15.9967571	10.62	20.2	134.2	0.22	1.32
423	25	N	54°31.77	E	10°02.36	14.07.200	10:04:26	14.50125774	8.97	21.13	39.9	0.52	6.65
424	1	N	54°31.77	E	10°02.36	20.08.200	09:49:09		18.9	15.61	269.1	0.03	0.17
424	5	N	54°31.77	E	10°02.36	20.08.200	09:49:09		18.87	15.9	267.6	0.01	0.07
424	10	N	54°31.77	E	10°02.36	20.08.200	09:49:09		14.79	19.13	263.5	0.01	0.01
424	15	N	54°31.77	E	10°02.36	20.08.200	09:49:09		12.56	20.47	90.2	0.01	0.03
424	20	N	54°31.77	E	10°02.36	20.08.200	09:49:09		12.06	21.56	70.1	0.01	0.04
424	25	N	54°31.77	E	10°02.36	20.08.200	09:49:09		11.65	23.36	51.4	0.12	0.74
425	1	N	54°31.77	E	10°02.36	15.09.200	09:55:47	11.75410995	16.21	17.93	278	0.02	0.06
425	5	N	54°31.77	E	10°02.36	15.09.200	09:55:47	11.52902253	16.21	17.94	277.4	0.01	0
425	10	N	54°31.77	E	10°02.36	15.09.200	09:55:47	11.53082523	16.21	17.94	276.9	0	0.05
425	15	N	54°31.77	E	10°02.36	15.09.200	09:55:47	11.55127516	16.21	17.94	276.1	0	0.1
425	20	N	54°31.77	E	10°02.36	15.09.200	09:55:47	11.34419306	12.94	21.91	69.5	0.34	0.98
425	25	N	54°31.77	E	10°02.36	15.09.200	09:55:47	12.10046259	12.56	22.74	41.4	0.77	2.64

426	1	N	54°31.77	E	10°02.36	19.10.200	9	11:48:26	11.84555526	10.94	19.31	296.6	0.05	0.04
426	5	N	54°31.77	E	10°02.36	19.10.200	9	11:48:26	11.68557968	10.95	19.32	296.9	0.01	0.1
426	10	N	54°31.77	E	10°02.36	19.10.200	9	11:48:26	12.43723482	10.94	19.33	295.7	0.02	0.05
426	15	N	54°31.77	E	10°02.36	19.10.200	9	11:48:26		10.93	19.39	295.5	0.02	0.13
426	20	N	54°31.77	E	10°02.36	19.10.200	9	11:48:26	10.63884954	10.85	19.92	295	0.04	0.26
426	25	N	54°31.77	E	10°02.36	19.10.200	9	11:48:26	10.28818017	11.06	20.37	279.2	0.09	0.66
428	1	N	54°31.77	E	10°02.36	15.12.200	9	09:46:42		5.7	17.17	359.5	0.01	0.08
428	5	N	54°31.77	E	10°02.36	15.12.200	9	09:46:42		6.18	17.37	356.6	0.02	0.01
428	10	N	54°31.77	E	10°02.36	15.12.200	9	09:46:42		6.48	17.52	340.4	0.04	0.73
428	15	N	54°31.77	E	10°02.36	15.12.200	9	09:46:42		6.91	17.94	318	0.16	2.43
428	20	N	54°31.77	E	10°02.36	15.12.200	9	09:46:42		8.7	22.2	266.2	0.23	4.8
428	25	N	54°31.77	E	10°02.36	15.12.200	9	09:46:42		8.97	24.28	219.1	0.27	5.32
429	1	N	54°31.77	E	10°02.36	19.01.201	0	09:50:36	14.9097378	1.27	17.45	388.6	0.29	3.62
429	5	N	54°31.77	E	10°02.36	19.01.201	0	09:50:36	14.71157483	1.27	17.46	390.2	0.29	3.74
429	10	N	54°31.77	E	10°02.36	19.01.201	0	09:50:36	14.74468908	1.28	17.46	388.2	0.29	3.88
429	15	N	54°31.77	E	10°02.36	19.01.201	0	09:50:36	15.37822538	1.35	17.51	386.6	0.29	3.93
429	20	N	54°31.77	E	10°02.36	19.01.201	0	09:50:36	14.74800504	1.44	17.53	324.2	0.32	4.81
429	25	N	54°31.77	E	10°02.36	19.01.201	0	09:50:36	15.23107307	5.71	21.29	210.1	0.42	7.05

431	1	N	54°31.77	E	10°02.36	19.03.201	09:48:06	16.12172686	0.99	16.61	442.5	0.07	0.12
431	5	N	54°31.77	E	10°02.36	19.03.201	09:48:06	13.86205625	1.03	16.6	443.4	0.06	0.13
431	10	N	54°31.77	E	10°02.36	19.03.201	09:48:06	14.72188448	1.03	16.59	433.4	0.08	0.32
431	15	N	54°31.77	E	10°02.36	19.03.201	09:48:06	14.52971583	0.42	16.84	357.2	0.11	1.36
431	20	N	54°31.77	E	10°02.36	19.03.201	09:48:06	13.0075641	1.53	20.7	290.5	0.11	1.99
431	25	N	54°31.77	E	10°02.36	19.03.201	09:48:06	12.43668835	1.66	21.14	298.1	0.09	1.88
432	1	N	54°31.77	E	10°02.36	26.04.201	10:28:12	12.79841347	7.93	13.79	359.5	0.03	0.12
432	5	N	54°31.77	E	10°02.36	26.04.201	10:28:12	13.01181393	7.46	14.17	359.2	0	0.02
432	10	N	54°31.77	E	10°02.36	26.04.201	10:28:12	14.55048308	4.69	18.44	357.9	0	0.26
432	15	N	54°31.77	E	10°02.36	26.04.201	10:28:12	13.96349591	3.94	19.68	314.6	0.05	0.77
432	20	N	54°31.77	E	10°02.36	26.04.201	10:28:12	15.6462077	3.17	21.61	243.4	0.11	1.71
432	25	N	54°31.77	E	10°02.36	26.04.201	10:28:12	17.80327949	3.06	22.13	232.9	0.17	2.21
433	1	N	54°31.77	E	10°02.36	19.05.201	10:40:55		9.23	13.54	340.6	0.03	0.11
433	5	N	54°31.77	E	10°02.36	19.05.201	10:40:55		9.22	13.54	341.1	0.02	0.02
433	10	N	54°31.77	E	10°02.36	19.05.201	10:40:55		9.19	13.54	336.9	0.02	0.13
433	15	N	54°31.77	E	10°02.36	19.05.201	10:40:55		7.38	16.32	306	0.03	0.43
433	20	N	54°31.77	E	10°02.36	19.05.201	10:40:55		3.88	20.71	211.7	0.4	2.21
433	25	N	54°31.77	E	10°02.36	19.05.201	10:40:55		3.42	21.71	167.3	0.66	3.05
434	1	N	54°31.77	E	10°02.36	02.06.201	10:16:43	10.71973487	12.23	13.05	326.6	0.07	0.06

434	5	N	54°31.77	E	10°02.36	02.06.201	0	10:16:43	14.75975941	12.21	13.07	330.4	0.06	0.03
434	10	N	54°31.77	E	10°02.36	02.06.201	0	10:16:43	12.08732091	11.7	13.5	324.4	0.06	0.11
434	15	N	54°31.77	E	10°02.36	02.06.201	0	10:16:43	13.72344449	7.43	17.91	297.1	0.05	0.23
434	20	N	54°31.77	E	10°02.36	02.06.201	0	10:16:43	27.22981073	4.39	20.6	234.4	0.34	1.8
434	25	N	54°31.77	E	10°02.36	02.06.201	0	10:16:43	28.50647121	3.66	21.54	114.6	0.5	3.33
435	1	N	54°31.77	E	10°02.36	01.07.201	0	10:05:47	8.811144459	17.76	12.73	298	0.01	0.07
435	5	N	54°31.77	E	10°02.36	01.07.201	0	10:05:47	8.828108436	17.55	12.71	295.8	0.01	0.01
435	10	N	54°31.77	E	10°02.36	01.07.201	0	10:05:47	9.968214495	14.08	13.99	284.3	0.04	0.05
435	15	N	54°31.77	E	10°02.36	01.07.201	0	10:05:47	12.07184966	11.05	16.2	280.8	0.05	0.13
435	20	N	54°31.77	E	10°02.36	01.07.201	0	10:05:47	14.58591298	7.32	18.786	188.8	0.22	0.93
435	25	N	54°31.77	E	10°02.36	01.07.201	0	10:05:47	14.53719245	4.29	21.114	70.9	0.17	3.15
436	1	N	54°31.77	E	10°02.36	10.08.201	0	09:46:58	8.026487238	19.55	12.5	276.7	0.05	0.2
436	5	N	54°31.77	E	10°02.36	10.08.201	0	09:46:58	8.763638788	19.5	12.65	275.2	0.04	0.02
436	10	N	54°31.77	E	10°02.36	10.08.201	0	09:46:58	11.41558313	16.14	15.57	245.8	0	0.04
436	15	N	54°31.77	E	10°02.36	10.08.201	0	09:46:58	14.63716024	11.44	18.94	157.7	0.02	0.17
436	20	N	54°31.77	E	10°02.36	10.08.201	0	09:46:58	16.25168123	7.47	22.12	75.7	0.22	6.61
436	25	N	54°31.77	E	10°02.36	10.08.201	0	09:46:58	12.38446619	9.59	24.74	28.5	0.65	6.08
437	1	N	54°31.77	E	10°02.36	21.09.201	0	10:00:32	10.13063779	14.25	15.34	285.4	0.01	0.11
437	5	N	54°31.77	E	10°02.36	21.09.201	0	10:00:32	14.75343466	14.21	15.55	286.5	0.01	0.01

437	10	N	54°31.77	E	10°02.36	21.09.201	0	10:00:32	11.76771206	14.09	16.56	272.2	0.01	0.05
437	15	N	54°31.77	E	10°02.36	21.09.201	0	10:00:32	11.38909853	13.71	17.44	205.5	0.09	0.27
437	20	N	54°31.77	E	10°02.36	21.09.201	0	10:00:32	16.3043826	10.85	21.56	34.1	0.34	2.61
437	25	N	54°31.77	E	10°02.36	21.09.201	0	10:00:32	11.6890804	9.52	22.33	10.3	0.2	4.56
438	1	N	54°31.77	E	10°02.36	13.10.201	0	10:59:35	14.05219992	12.41	16.24	300.1	0.01	0.09
438	5	N	54°31.77	E	10°02.36	13.10.201	0	10:59:35	12.53418193	12.45	16.31	299.5	0.01	0.01
438	10	N	54°31.77	E	10°02.36	13.10.201	0	10:59:35	11.08387916	12.92	16.85	295.9	0.01	0.03
438	15	N	54°31.77	E	10°02.36	13.10.201	0	10:59:35	9.667744891	13.06	17.03	280.2	0.02	0.13
438	20	N	54°31.77	E	10°02.36	13.10.201	0	10:59:35	10.48191104	13.09	19.87	179	0.05	0.42
438	25	N	54°31.77	E	10°02.36	13.10.201	0	10:59:35	10.9936946	11.4	21.21	26.6	0.3	2.21
439	1	N	54°31.77	E	10°02.36	16.11.201	0	10:01:22	12.93633166	8.93	19.42	305.8	0.37	2.59
439	5	N	54°31.77	E	10°02.36	16.11.201	0	10:01:22	13.15482046	8.91	19.4	296.7	0.38	2.82
439	10	N	54°31.77	E	10°02.36	16.11.201	0	10:01:22	14.96020003	9.54	20.3	276.3	0.46	3.35
439	15	N	54°31.77	E	10°02.36	16.11.201	0	10:01:22	13.40319814	9.57	20.75	267	0.37	3.18
439	20	N	54°31.77	E	10°02.36	16.11.201	0	10:01:22	11.43244327	9.92	22.67	246.6	0.14	2.23
439	25	N	54°31.77	E	10°02.36	16.11.201	0	10:01:22	10.60917105	9.93	22.74	243.8	0.15	2.4
442	1	N	54°31.77	E	10°02.36	18.02.201	1	09:52:20		1.4	18.46	384.5	0.24	6.18
442	5	N	54°31.77	E	10°02.36	18.02.201	1	09:52:20		1.4	18.46	386	0.23	6.19
442	10	N	54°31.77	E	10°02.36	18.02.201	1	09:52:20		1.4	18.46	385.9	0.23	6.26

442	15	N	54°31.77	E	10°02.36	18.02.201	1	09:52:20	11.78615009	0.48	18.53	383.4	0.24	6.29
442	20	N	54°31.77	E	10°02.36	18.02.201	1	09:52:20	13.00162066	0.59	22.67	329.2	0.1	6.08
442	25	N	54°31.77	E	10°02.36	18.02.201	1	09:52:20	12.46765936	0.45	23.05	325.7	0.09	5.9
443	1	N	54°31.77	E	10°02.36	08.03.201	1	10:01:22	13.65840736	0.63	14.24	479.4	0.24	0.02
443	5	N	54°31.77	E	10°02.36	08.03.201	1	10:01:22	13.65840736	0.63	16.22	439.2	0.22	0.77
443	10	N	54°31.77	E	10°02.36	08.03.201	1	10:01:22	13.65840736	0.63	17.17	425.7	0.15	0.91
443	15	N	54°31.77	E	10°02.36	08.03.201	1	10:01:22	13.65840736	0.63	17.84	400.4	0.19	2.56
443	20	N	54°31.77	E	10°02.36	08.03.201	1	10:01:22	14.05726777	1.08	18.79	365.6	0.21	3.9
443	25	N	54°31.77	E	10°02.36	08.03.201	1	10:01:22	14.05726777	1.08	22.3	297.9	0.27	5.9
444	1	N	54°31.77	E	10°02.36	19.04.201	1	10:30:13	17.1857872	6.9	17	391.7	0.02	0.03
444	5	N	54°31.77	E	10°02.36	19.04.201	1	10:30:13	22.01144957	6.56	16.95	387.2	0.03	0.01
444	10	N	54°31.77	E	10°02.36	19.04.201	1	10:30:13	20.98244598	3.9	17.48	346.3	0.05	0.53
444	15	N	54°31.77	E	10°02.36	19.04.201	1	10:30:13	20.98244598	3.9	18.67	325.6	0.04	0.73
444	20	N	54°31.77	E	10°02.36	19.04.201	1	10:30:13	18.33808326	4.19	20.947	302.3	0.06	1.65
444	25	N	54°31.77	E	10°02.36	19.04.201	1	10:30:13	18.41947846	4.64	21.575	298.5	0.06	1.81
445	1	N	54°31.77	E	10°02.36	13.05.201	1	09:50:37	10.84960819	11.46	14.06	337.1	0.06	0.03
445	5	N	54°31.77	E	10°02.36	13.05.201	1	09:50:37	11.75436917	11.52	14.19	340.2	0.06	0.01
445	10	N	54°31.77	E	10°02.36	13.05.201	1	09:50:37	13.57600214	11.49	15.75	330.8	0.05	0.05
445	15	N	54°31.77	E	10°02.36	13.05.201	1	09:50:37	11.29267812	10.75	16.59	312.8	0.05	0.11

445	20	54°31.77 N	10°02.36 E	13.05.201 1	09:50:37	6.868024379	6.26	18.87	270.6	0.16	0.93
445	25	54°31.77 N	10°02.36 E	13.05.201 1	09:50:37	17.01168751	4.4	20.88	241.5	0.26	2.36
446	1	54°31.77 N	10°02.36 E	21.06.201 1	10:25:49	8.935930495	15.4	15.58	290.8	0.05	0.06
446	5	54°31.77 N	10°02.36 E	21.06.201 1	10:25:49	9.663706879	15.01	15.87	286.8	0.06	0.04
446	10	54°31.77 N	10°02.36 E	21.06.201 1	10:25:49	10.58732895	11.68	17.69	265.4	0.05	0.01
446	15	54°31.77 N	10°02.36 E	21.06.201 1	10:25:49	11.88659613	8.19	20.22	225.3	0.1	0.52
446	20	54°31.77 N	10°02.36 E	21.06.201 1	10:25:49	14.26859117	6.96	21.76	170.5	0.32	4.54
446	25	54°31.77 N	10°02.36 E	21.06.201 1	10:25:49	16.0949749	6.91	22.12	162.2	0.29	5.25
447	1	54°31.77 N	10°02.36 E	25.07.201 1	09:48:36	11.36219366	16.03	16.44	268.8	0.07	0.03
447	5	54°31.77 N	10°02.36 E	25.07.201 1	09:48:36	10.46394201	15.65	16.87	250.8	0.07	0.03
447	10	54°31.77 N	10°02.36 E	25.07.201 1	09:48:36	13.17908757	14.34	17.85	208.1	0.1	0.51
447	15	54°31.77 N	10°02.36 E	25.07.201 1	09:48:36	15.11440411	11.74	20.26	179.9	0.15	1.51
447	20	54°31.77 N	10°02.36 E	25.07.201 1	09:48:36	15.36701649	10.92	21.44	170.7	0.16	2.33
447	25	54°31.77 N	10°02.36 E	25.07.201 1	09:48:36	16.2549769	9.43	22.46	144.3	0.16	3.43
448	1	54°31.77 N	10°02.36 E	01.08.201 1	11:06:18	8.302751584	17.81	14.2	289.2	0.01	0.03
448	5	54°31.77 N	10°02.36 E	01.08.201 1	11:06:18	7.985503409	17.77	14.23	286.8	0.01	0.01
448	10	54°31.77 N	10°02.36 E	01.08.201 1	11:06:18	9.233731323	16.26	15.89	254	0.01	0.02
448	15	54°31.77 N	10°02.36 E	01.08.201 1	11:06:18	9.092036357	14.6	17.54	204.4	0.03	0.1
448	20	54°31.77 N	10°02.36 E	01.08.201 1	11:06:18	13.41314969	10.39	21.4	128.7	0.12	1.48

448	25	N	54°31.77	E	10°02.36	01.08.201	1	11:06:18	12.89402973	9.36	22.84	117.7	0.14	3.01
449	1	N	54°31.77	E	10°02.36	21.09.201	1	11:06:18	9.642140171	13.184	20.648	202.5	0.02	0.01
449	5	N	54°31.77	E	10°02.36	21.09.201	1	11:06:18	9.655295593	13.132	20.656	187.7	0.03	0.03
449	10	N	54°31.77	E	10°02.36	21.09.201	1	11:06:18	9.215925766	12.844	21.711	88.3	0.08	0.09
449	15	N	54°31.77	E	10°02.36	21.09.201	1	11:06:18	9.352787965	12.959	22.57	108.5	0.14	0.25
449	20	N	54°31.77	E	10°02.36	21.09.201	1	11:06:18	8.418264811	12.201	23.272	85.4	0.23	0.56
449	25	N	54°31.77	E	10°02.36	21.09.201	1	11:06:18	7.273030731	12.222	23.544	97.6	0.19	0.54
451	1	N	54°31.77	E	10°02.36	08.11.201	1	11:07:35	13.59028665	10.64	20.82	287.6	0.05	0.24
451	5	N	54°31.77	E	10°02.36	08.11.201	1	11:07:35	12.67673689	10.64	20.81	287.9	0.05	0.23
451	10	N	54°31.77	E	10°02.36	08.11.201	1	11:07:35	13.39078496	10.64	20.83	286.7	0.05	0.21
451	15	N	54°31.77	E	10°02.36	08.11.201	1	11:07:35	12.83871018	10.64	20.87	288.3	0.03	0.15
451	20	N	54°31.77	E	10°02.36	08.11.201	1	11:07:35	10.49819479	10.65	20.94	288.6	0.01	0.07
451	25	N	54°31.77	E	10°02.36	08.11.201	1	11:07:35	9.162214307	11.45	22.18	161.4	0.52	1.05
453	1	N	54°31.77	E	10°02.36	11.01.201	2	11:19:51	12.19281252	5.28	21	337.8	0.15	5.16
453	5	N	54°31.77	E	10°02.36	11.01.201	2	11:19:51	14.26131651	5.24	21	337.4	0.15	5.18
453	10	N	54°31.77	E	10°02.36	11.01.201	2	11:19:51	14.37144511	5.25	21.01	337.6	0.16	5.27
453	15	N	54°31.77	E	10°02.36	11.01.201	2	11:19:51	13.77506756	5.31	21.1	326.4	0.18	5.51
453	20	N	54°31.77	E	10°02.36	11.01.201	2	11:19:51	13.67101996	6.22	22.11	286.2	0.22	6.32
453	25	N	54°31.77	E	10°02.36	11.01.201	2	11:19:51	11.9051395	6.55	22.39	272.4	0.27	6.38

455	1	N	54°31.77	E	10°02.36	13.03.201	2	10:26:25	16.2491368	3.217	16.034	429.8	0.07	0.05
455	5	N	54°31.77	E	10°02.36	13.03.201	2	10:26:25	17.47501977	3.19	16.036	429.8	0.06	0.02
455	10	N	54°31.77	E	10°02.36	13.03.201	2	10:26:25		3.259	16.061	430.1	0.05	0.01
455	15	N	54°31.77	E	10°02.36	13.03.201	2	10:26:25	17.51147265	3.4	16.077	422.7	0.11	0.07
455	20	N	54°31.77	E	10°02.36	13.03.201	2	10:26:25	18.52905454	2.479	17.753	367.3	0.44	4.96
455	25	N	54°31.77	E	10°02.36	13.03.201	2	10:26:25	20.13657094	2.067	18.969	351	0.55	7.44
456	1	N	54°31.77	E	10°02.36	10.04.201	2	12:50:17	16.40345583	5.167	16.295	355.6	0	0.01
456	5	N	54°31.77	E	10°02.36	10.04.201	2	12:50:17	15.51889356	5.16	16.297	355.3	0.01	0.02
456	10	N	54°31.77	E	10°02.36	10.04.201	2	12:50:17	16.77514632	5.141	16.317	351.4	0.01	0.05
456	15	N	54°31.77	E	10°02.36	10.04.201	2	12:50:17	16.604436	4.83	16.992	332.3	0.02	0.23
456	20	N	54°31.77	E	10°02.36	10.04.201	2	12:50:17	17.12842176	4.663	17.394	316.9	0.03	0.56
456	25	N	54°31.77	E	10°02.36	10.04.201	2	12:50:17	18.90655666	4.423	17.923	301.6	0.05	0.7
457	1	N	54°31.77	E	10°02.36	14.05.201	2	09:58:42	12.72445794	9.87	13.3	333.7	0.02	0.03
457	5	N	54°31.77	E	10°02.36	14.05.201	2	09:58:42	11.98188802	9.78	13.47	338.5	0.03	0.03
457	10	N	54°31.77	E	10°02.36	14.05.201	2	09:58:42		9.32	14.43	336	0.02	0.01
457	15	N	54°31.77	E	10°02.36	14.05.201	2	09:58:42	12.8783357	7.55	16.33	317.1	0.1	0.25
457	20	N	54°31.77	E	10°02.36	14.05.201	2	09:58:42		5.75	17.66	258.3	0.33	1.21
457	25	N	54°31.77	E	10°02.36	14.05.201	2	09:58:42	12.9756249	5.66	17.77	249.2	0.36	1.41
458	1	N	54°31.77	E	10°02.36	26.06.201	2	09:42:23	12.23938015	14.007	14.673	299.3	0.05	0.04

458	5	N	54°31.77	E	10°02.36	26.06.201	2	09:42:23	10.69672598	14.01	14.677	297.1	0.04	0.02
458	10	N	54°31.77	E	10°02.36	26.06.201	2	09:42:23	11.17102168	13.468	15.239	288.2	0.05	0.01
458	15	N	54°31.77	E	10°02.36	26.06.201	2	09:42:23	12.07722084	10.886	16.737	264.1	0.05	0.04
458	20	N	54°31.77	E	10°02.36	26.06.201	2	09:42:23	14.18150032	9.708	17.87	207.9	0.07	0.14
458	25	N	54°31.77	E	10°02.36	26.06.201	2	09:42:23	13.68324764	9.299	18.803	148.4	0.08	0.17
459	1	N	54°31.77	E	10°02.36	16.07.201	2	11:36:19	10.90418255	15.748	15.194	288.7	0.01	0.02
459	5	N	54°31.77	E	10°02.36	16.07.201	2	11:36:19	10.9233882	15.703	15.198	283.5	0.02	0.03
459	10	N	54°31.77	E	10°02.36	16.07.201	2	11:36:19	12.06949498	14.102	15.957	267.7	0.02	0.01
459	15	N	54°31.77	E	10°02.36	16.07.201	2	11:36:19	12.78066571	12.42	16.906	234.5	0.08	0.12
459	20	N	54°31.77	E	10°02.36	16.07.201	2	11:36:19	13.51841284	9.484	18.362	95.3	0.36	0.98
459	25	N	54°31.77	E	10°02.36	16.07.201	2	11:36:19	13.7775937	9.256	18.639	82.9	0.55	1.83
460	1	N	54°31.77	E	10°02.36	07.08.201	2	09:50:20	11.00600884	15.104	16.829	254.9	0.05	0.02
460	5	N	54°31.77	E	10°02.36	07.08.201	2	09:50:20	12.18696781	14.927	16.892	229.2	0.06	0.03
460	10	N	54°31.77	E	10°02.36	07.08.201	2	09:50:20	11.86321941	12.609	18.795	177.2	0.07	0.04
460	15	N	54°31.77	E	10°02.36	07.08.201	2	09:50:20	11.98363859	12.322	19.056	156.6	0.09	0.07
460	20	N	54°31.77	E	10°02.36	07.08.201	2	09:50:20	11.73897717	11.623	20.708	129.1	0.12	0.07
460	25	N	54°31.77	E	10°02.36	07.08.201	2	09:50:20	9.350190461	11.389	22.979	76.7	0.04	0.08
461	1	N	54°31.77	E	10°02.36	27.09.201	2	10:14:06	13.66490819	13.253	18.947	266.6	0.04	0.01
461	5	N	54°31.77	E	10°02.36	27.09.201	2	10:14:06	13.27666281	13.284	18.996	251.7	0.04	0.03

461	10	N	54°31.77	E	10°02.36	27.09.201	2	10:14:06	11.10117274	13.857	22.378	101.6	0.14	0.24
461	15	N	54°31.77	E	10°02.36	27.09.201	2	10:14:06	9.139116547	13.594	22.639	82.5	0.15	0.26
461	20	N	54°31.77	E	10°02.36	27.09.201	2	10:14:06	9.151297489	13.489	22.806	74.8	0.18	0.26
461	25	N	54°31.77	E	10°02.36	27.09.201	2	10:14:06	6.396170734	13.013	22.953	51.3	0.24	0.32
462	1	N	54°31.77	E	10°02.36	02.10.201	2	09:46:32	12.48744526	13.46	21.019	221	0.02	0.02
462	5	N	54°31.77	E	10°02.36	02.10.201	2	09:46:32	11.82860731	13.47	21.075	217.1	0.02	0.02
462	10	N	54°31.77	E	10°02.36	02.10.201	2	09:46:32	8.839588666	13.503	21.487	203.5	0.03	0.06
462	15	N	54°31.77	E	10°02.36	02.10.201	2	09:46:32	11.93192972	13.814	22.216	130.5	0.09	0.17
462	20	N	54°31.77	E	10°02.36	02.10.201	2	09:46:32	8.454898636	12.909	22.903	23.9	0.28	0.22
462	25	N	54°31.77	E	10°02.36	02.10.201	2	09:46:32	10.50957837	13.011	23.584	55	0.27	0.31
463	1	N	54°31.77	E	10°02.36	06.11.201	2	09:55:43	14.23460833	9.466	18.926	300.9	0.03	0.03
463	5	N	54°31.77	E	10°02.36	06.11.201	2	09:55:43	14.17289728	9.468	18.933	302.8	0.02	0.01
463	10	N	54°31.77	E	10°02.36	06.11.201	2	09:55:43	13.73938821	9.507	18.961	290.8	0.03	0
463	15	N	54°31.77	E	10°02.36	06.11.201	2	09:55:43	13.13901191	10.063	19.607	258.8	0.05	0.04
463	20	N	54°31.77	E	10°02.36	06.11.201	2	09:55:43	11.98632282	11.876	21.243	119.7	0.48	0.84
463	25	N	54°31.77	E	10°02.36	06.11.201	2	09:55:43	11.68592001	12.118	21.6	95.8	0.59	0.95
464	1	N	54°31.77	E	10°02.36	04.12.201	2	09:50:43	16.31790389	6.761	18.053	327.2	0.13	0.14
464	5	N	54°31.77	E	10°02.36	04.12.201	2	09:50:43	16.38910109	6.792	18.116	268.2	0.13	0.26
464	10	N	54°31.77	E	10°02.36	04.12.201	2	09:50:43	15.94714478	8.064	19.093	276.8	0.24	0.54

464	15	N	54°31.77	E	10°02.36	04.12.201	2	09:50:43	15.90196957	8.574	19.592	264.3	0.5	0.93
464	20	N	54°31.77	E	10°02.36	04.12.201	2	09:50:43	14.80977549	8.699	19.7	206.8	0.66	1.25
464	25	N	54°31.77	E	10°02.36	04.12.201	2	09:50:43	15.43561999	8.849	19.796	198.9	0.72	1.44
466	1	N	54°31.77	E	10°02.36	06.02.201	3	10:49:59	18.12632622	2.034	15.576	380.7	0.86	6
466	5	N	54°31.77	E	10°02.36	06.02.201	3	10:49:59	18.16439178	2.029	15.579	380.7	0.84	6.02
466	10	N	54°31.77	E	10°02.36	06.02.201	3	10:49:59	18.15450998	2.034	15.592	379.2	0.84	6.01
466	15	N	54°31.77	E	10°02.36	06.02.201	3	10:49:59	18.46177233	2.259	15.891	365.1	0.86	6.44
466	20	N	54°31.77	E	10°02.36	06.02.201	3	10:49:59	17.13237944	3.642	18.101	284.8	1.01	6.75
466	25	N	54°31.77	E	10°02.36	06.02.201	3	10:49:59	18.20536294	4.57	19.653	249.8	1.03	7.05
467	1	N	54°31.77	E	10°02.36	05.03.201	3	10:51:02	20.86836796	1.257	14.043	414.8	0.59	3.93
467	5	N	54°31.77	E	10°02.36	05.03.201	3	10:51:02	21.01090089	1.282	15.086	410.3	0.71	6.16
467	10	N	54°31.77	E	10°02.36	05.03.201	3	10:51:02	21.39500179	1.222	15.344	386.8	0.81	7.05
467	15	N	54°31.77	E	10°02.36	05.03.201	3	10:51:02	21.51627703	1.167	15.427	337.2	0.87	7.38
467	20	N	54°31.77	E	10°02.36	05.03.201	3	10:51:02	20.25118925	1.969	17.575	268.9	0.87	7.56
467	25	N	54°31.77	E	10°02.36	05.03.201	3	10:51:02	21.82257549	3.152	20.356	223.3	0.82	8
468	1	N	54°31.77	E	10°02.36	03.04.201	3	10:14:50	13.66908221	1.478	12.769	443.4	0.17	0.91
468	5	N	54°31.77	E	10°02.36	03.04.201	3	10:14:50	15.26746264	1.036	13.351	433.5	0.3	2.11
468	10	N	54°31.77	E	10°02.36	03.04.201	3	10:14:50	17.84835166	1.067	13.774	422.1	0.46	3.66
468	15	N	54°31.77	E	10°02.36	03.04.201	3	10:14:50	18.12853238	0.712	13.926	412.1	0.52	4.56

468	20	54°31.77 N	10°02.36 E	03.04.201 3	10:14:50	17.88084976	0.7	14.144	399.7	0.52	4.86
468	25	54°31.77 N	10°02.36 E	03.04.201 3	10:14:50	19.64593515	0.64	14.648	393.4	0.47	4.5
469	1	54°31.77 N	10°02.36 E	24.05.201 3	10:33:39	12.52146546	11.202	13.05	312.8	0.08	0.02
469	5	54°31.77 N	10°02.36 E	24.05.201 3	10:33:39	12.69276322	11.06	15.151	328	0.09	0.01
469	10	54°31.77 N	10°02.36 E	24.05.201 3	10:33:39	12.53203517	11.125	13.225	327.4	0.1	0.03
469	15	54°31.77 N	10°02.36 E	24.05.201 3	10:33:39	14.9061183	8.47	14.745	347	0.11	0.01
469	20	54°31.77 N	10°02.36 E	24.05.201 3	10:33:39	15.50821951	4.627	20.398	230	0.17	1.01
469	25	54°31.77 N	10°02.36 E	24.05.201 3	10:33:39	15.69377397	5.108	21.782	163.2	0.25	1.4
470	1	54°31.77 N	10°02.36 E	04.06.201 3	10:10:04	11.40978605	13.869	12.564	312.9	0.05	0.02
470	5	54°31.77 N	10°02.36 E	04.06.201 3	10:10:04	12.42384914	13.871	12.563	312.9	0.05	0.03
470	10	54°31.77 N	10°02.36 E	04.06.201 3	10:10:04	12.47490234	13.793	12.553	314	0.05	0.05
470	15	54°31.77 N	10°02.36 E	04.06.201 3	10:10:04	12.81760374	13.59	12.661	313.7	0.06	0.07
470	20	54°31.77 N	10°02.36 E	04.06.201 3	10:10:04	16.33099473	5.983	17.676	278.9	0.13	0.63
470	25	54°31.77 N	10°02.36 E	04.06.201 3	10:10:04	17.28640611	5.285	21.715	172.5	0.27	2.06
471	1	54°31.77 N	10°02.36 E	04.07.201 3	10:30:39	10.69100481	16.087	13.121	299.9	0.05	0.01
471	5	54°31.77 N	10°02.36 E	04.07.201 3	10:30:39	10.92013025	14.877	14.671	295.2	0.05	0.03
471	10	54°31.77 N	10°02.36 E	04.07.201 3	10:30:39	14.95527908	8.147	19.573	208.7	0.07	0.04
471	15	54°31.77 N	10°02.36 E	04.07.201 3	10:30:39	15.40382886	7.644	21.635	190.2	0.31	1.11
471	20	54°31.77 N	10°02.36 E	04.07.201 3	10:30:39	14.81771318	7.373	23.198	188.8	0.34	2.12

471	25	54°31.77 N	10°02.36 E	04.07.201 3	10:30:39	13.85235076	7.752	24.791	184.5	0.29	2.41
472	1	54°31.77 N	10°02.36 E	28.08.201 3	11:05:05	9.291755986	18.732	15.817	273.4	0.03	0.03
472	5	54°31.77 N	10°02.36 E	28.08.201 3	11:05:05	10.29425403	17.851	16.95	267.7	0.03	0.01
472	10	54°31.77 N	10°02.36 E	28.08.201 3	11:05:05	10.75322018	16.733	18.52	246.7	0.03	0.02
472	15	54°31.77 N	10°02.36 E	28.08.201 3	11:05:05	11.26516197	16.35	18.783	226	0.04	0.03
472	20	54°31.77 N	10°02.36 E	28.08.201 3	11:05:05	11.51000152	12.762	22.464	134.5	0.08	0.13
472	25	54°31.77 N	10°02.36 E	28.08.201 3	11:05:05	10.43105329	9.082	24.224	49	0.53	1.33
473	1	54°31.77 N	10°02.36 E	24.09.201 3	10:09:55	9.554878402	15.534	15.508	289.3	0.04	0.02
473	5	54°31.77 N	10°02.36 E	24.09.201 3	10:09:55	10.37583691	15.538	15.517	288.5	0.03	0.1
473	10	54°31.77 N	10°02.36 E	24.09.201 3	10:09:55	9.845582085	15.761	16.443	246.7	0.03	0.01
473	15	54°31.77 N	10°02.36 E	24.09.201 3	10:09:55	9.786742641	15.731	17.276	239.4	0.02	0.03
473	20	54°31.77 N	10°02.36 E	24.09.201 3	10:09:55	9.560336038	15.152	20.144	109.5	0.03	0.02
473	25	54°31.77 N	10°02.36 E	24.09.201 3	10:09:55	5.314754759	11.247	23.057	27.1	0.2	0.013
474	1	54°31.77 N	10°02.36 E	01.10.201 3	10:08:17	10.46384604	14.162	16.389	279	0.04	0.04
474	5	54°31.77 N	10°02.36 E	01.10.201 3	10:08:17	10.37615747	14.28	16.651	262.9	0.04	0.01
474	10	54°31.77 N	10°02.36 E	01.10.201 3	10:08:17	10.15729116	14.455	17.149	248	0.04	0.02
474	15	54°31.77 N	10°02.36 E	01.10.201 3	10:08:17	8.593077961	14.633	20.35	68.5	0.06	0.04
474	20	54°31.77 N	10°02.36 E	01.10.201 3	10:08:17	8.209142831	13.16	22.386	37.1	0.22	0.17
474	25	54°31.77 N	10°02.36 E	01.10.201 3	10:08:17	2.710086896	10.252	23.574	9.8	0.32	0.3

475	1	N	54°31.77	10°02.36	05.11.201	10:24:16	10.48866017	11.473	17.68	273.9	0.13	0.46
475	5	N	54°31.77	10°02.36	05.11.201	10:24:16	11.15269623	11.473	17.695	273.7	0.14	0.51
475	10	N	54°31.77	10°02.36	05.11.201	10:24:16	10.87847084	11.478	17.783	267	0.15	0.79
475	15	N	54°31.77	10°02.36	05.11.201	10:24:16	11.19499428	11.991	19.424	239.7	0.22	1.85
475	20	N	54°31.77	10°02.36	05.11.201	10:24:16	11.19535142	12.16	23.937	238.2	0.3	3.18
475	25	N	54°31.77	10°02.36	05.11.201	10:24:16	11.70352271	12.112	24.343	239.2	0.32	3.31
476	1	N	54°31.77	10°02.36	03.12.201	10:17:22	13.89339691	7.066	19.642	334.6	0.01	0.04
476	5	N	54°31.77	10°02.36	03.12.201	10:17:22	13.9209849	7.078	19.644	334.4	0.01	0.01
476	10	N	54°31.77	10°02.36	03.12.201	10:17:22	14.47821079	7.091	19.669	327.2	0.05	0.14
476	15	N	54°31.77	10°02.36	03.12.201	10:17:22	14.26020989	9.087	23.003	238.7	0.21	2.66
476	20	N	54°31.77	10°02.36	03.12.201	10:17:22	17.18439524	11.191	25.287	162.5	0.33	5.3
476	25	N	54°31.77	10°02.36	03.12.201	10:17:22	16.5895773	11.143	25.661	151.1	0.35	5.16
477	1	N	54°31.77	10°02.36	25.02.201	09:41:38	14.27574837	2.856	16.62	396.4	0.39	2.9
477	5	N	54°31.77	10°02.36	25.02.201	09:41:38	15.20458224	2.805	16.653	392.3	0.48	3.71
477	10	N	54°31.77	10°02.36	25.02.201	09:41:38	15.80760731	2.641	17.392	371.7	0.67	5.75
477	15	N	54°31.77	10°02.36	25.02.201	09:41:38	15.67082395	2.538	18.227	356.1	0.85	6.76
477	20	N	54°31.77	10°02.36	25.02.201	09:41:38	15.7504203	2.69	19.332	318.9	0.89	7.36
477	25	N	54°31.77	10°02.36	25.02.201	09:41:38	15.53819726	3.433	21.489	311	0.27	7.63
478	1	N	54°31.77	10°02.36	05.03.201	09:41:08	16.17226603	3.242	17.57	418.9	0.1	0.24

478	5	N	54°31.77	E	10°02.36	05.03.201	4	09:41:08	18.641766	2.866	18.119	359.6	0.53	4.95
478	10	N	54°31.77	E	10°02.36	05.03.201	4	09:41:08	19.07595902	2.752	18.864	333.4	0.5	6.92
478	15	N	54°31.77	E	10°02.36	05.03.201	4	09:41:08	16.71219343	3.436	20.255	345.8	0.24	6.32
478	20	N	54°31.77	E	10°02.36	05.03.201	4	09:41:08	16.02716413	3.519	20.862	326.2	0.19	7.2
478	25	N	54°31.77	E	10°02.36	05.03.201	4	09:41:08	17.29778351	3.652	21.751	301.6	0.15	8
479	1	N	54°31.77	E	10°02.36	15.04.201	4	09:54:34	12.07160658	7.286	17.058	348.2	0.01	0.41
479	5	N	54°31.77	E	10°02.36	15.04.201	4	09:54:34	12.77780541	7.278	17.091	349.2	0.06	0.44
479	10	N	54°31.77	E	10°02.36	15.04.201	4	09:54:34	12.67624445	7.44	17.502	347.4	0.12	0.46
479	15	N	54°31.77	E	10°02.36	15.04.201	4	09:54:34	12.64546052	7.365	18.141	345.9	0.16	0.49
479	20	N	54°31.77	E	10°02.36	15.04.201	4	09:54:34		6.846	19.611	337.8	0.22	0.51
479	25	N	54°31.77	E	10°02.36	15.04.201	4	09:54:34		5.765	22.47	258.7	0.34	2.2
480	1	N	54°31.77	E	10°02.36	07.05.201	4	09:50:38	12.32599858	11.093	15.218	326.4	0.33	0.57
480	5	N	54°31.77	E	10°02.36	07.05.201	4	09:50:38	13.32844081	11.117	16.101	318.9	0.38	0.58
480	10	N	54°31.77	E	10°02.36	07.05.201	4	09:50:38	13.80818081	9.646	17.44	306.6	0.4	0.75
480	15	N	54°31.77	E	10°02.36	07.05.201	4	09:50:38	14.43644959	7.875	18.992	283.8	0.45	1.22
480	20	N	54°31.77	E	10°02.36	07.05.201	4	09:50:38	15.04551708	6.606	20.926	237.1	0.58	2.7
480	25	N	54°31.77	E	10°02.36	07.05.201	4	09:50:38	15.47398882	6.058	22.182	199.8	0.69	3.72
481	1	N	54°31.77	E	10°02.36	21.06.201	4	10:23:37	9.990157577	17.016	14.31	287.9	0.07	0.03
481	5	N	54°31.77	E	10°02.36	21.06.201	4	10:23:37	9.955937014	16.998	14.332	289.5	0.06	0.01

481	10	N	54°31.77	E	10°02.36	21.06.201	4	10:23:37	10.14409438	16.902	15.212	294.3	0.06	0.03
481	15	N	54°31.77	E	10°02.36	21.06.201	4	10:23:37	12.03198786	13.177	16.205	280	0.07	0.03
481	20	N	54°31.77	E	10°02.36	21.06.201	4	10:23:37	13.63350318	9.701	18.822	169	0.11	0.09
481	25	N	54°31.77	E	10°02.36	21.06.201	4	10:23:37	15.34896521	7.483	20.736	99.8	0.1	0.14
482	1	N	54°31.77	E	10°02.36	08.07.201	4	09:47:10	9.730200066	18.113	15.471	281.6	0.11	0.05
482	5	N	54°31.77	E	10°02.36	08.07.201	4	09:47:10	9.735079801	17.981	15.569	281.7	0.13	0.02
482	10	N	54°31.77	E	10°02.36	08.07.201	4	09:47:10	10.8559898	15.149	18.259	267	0	0
482	15	N	54°31.77	E	10°02.36	08.07.201	4	09:47:10	10.97171543	14.097	20.105	239.6	0.01	0.01
482	20	N	54°31.77	E	10°02.36	08.07.201	4	09:47:10	11.93856763	12.092	21.476	174.2	0.05	0.04
482	25	N	54°31.77	E	10°02.36	08.07.201	4	09:47:10	11.45905403	10.921	22.54	120.6	0.08	0.12
483	1	N	54°31.77	E	10°02.36	28.08.201	4	10:26:01		16.7	15.589	282.7	0.03	0.06
483	5	N	54°31.77	E	10°02.36	28.08.201	4	10:26:01		16.543	16.245	286.3	0.04	0.05
483	10	N	54°31.77	E	10°02.36	28.08.201	4	10:26:01		13.886	21.71	161.3	0.02	0.03
483	15	N	54°31.77	E	10°02.36	28.08.201	4	10:26:01		14.548	24.496	174.9	0.02	0.04
483	20	N	54°31.77	E	10°02.36	28.08.201	4	10:26:01		14.328	24.588	153	0.03	0.05
483	25	N	54°31.77	E	10°02.36	28.08.201	4	10:26:01		13.66	25.374	116.3	0.03	0.11
484	1	N	54°31.77	E	10°02.36	23.09.201	4	09:43:06	18.11138052	16.507	16.236	280.3	0.06	0.03
484	5	N	54°31.77	E	10°02.36	23.09.201	4	09:43:06	17.01155035	16.502	16.234	278.1	0.08	0.03
484	10	N	54°31.77	E	10°02.36	23.09.201	4	09:43:06	14.96505489	16.551	16.276	276	0.06	0.02

484	15	N	54°31.77	E	10°02.36	23.09.201	4	09:43:06	14.69111903	16.604	16.511	273.9	0	0.01
484	20	N	54°31.77	E	10°02.36	23.09.201	4	09:43:06	11.76417917	16.788	16.606	264.2	0.01	0.03
484	25	N	54°31.77	E	10°02.36	23.09.201	4	09:43:06	5.863286141	13.181	25.082	0	0.23	0.25
485	1	N	54°31.77	E	10°02.36	21.10.201	4	10:10:45	15.84286739	14.337	17.824	278.6	0.16	0.01
485	5	N	54°31.77	E	10°02.36	21.10.201	4	10:10:45	13.77948259	14.361	17.899	273.2	0.18	0.02
485	10	N	54°31.77	E	10°02.36	21.10.201	4	10:10:45	24.89204545	14.6	18.675	250.6	0.21	0.12
485	15	N	54°31.77	E	10°02.36	21.10.201	4	10:10:45	24.84493786	14.602	19.033	243.6	0.24	0.12
485	20	N	54°31.77	E	10°02.36	21.10.201	4	10:10:45	27.53445387	14.607	19.436	212	0.24	0.06
485	25	N	54°31.77	E	10°02.36	21.10.201	4	10:10:45	21.91304447	13.55	24.146	0	0	0.27
486	1	N	54°31.77	E	10°02.36	18.11.201	4	09:50:49	20.43516987	11.556	20.725	269.1	0.5	2.69
486	5	N	54°31.77	E	10°02.36	18.11.201	4	09:50:49	25.20406319	11.545	20.723	269.5	0.52	3.31
486	10	N	54°31.77	E	10°02.36	18.11.201	4	09:50:49	25.56328166	11.546	20.73	268.8	0.56	3.32
486	15	N	54°31.77	E	10°02.36	18.11.201	4	09:50:49	24.52979377	11.561	20.75	268.7	0.59	3.41
486	20	N	54°31.77	E	10°02.36	18.11.201	4	09:50:49	15.58325773	11.646	20.856	263.7	0.6	3.66
486	25	N	54°31.77	E	10°02.36	18.11.201	4	09:50:49	21.78399724	13.021	23.779	163.3	0.46	5.22
487	1	N	54°31.77	E	10°02.36	16.12.201	4	09:50:52	15.58484597	6.616	19.53	318.2	1.24	7.13
487	5	N	54°31.77	E	10°02.36	16.12.201	4	09:50:52	16.01693801	6.62	19.536	317.6	1.34	7.14
487	10	N	54°31.77	E	10°02.36	16.12.201	4	09:50:52	15.57044886	6.631	19.563	309.5	1.37	7.35
487	15	N	54°31.77	E	10°02.36	16.12.201	4	09:50:52	15.08557738	6.693	19.659	312.9	1.11	7.58

487	20	N	54°31.77	E	10°02.36	16.12.201	4	09:50:52	14.60943459	7.296	20.821	288.8	0.9	6.44
487	25	N	54°31.77	E	10°02.36	16.12.201	4	09:50:52	14.85232452	7.979	23.783	262.3	0.42	6.37
488	1	N	54°31.77	E	10°02.36	06.01.201	5	09:54:24	15.45155804	5.606	23.643	332.4	0.69	7.97
488	5	N	54°31.77	E	10°02.36	06.01.201	5	09:54:24	14.46544849	5.611	23.658	334.1	0.75	8.14
488	10	N	54°31.77	E	10°02.36	06.01.201	5	09:54:24	14.98029753	5.649	23.708	331.9	0.86	8.54
488	15	N	54°31.77	E	10°02.36	06.01.201	5	09:54:24	15.31565345	6.277	24.21	310	0.5	7.9
488	20	N	54°31.77	E	10°02.36	06.01.201	5	09:54:24	15.7006478	6.997	25.244	284.4	0.43	7.32
488	25	N	54°31.77	E	10°02.36	06.01.201	5	09:54:24	14.98766795	7.159	24.478	273.6	0.43	7.23
489	1	N	54°31.77	E	10°02.36	23.02.201	5	09:52:42	14.06530394	3.451	23.325	355.3	0.31	4.41
489	5	N	54°31.77	E	10°02.36	23.02.201	5	09:52:42	14.85563626	3.467	23.356	353.7	0.42	4.74
489	10	N	54°31.77	E	10°02.36	23.02.201	5	09:52:42	15.06318571	3.683	23.727	337.4	0.58	6.84
489	15	N	54°31.77	E	10°02.36	23.02.201	5	09:52:42	15.13388706	3.913	24.086	318.1	0.73	7.91
489	20	N	54°31.77	E	10°02.36	23.02.201	5	09:52:42	15.39064269	4.049	24.282	305.1	0.9	8.55
489	25	N	54°31.77	E	10°02.36	23.02.201	5	09:52:42	15.67921369	4.056	24.292	305.5	1.05	8.6
490	1	N	54°31.77	E	10°02.36	17.03.201	5	10:01:02	13.06076516	4.527	18.303	376.9	0.02	0.05
490	5	N	54°31.77	E	10°02.36	17.03.201	5	10:01:02	13.28330417	4.389	18.586	372.3	0.01	0.03
490	10	N	54°31.77	E	10°02.36	17.03.201	5	10:01:02	15.09284436	4.239	18.938	325.3	0.02	0.29
490	15	N	54°31.77	E	10°02.36	17.03.201	5	10:01:02	14.48233481	3.45	21.427	347.8	0.06	1.98
490	20	N	54°31.77	E	10°02.36	17.03.201	5	10:01:02	13.87664114	3.715	23.12	316.4	0.16	5.17

490	25	N	54°31.77	E	10°02.36	17.03.201	10:01:02	16.25117995	3.932	23.619	291.7	0.3	6.81
491	1	N	54°31.77	E	10°02.36	21.04.201	09:55:36	13.441711115	8.264	16.058	352.2	0.15	0.02
491	5	N	54°31.77	E	10°02.36	21.04.201	09:55:36	13.62855031	7.745	16.156	353.9	0	0.02
491	10	N	54°31.77	E	10°02.36	21.04.201	09:55:36	13.28009601	6.79	16.351	346.2	0	0.03
491	15	N	54°31.77	E	10°02.36	21.04.201	09:55:36	14.49802964	6.247	17.184	322.3	0.03	0.31
491	20	N	54°31.77	E	10°02.36	21.04.201	09:55:36	15.25416501	4.498	20.001	270.6	0.14	2.81
491	25	N	54°31.77	E	10°02.36	21.04.201	09:55:36	18.82847704	4.207	22.179	226.5	0.32	5.3
492	1	N	54°31.77	E	10°02.36	12.05.201	10:35:59	13.29746734	10.691	16.564	329.7	0.04	0.01
492	5	N	54°31.77	E	10°02.36	12.05.201	10:35:59	12.50071885	10.613	16.589	328	0.04	0.03
492	10	N	54°31.77	E	10°02.36	12.05.201	10:35:59	13.09891272	9.406	17.071	316.2	0.04	0.07
492	15	N	54°31.77	E	10°02.36	12.05.201	10:35:59	13.26272582	9.175	17.419	311.8	0.05	0.27
492	20	N	54°31.77	E	10°02.36	12.05.201	10:35:59	15.58568442	5.623	20.202	240.7	0.21	2.95
492	25	N	54°31.77	E	10°02.36	12.05.201	10:35:59	16.4238096	4.943	20.943	218.1	0.29	4.08
493	1	N	54°31.77	E	10°02.36	04.06.201	09:48:51	11.22498243	12.036	16.592	306.2	0.04	0.03
493	5	N	54°31.77	E	10°02.36	04.06.201	09:48:51	11.57567681	11.706	16.877	303.2	0.06	0.21
493	10	N	54°31.77	E	10°02.36	04.06.201	09:48:51	11.58401624	9.566	18.495	287.7	0.23	1.77
493	15	N	54°31.77	E	10°02.36	04.06.201	09:48:51	12.46406546	9.134	18.987	274.5	0.27	2.53
493	20	N	54°31.77	E	10°02.36	04.06.201	09:48:51	13.61970481	7.397	20.298	204.1	0.33	5.14
493	25	N	54°31.77	E	10°02.36	04.06.201	09:48:51	14.57045684	6.478	20.988	180.4	0.37	3.63

495	1	N	54°31.77	10°02.36	14.07.201	09:33:48	9.409879276	16.818	15.016	291.8	0.08	0.01
495	5	N	54°31.77	10°02.36	14.07.201	09:33:48	9.644449109	16.683	15.233	289.6	0.08	0.01
495	10	N	54°31.77	10°02.36	14.07.201	09:33:48	9.777900401	15.495	16.235	261.6	0.09	0.11
495	15	N	54°31.77	10°02.36	14.07.201	09:33:48	10.7579344	13.881	17.364	247	0.09	0.08
495	20	N	54°31.77	10°02.36	14.07.201	09:33:48	11.22291208	11.377	18.536	202.9	0.15	0.32
495	25	N	54°31.77	10°02.36	14.07.201	09:33:48	13.00779609	7.944	20.314	115.4	0.25	2.71
496	1	N	54°31.77	10°02.36	04.08.201	09:58:41	7.14584304	17.122	16.389	287	0.05	0.02
496	5	N	54°31.77	10°02.36	04.08.201	09:58:41	6.625784595	16.89	16.434	287.9	0.02	0
496	10	N	54°31.77	10°02.36	04.08.201	09:58:41	8.231420659	15.016	17.205	262.5	0.03	0.05
496	15	N	54°31.77	10°02.36	04.08.201	09:58:41	8.586046923	11.582	19.065	180	0.07	0.13
496	20	N	54°31.77	10°02.36	04.08.201	09:58:41	11.97223953	10.021	19.841	92	0.2	2.53
496	25	N	54°31.77	10°02.36	04.08.201	09:58:41	13.26354727	9.976	20.212	79.9	0.26	4.42
497	1	N	54°31.77	10°02.36	10.09.201	09:50:23	8.960289189	16.548	14.028	286.8	0.07	0.03
497	5	N	54°31.77	10°02.36	10.09.201	09:50:23	9.576092355	16.854	14.381	283.4	0.03	0.01
497	10	N	54°31.77	10°02.36	10.09.201	09:50:23	9.785919012	16.883	14.546	280.3	0.03	0.02
497	15	N	54°31.77	10°02.36	10.09.201	09:50:23	9.213578155	16.835	14.686	256	0.07	0.16
497	20	N	54°31.77	10°02.36	10.09.201	09:50:23	8.811350317	14.834	18.058	80.4	0.75	2.41
497	25	N	54°31.77	10°02.36	10.09.201	09:50:23	8.972331429	14.006	19.568	57.8	0.73	3.14
499	1	N	54°31.77	10°02.36	05.11.201	10:06:48	11.04391337	11.068	16.64	316.8	0.03	0.02

499	5	N	54°31.77	10°02.36	05.11.201	10:06:48	11.74332536	11.054	16.641	315.5	0.03	0.02
499	10	N	54°31.77	10°02.36	05.11.201	10:06:48	11.30889343	11.053	16.656	311.9	0.03	0.04
499	15	N	54°31.77	10°02.36	05.11.201	10:06:48	10.88368371	11.452	16.98	277.3	0.13	0.84
499	20	N	54°31.77	10°02.36	05.11.201	10:06:48	9.326048272	12.8677	19.643	109.8	0.22	5.25
499	25	N	54°31.77	10°02.36	05.11.201	10:06:48	8.61625096	12.911	20.386	73.6	0.22	5.53
500	1	N	54°31.77	10°02.36	08.12.201	10:11:04	7.771754443	8.161	23.228	318.2	0.43	4.52
500	5	N	54°31.77	10°02.36	08.12.201	10:11:04	8.633903195	8.195	23.25	317.2	0.43	4.69
500	10	N	54°31.77	10°02.36	08.12.201	10:11:04	8.763792288	8.374	23.496	309.9	0.44	5.23
500	15	N	54°31.77	10°02.36	08.12.201	10:11:04	9.978250395	8.455	23.753	303.5	0.43	5.28
500	20	N	54°31.77	10°02.36	08.12.201	10:11:04	9.990960064	8.817	24.374	291.7	0.35	4.59
500	25	N	54°31.77	10°02.36	08.12.201	10:11:04	10.52952792	8.295	25.122	287.9	0.3	4.22
503	1	N	54°31.77	10°02.36	08.03.201	10:04:56	13.50831729	3.578	20.644	411.1	0.12	0.03
503	5	N	54°31.77	10°02.36	08.03.201	10:04:56	12.30642047	3.578	20.645	410.8	0.3	0.11
503	10	N	54°31.77	10°02.36	08.03.201	10:04:56	11.98317108	3.58	20.642	374.7	0.31	4.09
503	15	N	54°31.77	10°02.36	08.03.201	10:04:56	12.00940999	4.657	24.197	327.9	0.66	9.37
503	20	N	54°31.77	10°02.36	08.03.201	10:04:56	13.95538268	4.669	24.158	294.1	0.63	9.33
503	25	N	54°31.77	10°02.36	08.03.201	10:04:56	12.60122507	4.662	24.168	277.8	0.57	8.83
504	1	N	54°31.77	10°02.36	12.04.201	09:46:11	14.61098697	6.225	17.078	366.6	0.03	0.25
504	5	N	54°31.77	10°02.36	12.04.201	09:46:11	14.52977078	6.11	17.274	370.1	0.03	0.09

504	10	N	54°31.77	E	10°02.36	12.04.201	6	09:46:11	15.18077436	5.581	18.313	382.2	0.02	0.06
504	15	N	54°31.77	E	10°02.36	12.04.201	6	09:46:11	15.27109501	4.683	19.762	383.6	0.07	0.21
504	20	N	54°31.77	E	10°02.36	12.04.201	6	09:46:11	16.55420599	4.152	21.264	300.3	0.71	3.32
504	25	N	54°31.77	E	10°02.36	12.04.201	6	09:46:11	16.74793928	4.267	21.717	238.2	0.88	5.38
505	1	N	54°31.77	E	10°02.36	03.05.201	6	09:40:37	13.6785316	9.47	15.188	347.4	0	0.08
505	5	N	54°31.77	E	10°02.36	03.05.201	6	09:40:37	13.86085973	7.518	16.987	332.6	0	0.04
505	10	N	54°31.77	E	10°02.36	03.05.201	6	09:40:37	14.3659804	6.731	20.112	326.6	0.01	0.06
505	15	N	54°31.77	E	10°02.36	03.05.201	6	09:40:37	15.41067101	5.908	21.097	278.3	0.51	1.98
505	20	N	54°31.77	E	10°02.36	03.05.201	6	09:40:37	16.14020279	5.87	21.866	266	0.72	3.6
505	25	N	54°31.77	E	10°02.36	03.05.201	6	09:40:37	16.80537525	5.09	21.955	245.8	0.87	4.57
506	1	N	54°31.77	E	10°02.36	01.06.201	6	09:48:23	9.030063846	16.228	13.653	303.6	0	0.14
506	5	N	54°31.77	E	10°02.36	01.06.201	6	09:48:23	9.360917244	16.2	13.6	305.7	0	0.15
506	10	N	54°31.77	E	10°02.36	01.06.201	6	09:48:23	11.10294416	11.325	16.2	327.5	0	0.15
506	15	N	54°31.77	E	10°02.36	01.06.201	6	09:48:23	11.67085178	10.073	17.062	309.2	0	0.14
506	20	N	54°31.77	E	10°02.36	01.06.201	6	09:48:23	12.77308782	7.067	19.567	270.3	0.02	0.27
506	25	N	54°31.77	E	10°02.36	01.06.201	6	09:48:23	17.33733916	5.665	21.547	147.3	0.09	6.9
508	1	N	54°31.77	E	10°02.36	05.07.201	6	09:50:35	8.854322803	17.746	13.609	293.4	0	0.07
508	5	N	54°31.77	E	10°02.36	05.07.201	6	09:50:35	9.493988564	16.63	14.5	292.9	0	0.06
508	10	N	54°31.77	E	10°02.36	05.07.201	6	09:50:35	11.76207185	12.905	17.557	264.4	0	0.07

508	15	N	54°31.77	E	10°02.36	05.07.201	6	09:50:35	13.24466032	11.153	19.597	219.5	0.07	0.24
508	20	N	54°31.77	E	10°02.36	05.07.201	6	09:50:35	15.77920473	8.268	20.861	148.4	0.07	5.08
508	25	N	54°31.77	E	10°02.36	05.07.201	6	09:50:35	15.1789072	8.588	22.973	140.3	0.09	5.92
509	1	N	54°31.77	E	10°02.36	03.08.201	6	09:39:54		19.032	15.978	271.4	0	0.08
509	5	N	54°31.77	E	10°02.36	03.08.201	6	09:39:54		19.248	17.468	289.2	0	0.09
509	10	N	54°31.77	E	10°02.36	03.08.201	6	09:39:54		15.541	20.018	277.8	0	0.08
509	15	N	54°31.77	E	10°02.36	03.08.201	6	09:39:54		12.688	22.19	242.9	0	0.1
509	20	N	54°31.77	E	10°02.36	03.08.201	6	09:39:54		10.639	23.861	160.6	0.01	0.27
509	25	N	54°31.77	E	10°02.36	03.08.201	6	09:39:54		10.746	25.487	111.8	0.19	1.86
510	1	N	54°31.77	E	10°02.36	21.09.201	6	10:37:05	9.968709241	17.406	14.587	280.9	0	0.22
510	5	N	54°31.77	E	10°02.36	21.09.201	6	10:37:05	10.1499446	17.777	15.498	279.7	0	0.15
510	10	N	54°31.77	E	10°02.36	21.09.201	6	10:37:05	10.17933056	17.968	16.432	268.8	0	0.15
510	15	N	54°31.77	E	10°02.36	21.09.201	6	10:37:05	9.833734749	18.628	17.738	261.7	0	0.15
510	20	N	54°31.77	E	10°02.36	21.09.201	6	10:37:05	9.888524344	17.839	19.953	219	0	0.15
510	25	N	54°31.77	E	10°02.36	21.09.201	6	10:37:05	2.146954365	11.32	25.366	0	0	0.13
511	1	N	54°31.77	E	10°02.36	19.10.201	6	10:21:13	6.119216502	12.274	16.328	307.1	0	0
511	5	N	54°31.77	E	10°02.36	19.10.201	6	10:21:13	5.87915901	12.285	16.334	305.3	0	0.02
511	10	N	54°31.77	E	10°02.36	19.10.201	6	10:21:13	7.27332795	12.355	16.585	277	0.01	0.1
511	15	N	54°31.77	E	10°02.36	19.10.201	6	10:21:13	6.555879723	13.382	17.697	255.2	0.08	0.34

511	20	N	54°31.77	E	10°02.36	19.10.201	6	10:21:13	5.244062408	14.784	21.532	96.2	0.58	1.58
511	25	N	54°31.77	E	10°02.36	19.10.201	6	10:21:13	5.493895348	12.253	24.846	0	0.08	0.14
512	1	N	54°31.77	E	10°02.36	08.11.201	6	10:02:27	6.889549874	9.533	15.168	309.3	0.06	0.01
512	5	N	54°31.77	E	10°02.36	08.11.201	6	10:02:27	6.967803196	9.549	15.164	308.9	0.04	0.02
512	10	N	54°31.77	E	10°02.36	08.11.201	6	10:02:27	9.175603521	9.565	15.169	308.9	0.04	0.03
512	15	N	54°31.77	E	10°02.36	08.11.201	6	10:02:27	6.959702936	9.566	15.171	308.9	0.04	0.06
512	20	N	54°31.77	E	10°02.36	08.11.201	6	10:02:27	7.109401032	9.796	15.454	301.8	0.04	0.09
512	25	N	54°31.77	E	10°02.36	08.11.201	6	10:02:27	6.635359921	12.171	22.248	0	0.42	1.12
513	1	N	54°31.77	E	10°02.36	06.12.201	6	09:54:39	6.822491396	6.258	16.519	341.1	0.02	0.04
513	5	N	54°31.77	E	10°02.36	06.12.201	6	09:54:39	5.903748442	6.259	16.523	341	0.02	0.01
513	10	N	54°31.77	E	10°02.36	06.12.201	6	09:54:39	6.191312577	6.272	16.55	339.5	0.03	0.06
513	15	N	54°31.77	E	10°02.36	06.12.201	6	09:54:39	6.513092552	6.483	16.691	311.5	0.07	0.4
513	20	N	54°31.77	E	10°02.36	06.12.201	6	09:54:39	6.791885461	8.219	19.665	194.7	0.32	2.11
513	25	N	54°31.77	E	10°02.36	06.12.201	6	09:54:39	7.646939962	10.173	20.572	98.1	0.65	2.51
514	1	N	54°31.77	E	10°02.36	10.01.201	7	09:57:46	9.041669563	4.327	21.059	345.4	0.02	0.01
514	5	N	54°31.77	E	10°02.36	10.01.201	7	09:57:46	9.177983056	4.333	21.061	345.1	0.02	0.1
514	10	N	54°31.77	E	10°02.36	10.01.201	7	09:57:46	8.46147916	4.423	21.124	340.9	0.03	0.31
514	15	N	54°31.77	E	10°02.36	10.01.201	7	09:57:46	8.368859371	5.607	22.134	301.7	0.09	0.82
514	20	N	54°31.77	E	10°02.36	10.01.201	7	09:57:46	8.071092811	5.457	23.211	299.8	0.54	2.91

514	25	N	54°31.77	E	10°02.36	7	10.01.201	09:57:46	9.239491029	5.3	23.7	304.6	0.28	1.2
516	1	N	54°31.77	E	10°02.36	7	13.03.201	10:26:42	9.542190746	3.749	16.357	410.7	0.07	0.01
516	5	N	54°31.77	E	10°02.36	7	13.03.201	10:26:42	10.19027286	3.623	16.747	393.2	0.1	0.07
516	10	N	54°31.77	E	10°02.36	7	13.03.201	10:26:42	10.04812171	2.939	19.271	344.9	0.35	4.02
516	15	N	54°31.77	E	10°02.36	7	13.03.201	10:26:42	11.11926152	3.012	20.041	325.4	0.38	4.5
516	20	N	54°31.77	E	10°02.36	7	13.03.201	10:26:42	10.87916975	3.23	20.43	322.4	0.33	4.27
516	25	N	54°31.77	E	10°02.36	7	13.03.201	10:26:42	13.9339288	3.257	20.618	318.5	0.35	4.3
517	1	N	54°31.77	E	10°02.36	7	10.04.201	10:35:37	8.938131852	7.153	16.821	350.2	0.05	0.01
517	5	N	54°31.77	E	10°02.36	7	10.04.201	10:35:37	8.547087455	7.153	16.82	350.64	0.07	0.03
517	10	N	54°31.77	E	10°02.36	7	10.04.201	10:35:37	8.816543654	7.143	16.821	348.39	0.08	0.76
517	15	N	54°31.77	E	10°02.36	7	10.04.201	10:35:37	10.37617188	6.2	17.283	328.49	0.12	1.29
517	20	N	54°31.77	E	10°02.36	7	10.04.201	10:35:37	10.49193686	3.467	20.024	268.13	0.3	4.78
517	25	N	54°31.77	E	10°02.36	7	10.04.201	10:35:37	12.51335735	3.474	20.187	261.08	0.23	5.05
519	1	N	54°31.77	E	10°02.36	7	21.06.201	10:16:02	10.92599046	17.35	16.098	294.4	0.06	1.04
519	5	N	54°31.77	E	10°02.36	7	21.06.201	10:16:02	11.70436928	17.284	16.256	295.59	0.07	1.85
519	10	N	54°31.77	E	10°02.36	7	21.06.201	10:16:02	12.65511503	14.563	16.944	299.07	0.06	2.66
519	15	N	54°31.77	E	10°02.36	7	21.06.201	10:16:02	13.24292187	12.998	17.535	276.58	0.18	3.78
519	20	N	54°31.77	E	10°02.36	7	21.06.201	10:16:02	16.21536787	8.977	19.134	183.53	1	9.58
519	25	N	54°31.77	E	10°02.36	7	21.06.201	10:16:02	17.71534508	8.567	20.372	137.58	0.31	12.18

520	1	N	54°31.77	10°02.36	17.07.201	7	10:50:00	9.533047828	16.968	16.385	280.36	0.04	6.58
520	5	N	54°31.77	10°02.36	17.07.201	7	10:50:00	9.744741176	16.943	16.399	278.33	0	8.01
520	10	N	54°31.77	10°02.36	17.07.201	7	10:50:00	12.38792453	15.639	17.579	247.64	0.03	8.96
520	15	N	54°31.77	10°02.36	17.07.201	7	10:50:00	14.16502283	12.621	20.568	169.23	0.15	10.53
520	20	N	54°31.77	10°02.36	17.07.201	7	10:50:00	14.3679753	11.623	21.862	128.24	0.55	15.58
520	25	N	54°31.77	10°02.36	17.07.201	7	10:50:00	15.87362878	10.763	22.333	91.01	0.54	17.92
521	1	N	54°31.77	10°02.36	01.08.201	7	09:58:53	10.12922826	18.712	14.938	278.36	0.02	0.02
521	5	N	54°31.77	10°02.36	01.08.201	7	09:58:53	11.07	18.402	16.232	277.01	0.01	0.03
521	10	N	54°31.77	10°02.36	01.08.201	7	09:58:53	10.32646383	17.223	17.193	254.6	0.01	0.1
521	15	N	54°31.77	10°02.36	01.08.201	7	09:58:53	13.76	15.215	19.105	209.44	0.01	0.11
521	20	N	54°31.77	10°02.36	01.08.201	7	09:58:53	13.74612202	12.796	20.72	145.42	0.06	0.36
521	25	N	54°31.77	10°02.36	01.08.201	7	09:58:53	14.73806811	10.808	22.028	53.1	0.61	4.71
522	1	N	54°31.77	10°02.36	12.09.201	7	09:55:48	9.067516386	15.001	20.119	146.8	0.02	0.28
522	5	N	54°31.77	10°02.36	12.09.201	7	09:55:48	8.832308671	14.968	20.133	135.92	0.01	0.33
522	10	N	54°31.77	10°02.36	12.09.201	7	09:55:48	8.220801321	14.207	21.274	55.04	0.06	0.42
522	15	N	54°31.77	10°02.36	12.09.201	7	09:55:48	9.838427412	13.547	22.225	24.61	0.23	1.04
522	20	N	54°31.77	10°02.36	12.09.201	7	09:55:48	9.981064103	13.612	22.278	27.98	0.24	1.22
522	25	N	54°31.77	10°02.36	12.09.201	7	09:55:48	9.557144944	13.532	22.77	28.64	0.35	2.06
523	1	N	54°31.77	10°02.36	24.10.201	7	10:43:32	10.84227438	13.184	17.988	267.67	0.12	0.02

523	5	N	54°31.77 E	10°02.36 7	24.10.201	10:43:32	10.53213244	13.185	17.99	258.71	0.17	0.03
523	10	N	54°31.77 E	10°02.36 7	24.10.201	10:43:32	10.16654524	13.185	17.992	187.22	0.22	0.11
523	15	N	54°31.77 E	10°02.36 7	24.10.201	10:43:32	10.05492629	13.188	22.114	164.67	0.34	1.62
523	20	N	54°31.77 E	10°02.36 7	24.10.201	10:43:32	9.858401259	13.19	22.114	152.52	0.22	0.93
523	25	N	54°31.77 E	10°02.36 7	24.10.201	10:43:32	10.19879532	13.192	22.111	172.33	0.22	0.87
524	1	N	54°31.77 E	10°02.36 7	09.11.201	10:36:59	35.59665908	11.106	18.367	305.82	0	0.02
524	5	N	54°31.77 E	10°02.36 7	09.11.201	10:36:59	37.82565787	11.104	18.369	300.24	0	0.08
524	10	N	54°31.77 E	10°02.36 7	09.11.201	10:36:59	34.89039037	11.103	18.366	294.15	0	0.1
524	15	N	54°31.77 E	10°02.36 7	09.11.201	10:36:59	36.22026741	13.126	21.461	243.63	0.04	0.2
524	20	N	54°31.77 E	10°02.36 7	09.11.201	10:36:59	33.89980546	13.128	21.46	165.12	0.41	1.47
524	25	N	54°31.77 E	10°02.36 7	09.11.201	10:36:59	33.75445882	13.125	21.458	100.72	0.89	2.74
525	1	N	54°31.77 E	10°02.36 7	19.12.201	10:05:58	11.76287194	5.766	19.538	331.6	0.28	1.3
525	5	N	54°31.77 E	10°02.36 7	19.12.201	10:05:58	12.96343516	5.767	19.535	332	0.28	1.35
525	10	N	54°31.77 E	10°02.36 7	19.12.201	10:05:58	12.89773412	5.572	19.569	331.52	0.32	1.97
525	15	N	54°31.77 E	10°02.36 7	19.12.201	10:05:58	13.06728152	5.63	19.617	329.77	0.35	2.28
525	20	N	54°31.77 E	10°02.36 7	19.12.201	10:05:58	11.6778542	5.844	19.692	320.67	0.45	2.83
525	25	N	54°31.77 E	10°02.36 7	19.12.201	10:05:58	11.96373705	6.446	19.84	305.26	0.55	3.49
526	1	N	54°31.77 E	10°02.36 10.012018	10.012018	10:05:03				345.77	0.32	3.57
526	5	N	54°31.77 E	10°02.36 10.012018	10.012018	10:05:03				345.79	0.31	3.33

526	10	N	54°31.77 E	10°02.36	10.012018	10:05:03				345.59	0.32	3.25
526	15	N	54°31.77 E	10°02.36	10.012018	10:05:03				345.15	0.32	2.91
526	20	N	54°31.77 E	10°02.36	10.012018	10:05:03				344.44	0.33	2.94
526	25	N	54°31.77 E	10°02.36	10.012018	10:05:03				343.81	0.33	2.97
527	1	N	54°31.77 E	10°02.36	20.02.201	12:01:42				393.212		
527	5	N	54°31.77 E	10°02.36	20.02.201	12:01:42				388.926	0.55	3.99
527	10	N	54°31.77 E	10°02.36	20.02.201	12:01:42				366.798	0.54	4.22
527	15	N	54°31.77 E	10°02.36	20.02.201	12:01:42				354.434	0.56	4.99
527	20	N	54°31.77 E	10°02.36	20.02.201	12:01:42				319.444	0.61	5.49
527	25	N	54°31.77 E	10°02.36	20.02.201	12:01:42				294.359	0.65	5.65
528	1	N	54°31.77 E	10°02.36	26.03.201	09:53:23	16.36015508	1.815	13.532	426.88	0.66	6.13
528	5	N	54°31.77 E	10°02.36	26.03.201	09:53:23	16.92950998	1.807	13.532	426.99	0.11	0.27
528	10	N	54°31.77 E	10°02.36	26.03.201	09:53:23	16.8797354	1.804	13.526	421.55	0.1	0.24
528	15	N	54°31.77 E	10°02.36	26.03.201	09:53:23	17.2158116	1.39	13.628	416.27	0.1	0.61
528	20	N	54°31.77 E	10°02.36	26.03.201	09:53:23	16.92045529	1.22	13.854	405.9	0.11	1.11
528	25	N	54°31.77 E	10°02.36	26.03.201	09:53:23	17.20107283	1.072	14.108	398.37	0.13	1.17
529	1	N	54°31.77 E	10°02.36	18.04.201	09:55:01				406.79	0.15	1.27
529	5	N	54°31.77 E	10°02.36	18.04.201	09:55:01				401.96	0.06	0.03
529	10	N	54°31.77 E	10°02.36	18.04.201	09:55:01				390.42	0.05	0.04
529	10	N	54°31.77 E	10°02.36	8	09:55:01				390.42	0.05	0.09

529	15	N	54°31.77	E	10°02.36	18.04.201	8	09:55:01		391.67	0.04	0.06		
529	20	N	54°31.77	E	10°02.36	18.04.201	8	09:55:01		388.26	0.04	0.07		
529	25	N	54°31.77	E	10°02.36	18.04.201	8	09:55:01		384.18	0.04	0.09		
530	1	N	54°31.77	E	10°02.36	08.05.201	8	10:08:43		369.182	0.03	0.01		
530	5	N	54°31.77	E	10°02.36	08.05.201	8	10:08:43		371.819	0.03	0.04		
530	10	N	54°31.77	E	10°02.36	08.05.201	8	10:08:43		359.393	0.03	0.02		
530	15	N	54°31.77	E	10°02.36	08.05.201	8	10:08:43		324.163	0.04	0.17		
530	20	N	54°31.77	E	10°02.36	08.05.201	8	10:08:43		305.608	0.06	0.53		
530	25	N	54°31.77	E	10°02.36	08.05.201	8	10:08:43		286.435	0.07	0.96		
531	1	N	54°31.77	E	10°02.36	21.06.201	8	10:16:12		294.2	0.04	0.03		
531	5	N	54°31.77	E	10°02.36	21.06.201	8	10:16:12		288.18	0.04	0.01		
531	10	N	54°31.77	E	10°02.36	21.06.201	8	10:16:12		225.07	0.07	0.18		
531	15	N	54°31.77	E	10°02.36	21.06.201	8	10:16:12		228.13	0.14	1.06		
531	20	N	54°31.77	E	10°02.36	21.06.201	8	10:16:12		217.76	0.17	1.89		
531	25	N	54°31.77	E	10°02.36	21.06.201	8	10:16:12		187.03	0.2	3.33		
533	1	N	54°31.77	E	10°02.36	01.08.201	8	10:16:39	11.24111396	21.761	15.453	264.13	0.08	0.09
533	5	N	54°31.77	E	10°02.36	01.08.201	8	10:16:39	10.85883851	21.772	15.434	280.3	0.09	0.02
533	10	N	54°31.77	E	10°02.36	01.08.201	8	10:16:39	11.75029295	21.757	15.439	295.66	0.11	0.04
533	15	N	54°31.77	E	10°02.36	01.08.201	8	10:16:39	11.56237969	10.469	24.254	297.61	0.15	0.03

533	20	N	54°31.77	E	10°02.36	01.08.201	8	10:16:39	11.46887213	10.458	24.312	192.87	0.15	0.03			
533	25	N	54°31.77	E	10°02.36	01.08.201	8	10:16:39	7.677135489	10.483	24.244	67.36	0.22	0.41			
539	1	N	54°31.77	E	10°02.36	26.02.201	9	10:09:01	15.95786294	3	18.395	400.29	0.04	0.02	-27.1177	3	184.78
539	5	N	54°31.77	E	10°02.36	26.02.201	9	10:09:01	16.92261254	3.763	3	387.24	0.06	0.17	-15.2703	3	197.02
539	10	N	54°31.77	E	10°02.36	26.02.201	9	10:09:01	15.06008152	3.70233	19.6366	354.67	0.19	1.83	15.0552	5	9.20008
539	15	N	54°31.77	E	10°02.36	26.02.201	9	10:09:01	14.77935386	3.68166	19.9406	338.94	0.27	2.73	29.8820	2	9.04935
539	20	N	54°31.77	E	10°02.36	26.02.201	9	10:09:01	17.6949908	4.31766	21.5183	282.45	0.44	4.3	75.6559	7	10.8649
539	25	N	54°31.77	E	10°02.36	26.02.201	9	10:09:01	18.95002285	4.61066	21.9503	249.83	0.58	4.74	103.993	8	11.6600
540	1	N	54°31.77	E	10°02.36	20.03.201	9	9:53:38	9.306010249	7	3	249.83	0.58	4.74	8	2	225.70
540	5	N	54°31.77	E	10°02.36	20.03.201	9	9:53:38	9.025601019	4.772	19.552	367.41	0.03	0.03	-6.74842	5.79601	115.07
540	10	N	54°31.77	E	10°02.36	20.03.201	9	9:53:38	8.743894057	4.76966	19.5516	367.07	0.02	0.02	-6.39491	1	111.61
540	15	N	54°31.77	E	10°02.36	20.03.201	9	9:53:38	8.778630137	4.74866	19.6583	355.73	0.02	0.19	4	4	108.51
540	20	N	54°31.77	E	10°02.36	20.03.201	9	9:53:38	9.590284267	7	3	355.73	0.02	0.19	4	4	108.51
540	25	N	54°31.77	E	10°02.36	20.03.201	9	9:53:38	8.836097878	7	3	355.73	0.02	0.19	4	4	108.51
541	1	N	54°31.77	E	10°02.36	24.04.201	9	10:43:49	14.1066901	4.73	19.87	346.7	0.08	1.45	6	5.46863	108.73
541	5	N	54°31.77	E	10°02.36	24.04.201	9	10:43:49	13.92266628	4.63166		346.7	0.08	1.45	6	5.46863	108.73
541	10	N	54°31.77	E	10°02.36	24.04.201	9	10:43:49	14.62565406	7	20.282	324.31	0.23	3.08	34.8957	4	3.98028
541	15	N	54°31.77	E	10°02.36	24.04.201	9	10:43:49	15.32092314	7	20.282	324.31	0.23	3.08	4	4	119.40
541	20	N	54°31.77	E	10°02.36	24.04.201	9	10:43:49	14.27625416	4.929	21.606	276.28	0.22	2.25	76.2106	5.53609	
541	25	N	54°31.77	E	10°02.36	24.04.201	9	10:43:49	14.27625416	4.929	21.606	276.28	0.22	2.25	6	8	110.77
541	1	N	54°31.77	E	10°02.36	24.04.201	9	10:43:49	14.1066901	8.7805	16.6085	342.56	0.04	0.05	-8.50591	8.71669	171.15
541	5	N	54°31.77	E	10°02.36	24.04.201	9	10:43:49	13.92266628	8.63	7	344.36	0.03	0.09	-9.50723	6	169.74
541	10	N	54°31.77	E	10°02.36	24.04.201	9	10:43:49	14.62565406	8.458	17.2415	343.56	0.01	0.03	-8.36623	4	178.57
541	15	N	54°31.77	E	10°02.36	24.04.201	9	10:43:49	15.32092314	7.357	18.8825	345.11	0.01	0.03	-4.86176	3	189.24
541	20	N	54°31.77	E	10°02.36	24.04.201	9	10:43:49	14.27625416	6.93	7	325.63	0.03	0.07	16.6729	4	176.76

		54°31.77	10°02.36	24.04.201		6.12033							8.24691	
541	25	N	E	9	10:43:49	12.94691169	3	20.714	197.27	0.17	0.99	145.54	2	162.01
		54°31.77	10°02.36	28.05.201					326.488				9.52864	
542	1	N	E	9	10:24:20	15.32864803	12.1205	14.7205	2	0.06	0.03	-12.8248	8	188.34
		54°31.77	10°02.36	28.05.201				14.9126	326.703				5.82444	
542	5	N	E	9	10:24:20	9.314443648	11.703	7	5	0.04	0.01	-10.5793	4	118.10
		54°31.77	10°02.36	28.05.201					313.116			11.4277	2.46762	
542	10	N	E	9	10:24:20	3.92762286	10.184	15.879	2	0.03	0.01	1	3	50.25
		54°31.77	10°02.36	28.05.201				18.2483	258.571			71.4418	3.00399	
542	15	N	E	9	10:24:20	4.753996766	8.611	3	8	0.04	0.09	9	7	61.53
		54°31.77	10°02.36	28.05.201					200.409			132.214	4.81592	
542	20	N	E	9	10:24:20	7.605920763	7.8515	19.128	9	0.16	0.76	1	1	98.85
		54°31.77	10°02.36	28.05.201					149.103			185.592	4.16781	
542	25	N	E	9	10:24:20	6.577816541	7.2735	19.717	1	0.26	1.72	2	7	85.73
		54°31.77	10°02.36	26.06.201			19.4276	14.5003					4.68717	
543	1	N	E	9	11:24:30	7.477172123	7	3	304.83	0.04	0.02	-34.1456	2	94.35
		54°31.77	10°02.36	26.06.201									4.95225	
543	5	N	E	9	11:24:30	7.902255134	17.608	14.72	293.62	0.05	0.11	-13.9238	5	100.10
		54°31.77	10°02.36	26.06.201			13.8654	16.2676				38.0111	5.35871	
543	10	N	E	9	11:24:30	8.508716551	7	7	260.03	0.03	0.13	4	7	109.05
		54°31.77	10°02.36	26.06.201			12.6043					54.5264	5.82373	
543	15	N	E	9	11:24:30	9.233732505	3	16.799	250.31	0.05	0.2	7	3	118.64
		54°31.77	10°02.36	26.06.201			9.22966						8.09216	
543	20	N	E	9	11:24:30	12.78216757	7	18.816	150.65	0.21	1.09	171.193	8	166.00
		54°31.77	10°02.36	26.06.201				19.7713				210.090	5.39639	
543	25	N	E	9	11:24:30	8.506396679	8.221	3	116.48	0.2	1.78	8	7	111.30
		54°31.77	10°02.36	31.07.201				14.3713					3.65565	
544	1	N	E	9	10:10:16	5.895659485	19.553	3	269.6	0.0095	0.059	-0.14772	9	70.59
		54°31.77	10°02.36	31.07.201			18.6903					6.57561	3.56597	
544	5	N	E	9	10:10:16	5.695971421	3	16.268	264.23	0.0465	0.047	2	1	71.22
		54°31.77	10°02.36	31.07.201			18.5913					8.96592	4.23218	
544	10	N	E	9	10:10:16	6.772185546	3	16.747	261.54	0.0985	0.017	4	6	85.18
		54°31.77	10°02.36	31.07.201			17.4663					47.1570	3.95801	
544	15	N	E	9	10:10:16	6.30801822	3	17.376	227.51	0.0945	0.066	3	8	79.84
		54°31.77	10°02.36	31.07.201								216.914	4.07767	
544	20	N	E	9	10:10:16	6.45767765	11.465	20.827	84.07	0.1005	-0.024	5	8	83.18
		54°31.77												
544	25	N	10°02.36E		10:10:16		9.69	21.55	46.35	0.1695	-0.007	264.386		

545	1	N	54°31.77	10°02.36	27.08.201	9	10:39:15	4.952470226	19.813	15.748	274.576	0.0885	0.066	-8.44365	3.11247	63.17
			54°31.77	10°02.36	27.08.201				17.8253		247.040			25.2689	3.90203	
545	5	N	54°31.77	10°02.36	27.08.201	9	10:39:15	6.182039412	3	17.931	2	0.0935	-0.026	8	9	79.69
			54°31.77	10°02.36	27.08.201				15.2513	20.2543					5.00189	
545	10	N	54°31.77	10°02.36	27.08.201	9	10:39:15	7.881891733	3	3	145.466	0.0375	-0.026	134.836	2	103.21
			54°31.77	10°02.36	27.08.201					21.1003	54.7284			232.684	3.92419	
545	15	N	54°31.77	10°02.36	27.08.201	9	10:39:15	6.164194868	13.44	3	3	0.0685	-0.045	3	5	81.32
			54°31.77	10°02.36	27.08.201						74.2306					
545	20	N	54°31.77	10°02.36	27.08.201	9	10:39:15		13.45	22.09	9	0.1345	-0.038	211.818		
			54°31.77	10°02.36	27.08.201						36.5957			251.085		
545	25	N	54°31.77	10°02.36	27.08.201	9	10:39:15		12.94	22.43	6	0.1365	-0.04	6		
			54°31.77	10°02.36E							292.737	0.23533		27.8309		
547	1	N	54°31.77	10°02.36E	29.09.201		10:39:15		9.49	20.1	1	3	1.2	5		
			54°31.77	10°02.36	29.09.201	9			9.58233	20.1966	286.755	0.35733		32.8284	6.99248	
547	5	N	54°31.77	10°02.36	29.09.201	9	9:52:02	11.34248256	3	7	5	3	1.74	7	3	136.43
			54°31.77	10°02.36	29.09.201				10.2193	20.7193	269.158	0.41566		44.5491	15.1040	
547	10	N	54°31.77	10°02.36	29.09.201	9	9:52:02	24.45404717	3	3	3	7	1.9	7	5	295.02
			54°31.77	10°02.36	29.09.201				10.1413	20.6713	249.335	0.40366		64.5574		
547	15	N	54°31.77	10°02.36	29.09.201	9	9:52:02	13.39096034	3	3	6	7	2.669	8	8.27096	162.02
			54°31.77	10°02.36E							122.569		6.77266	176.524		
547	20	N	54°31.77	10°02.36E			9:52:02		11.65	21.66	5	0.221	7	8		
			54°31.77	10°02.36E							56.7556	0.30233		233.691		
547	25	N	54°31.77	10°02.36E			9:52:02		12.56	22.44	9	3	8.49	7		
			54°31.77	10°02.36	10.12.201								1.20566	141.478	6.29583	
548	1	N	54°31.77	10°02.36	10.12.201	9	10:02:23	10.22583688			322.719	0.299	7	4	7	123.35
			54°31.77	10°02.36	10.12.201						307.252	0.43966	2.04666	156.596	5.91293	
548	5	N	54°31.77	10°02.36	10.12.201	9	10:02:23	9.602935366			9	7	7	7	5	116.19
			54°31.77	10°02.36	10.12.201						291.240		2.87433	172.249	7.71260	
548	10	N	54°31.77	10°02.36	10.12.201	9	10:02:23	12.52260708			3	0.558	3	2	7	151.52
			54°31.77	10°02.36E							268.091	0.53966	3.36066	194.877		
548	15	N	54°31.77	10°02.36E			10:02:23				8	7	7	4		
			54°31.77	10°02.36	10.12.201						255.875	0.44633	3.85366	206.818	6.04400	
548	20	N	54°31.77	10°02.36	10.12.201	9	10:02:23	9.79400887			6	3	7	9	9	118.87
			54°31.77	10°02.36	10.12.201						263.585		3.73233	199.282	4.72794	
548	25	N	54°31.77	10°02.36	07.01.202	9	10:02:23	7.727946126			5	0.268	3	3	6	93.79
			54°31.77	10°02.36	07.01.202				5.81633	20.3053	322.073		4.11166	26.9551	9.16808	
549	1	N	54°31.77	10°02.36	07.01.202	0	9:40:11	14.77808548	3	3	9	0.262	7	9	5	180.17

549	5	N	E	0	9:40:11	17.86916426	5.91233	20.3776	318.665	0.26566	4.14633	29.3309	11.0891	217.87
549	10	N	E	0	9:40:11	14.93169105	5.96733	20.454	313.987	0.27166	4.17433	33.2795	9.28169	182.68
549	15	N	E	0	9:40:11	14.1725595	7.16666	3	270.240	0.33033	4.95033	64.3834	8.78255	174.79
549	20	N	E	0	9:40:11	17.57156619	8.06933	7	216.511	0.26133	4.90033	107.527	10.9015	213.29
549	25	N	E	0	9:40:11	14.2606891	8.31333	3	200.543	0.22866	4.505	120.558	8.88068	175.14
557	1	N	E	0	7:41:17		16.09	16.51	268.712	0.021	0	15.9050	7	
557	5	N	E	0	7:41:17		15.85	17.08	219.814	0.026	0	64.1083	4	
557	10	N	E	0	7:41:17		14.51	19.81	54.5659	0.084	0.07	228.728	5	
557	15	N	E	0	7:41:17	5.646546154	13.6975	20.4965	279.244	0.462	0.807	279.244	3.52654	69.76
557	20	N	E	0	7:41:17	7.926579465	13.084	7	21.2206	0.378	1.154	288.132	4.92657	98.89
557	25	N	E	0	7:41:17	9.11411063	13.0633	21.3496	288.029	0.391	1.87	288.029	5.71411	113.80
558	1	N	E	0	8:12:09	8.954984433	12.8553	16.144	298.804			298.804	5.56498	109.54
558	5	N	E	0	8:12:09	8.086846091	13.0316	16.3956	297.207			297.207	5.02684	99.07
558	10	N	E	0	8:12:09	6.079043947	12.8553	16.5925	295.508			295.508	3.77904	74.53
558	15	N	E	0	8:12:09		13.2	16.64	295.687			295.687	5	
558	20	N	E	0	8:12:09		13.08	16.97	295.843			295.843	8	
558	25	N	E	0	8:12:09		13.75	18.97	288.075			288.075	1	
559	1	N	E	1	9:23:33	15.10588165	1.462	17.8365	20.5951	0.5425	4.667	20.5951	9.38588	184.32
559	5	N	E	1	9:23:33	16.31100277	1.74466	18.0183	25.0740	0.5345	4.991	25.0740	10.141	199.23

		54°31.77	10°02.36	17.02.202					361.259			30.9301	9.90803	
559	10	N	E	1	9:23:33	15.91803353	1.736	18.281	8	0.5585	5.294	2	4	195.32
		54°31.77	10°02.36	17.02.202			1.77733	18.3116				28.5156	9.82257	
559	15	N	E	1	9:23:33	15.80257901	3	7	363.221	0.5645	5.355	2	9	192.71
		54°31.77	10°02.36	17.02.202				18.3053	363.036			29.9991		
559	20	N	E	1	9:23:33	16.95489636	1.65	3	7	0.5915	5.428	7	10.5449	207.39
		54°31.77	10°02.36	17.02.202			1.43666		365.051			29.9881		
559	25	N	E	1	9:23:33	14.80424019	7	18.386	2	0.6485	5.73	6	9.24424	188.60
		54°31.77	10°02.36	16.03.202					385.470				9.82033	
560	1	N	E	1	9:18:53	15.60033394	3.01	17.808	9	0.0315	0.073	-4.04945	4	198.05
		54°31.77							381.918					
560	5	N	10°02.36E		9:18:53		2.94	17.84	3	0.0545	0.659	0.01405		
		54°31.77	10°02.36	16.03.202					364.726			16.3186	10.0656	
560	10	N	E	1	9:18:53	15.9856244	2.968	17.932	2	0.0525	0.767	7	2	203.07
		54°31.77	10°02.36	16.03.202					377.175			4.24212	10.6025	
560	15	N	E	1	9:18:53	16.83253463	2.952	17.956	5	0.0645	1.138	1	3	213.86
		54°31.77	10°02.36	16.03.202					345.276			34.5005		
560	20	N	E	1	9:18:53	16.52590273	2.797	18.911	8	0.1365	2.099	9	10.4359	211.64
		54°31.77	10°02.36	16.03.202					333.381			39.8462	10.6134	
560	25	N	E	1	9:18:53	16.76341329	3.201	19.9	4	0.1405	2.229	5	1	215.77
		54°31.77	10°02.36	17.04.202				17.9536	352.318			12.1523	8.88598	
561	1	N	E	1	7:58:18	14.15598419	4.729	7	9	0.076	0.192	7	4	178.11
		54°31.77	10°02.36	17.04.202				17.9526	350.052			14.3698	9.23900	
561	5	N	E	1	7:58:18	14.70900298	4.729	7	9	0.04	0.152	3	3	185.06
		54°31.77	10°02.36	17.04.202			4.71066	17.9593	348.602			15.9344	9.15489	
561	10	N	E	1	7:58:18	14.55489856	7	3	6	0.04	0.163	1	9	183.69
		54°31.77	10°02.36	17.04.202			4.68666	18.1396	321.975			41.7475	9.38476	
561	15	N	E	1	7:58:18	14.91476149	7	7	6	0.044	0.166	3	1	188.92
		54°31.77	10°02.36	17.04.202			4.23433	21.2163				97.4429	9.63301	
561	20	N	E	1	7:58:18	15.2130149	3	3	261.637	0.079	0.218	4	5	195.81
		54°31.77	10°02.36	17.04.202			4.21166	21.3616	256.846			101.981	9.17883	
561	25	N	E	1	7:58:18	14.47883099	7	7	9	0.195	0.345	8	1	186.53
		54°31.77	10°02.36	26.05.202			8.89533		314.026			14.6051		
562	1	N	E	1	9:54:48	12.15692024	3	18.494	1	0.028	0	3	7.67692	155.30
		54°31.77	10°02.36	26.05.202			8.82366	18.5223	312.959			16.1200	7.84896	
562	5	N	E	1	9:54:48	12.41896772	7	3	9	0.015	0	9	8	159.14
		54°31.77	10°02.36	26.05.202				18.8566	305.892			26.3389	8.11155	
562	10	N	E	1	9:54:48	12.81155766	8.289	7	9	0.017	0	2	8	164.47

562	15	N	E	1	9:54:48	13.75582808	7.41	3	6	0.03	0.003	46.4219	8.73582	178.70
		54°31.77	10°02.36	26.05.202				19.7593	290.290					
		54°31.77	10°02.36	26.05.202				21.3616	211.902				9.32578	
562	20	N	E	1	9:54:48	14.62578874	6.122	7	6	0.262	1.176	129.786	9	192.50
		54°31.77	10°02.36	26.05.202			5.94666	21.8696	180.137			161.133	9.39977	
562	25	N	E	1	9:54:48	14.66977195	7	7	6	0.29	1.182	6	2	194.25
		54°31.77	10°02.36	09.06.202			15.5126	14.6656	314.506				7.11436	
563	1	N	E	1	10:43:50	11.38436494	7	7	7	0.021	0	-22.3667	5	141.45
		54°31.77	10°02.36	09.06.202				15.8473	313.742				7.12810	
563	5	N	E	1	10:43:50	11.3981017	15.173	3	8	0.021	0	-21.664	2	142.46
		54°31.77	10°02.36	09.06.202				16.1073	314.002				7.57222	
563	10	N	E	1	10:43:50	12.10222175	15.102	3	9	0.049	0	-21.9499	2	150.98
		54°31.77	10°02.36	09.06.202			11.2153		306.319			8.01418		
563	15	N	E	1	10:43:50	13.32712998	3	17.318	7	0.034	0.008	4	8.36713	167.91
		54°31.77	10°02.36	09.06.202			8.93233	19.0023	259.517			66.5681		
563	20	N	E	1	10:43:50	14.9790296	3	3	9	0.09	0.1	2	9.43903	190.77
		54°31.77	10°02.36	09.06.202			6.44433	21.2966	171.543			166.785	9.93284	
563	25	N	E	1	10:43:50	15.6628487	3	7	7	0.251	1.031	8	9	202.10
		54°31.77	10°02.36	20.07.202					82.9381			176.401		
564	1	N	E	1	9:57:53	8.812450474	21.421	12.145	5	0.164	-0.002	1	5.48245	108.11
		54°31.77	10°02.36	20.07.202					122.507				5.71474	
564	5	N	E	1	9:57:53	9.184741947	21.429	12.22	8	0.431	0	137.57	2	112.72
		54°31.77	10°02.36	20.07.202					284.834				5.95293	
564	10	N	E	1	9:57:53	9.56293888	21.015	12.695	5	0.061	0	-19.7962	9	117.65
		54°31.77	10°02.36	20.07.202					271.760			24.6168	7.61165	
564	15	N	E	1	9:57:53	12.13165873	14.075	16.623	9	0.172	0.026	6	9	152.75
		54°31.77	10°02.36	20.07.202					252.439			69.7615	9.89918	
564	20	N	E	1	9:57:53	15.66918606	9.063	20.361	6	0.232	1.103	2	6	201.11
		54°31.77	10°02.36	20.07.202					265.815			58.9072	10.2495	
564	25	N	E	1	9:57:53	16.189562	8.534	21.162	6	0.799	2.9	6	6	208.64
		54°31.77	10°02.36	01.09.202					269.935				7.05781	
567	1	N	E	1	10:09:53	11.27781539	17.056	15.979	4	0.048	0	10.1903	5	140.49
		54°31.77	10°02.36	01.09.202					263.373			16.9811	8.21036	
567	5	N	E	1	10:09:53	13.12036491	16.988	15.978	6	0.032	0	6	5	163.44
		54°31.77	10°02.36	01.09.202					232.523			48.6220	8.12512	
567	10	N	E	1	10:09:53	12.97512573	16.666	16.161	1	0.094	0.092	8	6	162.28
		54°31.77	10°02.36	01.09.202					105.663			186.608		
567	15	N	E	1	10:09:53	15.70302967	12.547	22.082	1	0.56	0.807	6	9.95303	202.45

		54°31.77	10°02.36	01.09.202					32.0562			261.327	17.4167	
567	20	N	E	1	10:09:53	27.41673295	11.939	22.654	1	0.444	1.154	7	3	355.59
		54°31.77	10°02.36	01.09.202								296.730	11.3911	
567	25	N	E	1	10:09:53	17.90115951	11.112	23.319	0	0.391	1.95	3	6	233.68
		54°31.77	10°02.36	06.10.202					271.515			20.2051	5.80854	
568	1	N	E	1	10:00:46	9.238545851	14.675	17.205	3	0.048	0	8	6	116.48
		54°31.77	10°02.36	06.10.202					263.592			25.3536	5.97044	
568	5	N	E	1	10:00:14	9.480442011	14.857	18.08	1	0.032	0	1	2	120.07
		54°31.77	10°02.36	06.10.202					247.038			41.5311	6.08761	
568	10	N	E	1	9:59:43	9.667611964	14.705	18.599	3	0.094	0.092	7	2	122.77
		54°31.77	10°02.36	06.10.202					223.876			61.2071	6.55719	
568	15	N	E	1	9:59:10	10.35719236	14.561	20.81	8	0.56	0.807	1	2	133.43
		54°31.77	10°02.36	06.10.202					158.406			130.527	5.42401	
568	20	N	E	1	9:58:09	8.544015514	13.285	22.089	2	0.444	1.154	8	6	110.79
		54°31.77	10°02.36	06.10.202					101.746				4.83642	
568	25	N	E	1	9:57:39	7.626426552	12.747	22.386	3	0.391	0.095	188.658	7	98.74
		54°31.77	10°02.36	03.11.202					283.518			20.2880	7.00828	
569	1	N	E	1	10:51:50	11.07828492	11.717	20.839	4	0.437	1.775	7	5	142.20
		54°31.77	10°02.36	03.11.202					276.630			19.6686		
569	5	N	E	1	10:51:24	11.21465041	12.445	22.331	8	0.479	2.832	8	7.11465	145.50
		54°31.77	10°02.36	03.11.202					255.575				7.87265	
569	10	N	E	1	10:50:50	12.40265621	12.28	22.429	2	0.477	2.801	41.1015	6	161.00
		54°31.77	10°02.36	03.11.202					227.596			68.3518	7.56618	
569	15	N	E	1	10:50:12	11.89618389	12.129	23.004	9	0.234	2.336	7	4	154.88
		54°31.77	10°02.36	03.11.202					178.323			116.816	7.11659	
569	20	N	E	1	10:49:26	11.18659232	11.958	23.429	2	0.206	2.169	7	2	145.96
		54°31.77	10°02.36	03.11.202								164.478	6.33364	
569	25	N	E	1	10:48:46	9.943644593	11.926	23.554	129.538	0.215	2.026	5	5	130.22
		54°31.77	10°02.36	02.02.202					350.366			11.0433	9.27438	
570	1	N	E	2	9:46:56	14.64438914	4.606	19.689	1	0.771	6.898	6	9	187.49
		54°31.77	10°02.36	02.02.202					351.637			9.78264	9.53506	
570	5	N	E	2	9:46:26	15.04506145	4.608	19.689	9	0.777	6.923	2	1	193.80
		54°31.77	10°02.36	02.02.202					347.715			13.6275	10.4090	
570	10	N	E	2	9:45:51	16.41904333	4.607	19.688	9	0.771	6.976	6	4	211.50
		54°31.77	10°02.36	02.02.202					299.351			60.8699	9.60015	
570	15	N	E	2	9:45:12	14.75015275	4.611	19.688	1	0.805	6.984	3	3	190.59
		54°31.77	10°02.36	02.02.202					293.142			66.9345	9.36015	
570	20	N	E	2	9:44:37	14.75015275	4.611	19.69	2	0.78	6.979	1	3	190.59

		54°31.77	10°02.36	02.02.202					278.943			77.2360	9.26158	
570	25	N	E	2	9:43:53	14.65158184	4.987	19.821	3	0.33	3.198	5	2	187.14
		54°31.77	10°02.36	02.03.202					342.973			17.7386	9.36839	
570	1	N	E	2	9:34:41	14.76839929	4.304	21.04	5	0.582	7.322	1	9	190.50
		54°31.77	10°02.36	02.03.202					335.720			24.8312	9.17863	
570	5	N	E	2	9:34:14	14.46863675	4.304	21.039	1	0.585	7.309	8	7	186.63
		54°31.77	10°02.36	02.03.202					319.770				9.58454	
570	10	N	E	2	9:33:38	15.11454846	4.33	21.078	3	0.6	7.439	40.1023	8	195.00
		54°31.77	10°02.36	02.03.202					308.263			50.4748	9.96843	
570	15	N	E	2	9:33:03	15.6984361	4.397	21.201	1	0.624	7.771	8	6	203.28
		54°31.77	10°02.36	02.03.202					293.142			63.0077	9.87306	
570	20	N	E	2	9:32:04	15.53306195	4.569	21.523	2	0.707	8.175	1	2	201.47
		54°31.77	10°02.36	02.03.202					290.938			61.8963	10.2109	
570	25	N	E	2	9:30:50	16.11093084	4.686	22.499	4	0.861	7.317	2	3	206.82
		54°31.77	10°02.36	12.04.202					368.614				9.96658	
571	1	N	E	2	8:59:32	15.99658109	5.605	13.446	6	0	0.401	-0.85247	1	196.28
		54°31.77	10°02.36	12.04.202					370.614				9.93102	
571	5	N	E	2	8:59:07	15.94102216	5.603	13.445	4	0	0.061	-2.78707	2	195.60
		54°31.77	10°02.36	12.04.202					370.476				9.66193	
571	10	N	E	2	8:58:37	15.45193297	5.535	13.502	2	0.044	0.091	-2.18185	3	191.42
		54°31.77	10°02.36	12.04.202					348.020			17.1778	9.68970	
571	15	N	E	2	8:58:08	15.43970469	5.28	15.547	6	0.021	0.644	3	5	193.28
		54°31.77	10°02.36	12.04.202					281.416			75.6324	9.82738	
571	20	N	E	2	8:57:39	15.50738704	4.8	20.166	4	0.072	0.894	3	7	199.38
		54°31.77	10°02.36	12.04.202					266.890			89.0007	10.2771	
571	25	N	E	2	8:57:10	16.20711703	4.815	20.467	5	0.298	3.048	9	2	208.70
		54°31.77	10°02.36	03.05.202			10.1696		290.032			38.0067	8.91695	
572	1	N	E	2	9:29:44	14.21695731	7	13.952	4	0	0.107	7	7	177.48
		54°31.77	10°02.36	03.05.202			9.73233	14.1833	291.085			39.7260	9.97989	
572	5	N	E	2	9:29:44	15.90989818	3	3	2	0.032	0.188	8	8	198.90
		54°31.77	10°02.36	03.05.202			7.06433	15.6966	287.838			60.4665	9.86202	
572	10	N	E	2	9:29:44	15.67202191	3	7	6	0.702	1.147	7	2	197.52
		54°31.77	10°02.36	03.05.202					247.802			106.271	9.73963	
572	15	N	E	2	9:29:44	15.41963608	5.759	17.5665	3	0.061	0.638	1	6	196.83
		54°31.77	10°02.36	03.05.202			5.03966					170.253	10.2910	
572	20	N	E	2	9:29:44	16.1910651	7	19.879	183.185	0.657	2.852	2	7	209.66
		54°31.77	10°02.36	03.05.202			4.98866		168.691			183.983		
572	25	N	E	2	9:29:44	5.758008797	7	20.257	2	0.707	3.698	7		74.24

		54°31.77	10°02.36	12.07.202			18.3226						8.27062	
573	1	N	E	2	7:42:33	13.1606255	7	14.43	325.01	0	0	-47.991	5	164.94
		54°31.77	10°02.36	12.07.202				14.7523					8.50859	
573	5	N	E	2	7:42:33	13.54859373	18.159	3	317.65	0	0	-40.4406	4	170.44
		54°31.77	10°02.36	12.07.202			15.6433	16.0403					9.70958	
573	10	N	E	2	7:42:33	15.4195868	3	3	298.77	0	0	-10.115	7	193.40
		54°31.77	10°02.36	12.07.202			11.2816					70.5634	12.7648	
573	15	N	E	2	7:42:33	20.15485982	7	18.08	240.369	0.054	0.254	5	6	256.96
		54°31.77	10°02.36	12.07.202								152.219	13.4386	
573	20	N	E	2	7:42:33	21.1486079	9.1175	19.5085	169.452	0.137	2.381	7	1	273.53
		54°31.77	10°02.36	12.07.202			8.57566					176.152	13.9224	
573	25	N	E	2	7:42:33	21.95244494	7	20.763	146.398	0.197	4.864	6	4	283.11
		54°31.77	10°02.36	30.08.202			19.9973	13.1866	263.822			5.07300	6.84487	
574	1	N	E	2	7:46:11	10.93487192	3	7	9	0	0	6	2	135.84
		54°31.77	10°02.36	30.08.202			19.9986	13.2906	260.805			7.85524	6.80515	
574	5	N	E	2	7:46:11	10.88515373	7	7	5	0	0	6	4	135.31
		54°31.77	10°02.36	30.08.202			19.9656		267.085			1.18118	6.74565	
574	10	N	E	2	7:46:11	10.76565546	7	13.746	9	0	0	1	5	134.51
		54°31.77	10°02.36	30.08.202			19.9723		254.928			12.6426	6.80502	
574	15	N	E	2	7:46:11	10.8450248	3	13.999	2	0	0	5	5	135.71
		54°31.77	10°02.36	30.08.202			14.6633	19.4423	115.477			168.922	7.01270	
574	20	N	E	2	7:46:11	11.06270755	3	3	8	0.061	0	3	8	142.84
		54°31.77	10°02.36	30.08.202			10.3773	21.7023				302.116		
574	25	N	E	2	7:46:11	6.52086013	3	3	2.61232	0.089	0.637	7	4.13086	83.59
		54°31.77	10°02.36	28.09.202				13.7426	281.802			11.7874		
575	1	N	E	2	7:42:33	15.10296979	15.415	7	6	0.059	0.095	2	9.41297	185.89
		54°31.77	10°02.36	28.09.202			15.4603	13.7903	269.782			23.1838	8.50302	
575	5	N	E	2	7:42:33	13.62302568	3	3	6	0.168	0.247	1	6	167.71
		54°31.77	10°02.36	28.09.202								278.844		
575	10	N	E	2	7:42:33	14.47005036	16.167	16.091		0.141	0.398	6	9.08005	181.41
		54°31.77	10°02.36	28.09.202					197.670			85.6390	8.89675	
575	15	N	E	2	7:42:33	14.10675761	15.46	18.465	5	0.131	0.456	7	8	179.01
		54°31.77	10°02.36	28.09.202			15.2853		50.0292			230.618		
575	20	N	E	2	7:42:33	12.93112999	3	18.668	2	0.614	1.092	2	8.16113	164.26
		54°31.77	10°02.36	28.09.202			11.8906	20.9516				4.32762		
575	25	N	E	2	7:42:33	6.817627614	7	7	0	0.21	0.366	296.103	8	87.89
		54°31.77	10°02.36	11.10.202			14.3633	17.5286	232.620			59.5236	6.98866	
576	1	N	E	2	7:42:33	11.1486674	3	7	1	0	0	6	7	138.91

		54°31.77	10°02.36	11.10.202		14.5423	17.7093	220.251					7.07285	
576	5	N	E	2	7:42:33	11.26285362	3	3	4	0.038	0.232	70.2259	4	141.07
		54°31.77	10°02.36	11.10.202				18.9713	77.7394			205.276	7.28118	
576	10	N	E	2	7:42:33	11.57118544	14.894	3	3	0.405	3.898	5	5	145.69
		54°31.77	10°02.36	11.10.202			14.5966		122.571			161.858	7.24666	
576	15	N	E	2	7:42:33	11.49666677	7	19.744	4	0.346	3.516	3	7	145.72
		54°31.77	10°02.36	11.10.202				20.3483	159.365			125.883	7.82242	
576	20	N	E	2	7:42:33	12.38242647	14.42	3	9	0.148	1.186	1	6	157.46
		54°31.77	10°02.36	11.10.202			14.1913	20.9696	110.717			173.706	7.41239	
576	25	N	E	2	7:42:33	11.72239803	3	7	3	0.1	0.98	2	8	150.03
		54°31.77	10°02.36	09.11.202					226.989			67.4019	8.55795	
577	1	N	E	2	7:42:33	13.66795723	12.645	22.083	2	0.259	1.615	9	7	169.22
		54°31.77	10°02.36	09.11.202			12.6626	22.1266	217.909			76.0898	8.62252	
577	5	N	E	2	7:42:33	13.78252809	7	7	7	0.251	1.648	4	8	170.71
		54°31.77	10°02.36	09.11.202			12.7343	22.3583	212.353			80.6646	8.74210	
577	10	N	E	2	7:42:33	13.97210467	3	3	6	0.35	2.135	7	5	173.22
		54°31.77	10°02.36	09.11.202			12.8023		189.898				7.69752	
577	15	N	E	2	7:42:33	12.27752585	3	22.434	3	0.32	2.562	102.063	6	152.76
		54°31.77	10°02.36	09.11.202			12.9953					138.719	8.62396	
577	20	N	E	2	7:42:33	13.72396103	3	22.862	150.419	0.372	3.947	5	1	171.69
		54°31.77	10°02.36	09.11.202			13.0266		84.6580			201.491	8.53725	
577	25	N	E	2	7:42:33	13.5572534	7	23.611	1	0.275	2.965	5	3	170.66
		54°31.77	10°02.36	08.12.202			6.02566	14.9946	340.359			19.4493	8.14981	
578	1	N	E	2	7:42:33	13.59981909	7	7	1	0.432	2.931	2	9	148.63
		54°31.77	10°02.36	08.12.202			6.53666		334.410			19.0507	7.60561	
578	5	N	E	2	7:42:33	12.66561699	7	15.812	9	0.396	2.795	3	7	139.22
		54°31.77	10°02.36	08.12.202			6.81533	17.6883	327.321			19.4734	8.05250	
578	10	N	E	2	7:42:33	13.36250158	3	3	9	0.427	3.324	9	2	148.64
		54°31.77	10°02.36	08.12.202				19.2193	319.648			22.5587	7.51124	
578	15	N	E	2	7:42:33	12.40124451	6.945	3	1	0.449	3.526	8	5	139.53
		54°31.77	10°02.36	08.12.202			7.32333	20.5956	307.878			28.1105	7.61072	
578	20	N	E	2	7:42:33	12.53072461	3	7	9	0.68	5.288	6	5	142.00
		54°31.77	10°02.36	08.12.202					207.009			125.571	7.85402	
578	25	N	E	2	7:42:33	12.9340279	7.4315	20.738	8	0.609	4.869	5	8	146.64
		54°31.77	10°02.36	26.01.202					332.737			22.9145		
579	1	N	E	3	7:42:33	15.36357012	4.777	21.349	4	0.327	7.627	8	9.54357	185.20
		54°31.77	10°02.36	26.01.202			4.80133	21.3716	335.263			20.1839	10.0710	
579	5	N	E	3	7:42:33	16.20105462	3	7	6	0.331	7.706	8	5	195.33

		54°31.77	10°02.36	26.01.202		4.87766	21.4226	335.812			18.8765	10.1624		
579	10	N	E	3	7:42:33	16.34246	7	7	4	0.388	7.998	5	6	197.70
		54°31.77	10°02.36	26.01.202			5.39966	21.8133	323.675			25.4477	9.10170	
579	15	N	E	3	7:42:33	14.65170891	7	3	2	0.328	7.681	4	9	176.49
		54°31.77	10°02.36	26.01.202			6.08266	23.0383	296.220				9.40053	
579	20	N	E	3	7:42:33	15.0905389	7	3	4	0.552	9.078	43.9874	9	183.61
		54°31.77	10°02.36	26.01.202			6.33766					152.310	9.81014	
579	25	N	E	3	7:42:33	15.71014872	7	23.612	182.059	0.533	8.811	2	9	191.65
		54°31.77	10°02.36	26.02.202									5.09494	
580	1	N	E	3	7:42:33	8.018899244	4.035	21.204	371.45	0.313	7.213	-8.11021	1	103.61
		54°31.77	10°02.36	26.02.202									5.62429	
580	5	N	E	3	7:42:33	8.852023443	4.041	21.211	372.12	0.314	7.299	-8.83503	8	114.37
		54°31.77	10°02.36	26.02.202									5.88245	
580	10	N	E	3	7:42:33	9.252846652	4.049	21.216	369.56	0.303	8.284	-6.41544	1	119.63
		54°31.77	10°02.36	26.02.202									5.32318	
580	15	N	E	3	7:42:33	8.364390816	4.086	21.231	368.95	0.627	8.957	-6.18268	8	108.63
		54°31.77	10°02.36	26.02.202								50.7012	5.33015	
580	20	N	E	3	7:42:33	8.366846043	5.363	22.23	297.19	0.575	8.704	7	7	108.90
		54°31.77	10°02.36	26.02.202								111.443		
580	25	N	E	3	7:42:33	10.20630466	5.981	23.13	227.84	0.87	9.026	5	6.51631	133.70
		54°31.77	10°02.36	26.03.202								16.8065	5.63873	
581	1	N	E	3	7:42:33	8.920506394	4.304	20.348	345.6	0.035	0.408	1	1	113.29
		54°31.77	10°02.36	26.03.202								25.5955		
581	5	N	E	3	7:42:33	9.22588469	4.351	20.631	335.5	0.045	0.753	9	5.83509	117.34
		54°31.77	10°02.36	26.03.202								24.1143	5.52105	
581	10	N	E	3	7:42:33	8.704228687	4.376	20.627	336.8	0.033	0.377	3	2	111.84
		54°31.77	10°02.36	26.03.202								28.3449	5.22384	
581	15	N	E	3	7:42:33	8.221261061	4.426	20.678	331.9	0.031	0.272	7	7	105.98
		54°31.77	10°02.36	26.03.202								62.6035	5.51114	
581	20	N	E	3	7:42:33	8.639998606	4.472	20.82	296.1	0.072	0.802	6	1	111.80
		54°31.77	10°02.36	26.03.202								58.0032	5.76499	
581	25	N	E	3	7:42:33	9.009322548	4.521	20.932	300.1	0.056	0.665	5	7	118.45
		54°31.77	10°02.36	26.04.202										
582	1	N	E	3	7:42:33	14.6757433	7.908	12.068		0.015	0.063		9.1013	177.14
		54°31.77	10°02.36	26.04.202									8.98087	
582	5	N	E	3	7:42:33	14.41640471	7.794	14.928		0.042	1.111		5	176.04
		54°31.77	10°02.36	26.04.202									8.14082	
582	10	N	E	3	7:42:33	12.94031527	6.924	17.112		1.871	2.372		9	160.79

EB-G-1	15	54.4791	9.905416	03.06.202 2	18.41	7.27	18.01	289.44	0.30	4.20	52.0662	11.5763		
EB-G-1	20	54.4791	9.905416	03.06.202 2	19.51	5.66	19.23	247.90	0.53	6.82	103.143	12.2921	2	5 231.00
EB-G-1	22	54.4791	9.905416	03.06.202 2	17.00	5.86	19.07	204.59	0.46	4.51	144.184	10.7219	8	8 246.45
EB-G-2	0	54.48911	9.939163	03.06.202 2	14.80	13.70	15.15	279.79	0.02	1.48	21.7193	9.24066	7	8 214.57
EB-G-2	5	54.48911	9.939163	03.06.202 2	15.33	13.14	15.00	299.73	0.02	1.21	6.04633	9.58303	2	1 182.57
EB-G-2	10	54.48911	9.939163	03.06.202 2	13.97	12.25	15.23	296.71	0.09	1.91	14.3828	8.74271	7	2 189.52
EB-G-2	15	54.48911	9.939163	03.06.202 2	18.03	7.99	17.60	292.09	0.30	5.43	44.7413		8	6 172.89
EB-G-2	20	54.48911	9.939163	03.06.202 2	19.57	5.66	19.28	251.33	0.56	8.89	99.6467		9	11.3433 226.47
EB-G-2	22	54.48911	9.939163	03.06.202 2	15.59	5.59	19.37	182.49	0.49	7.88	167.343	9.83532	8	8 248.00
MB-G-1	0	54.26493	11.43442	31.05.202 2	15.05	13.86	12.84	247.53	0.04	1.76	56.4922		9	9 198.21
MB-G-1	5	54.26493	11.43442	31.05.202 2	15.53	13.36	12.79	289.56	0.00	1.12	18.7324	9.53398	6	9.23905 176.62
MB-G-1	10	54.26493	11.43442	31.05.202 2	14.07	13.24	13.01	289.56	0.01	1.91	19.0347	8.64746	7	9 182.28
MB-G-1	15	54.26493	11.43442	31.05.202 2	15.04	13.18	13.15	288.31	0.04	3.01	20.4033	9.24629	2	7 165.79
MB-G-1	21	54.26493	11.43442	31.05.202 2	18.90	7.49	21.43	211.32	0.18	5.95	119.353		7	9 177.33
MB-G-2	0	54.26359	11.42652	31.05.202 2	14.24	13.60	12.86	295.43	0.01	1.76	11.2699	8.70522	1	11.8196 232.63
MB-G-2	5	54.26359	11.42652	31.05.202 2	14.70	13.96	12.75	208.63	0.01	1.82	94.0237	9.01055	8	7 165.56
MB-G-2	10	54.26359	11.42652	31.05.202 2	13.42	13.79	12.79	287.68	0.03	1.80	17.7822		9	7 171.40
MB-G-2	15	54.26359	11.42652	31.05.202 2	15.17	13.19	13.15	288.28	0.06	3.42	20.4075	8.98617	7	8.2156 156.94
													6	8 178.30

MET1-REF	20	54.57352	19.15138	26.05.2022	20:20	9.90	9.07	7.44	349.01	0.04	0.16	2.72952	5.86486			
MET1-REF	30	54.57352	19.15138	26.05.2022	20:20	13.41	4.65	7.50	364.87	0.03	0.22	26.4682	7.85070	9	7	105.37
MET1-REF	40	54.57352	19.15138	26.05.2022	20:20	13.77	4.32	7.57	365.80	0.03	0.24	28.6072	8.06694	5	5	138.13
MET1-REF	50	54.57352	19.15138	26.05.2022	20:20	13.40	4.09	7.60	353.36	0.01	0.24	42.9634	7.85328	6	9	141.85
MET1-REF	60	54.57352	19.15138	26.05.2022	20:20	14.22	4.13	7.69	323.49	0.04	0.51	71.5631	8.32814	9	2	138.58
MET1-REF	70	54.57352	19.15138	26.05.2022	20:20	19.81	6.34	10.40	36.56	0.58	2.92	324.392	11.6819	6	2	207.73
MET1-REF	77	54.57352	19.15138	26.05.2022	20:20	17.31	6.81	11.17	7.17	0.59	2.33	347.266	10.2245	7	8	182.42
MET1-MP	0	54.57147	19.165	26.05.2022	22:00	9.11	10.68	7.14	325.12	0.02	0.23	14.1327	5.41431	1	5	97.69
MET1-MP	10	54.57147	19.165	26.05.2022	22:00	9.35	10.66	7.22	251.90	0.02	0.42	85.6098	5.55031	2	4	100.33
MET1-MP	20	54.57147	19.165	26.05.2022	22:00	9.35	9.02	7.43	348.68	0.01	0.36	3.44232	5.56036	6	1	100.76
MET1-MP	30	54.57147	19.165	26.05.2022	22:00	11.70	4.89	7.51	361.33	0.01	0.53	27.5186	7.03632	2	9	129.80
MET1-MP	40	54.57147	19.165	26.05.2022	22:00	13.91	4.50	7.58	365.63	0.02	0.49	26.9490	8.36829	6	2	154.40
MET1-MP	50	54.57147	19.165	26.05.2022	22:00	14.14	4.34	7.60	358.84	0.01	0.47	35.1725	8.51463	6	8	157.54
MET1-MP	60	54.57147	19.165	26.05.2022	22:00	13.79	4.21	7.66	350.39	0.03	0.68	44.4858	8.31220	3	4	154.15
MET1-MP	70	54.57147	19.165	26.05.2022	22:00	17.42	6.23	10.33	93.04	0.41	2.16	270.324	10.5601	1	2	197.36
MET1-MP	77	54.57147	19.165	26.05.2022	22:00	20.32	6.76	11.06	21.77	0.74	1.76	333.666	12.3343	5	8	231.21
AB-G-1	0	54.73107	13.4924	30.05.2022	02:50	9.29	12.04	8.70	318.18	0.02	1.45	7.62340	5.56026	6	9	101.43
AB-G-1	10	54.73107	13.4924	30.05.2022	02:50	8.59	11.91	8.90	303.08	0.01	0.76	22.8909	5.14202	2	4	94.21

AB-G-1	20	54.73107	13.4924	30.05.202	2	02:50	9.23	12.78	10.02	290.54	0.01	1.89	26.8926	5.54035	6	101.80
AB-G-1	30	54.73107	13.4924	30.05.202	2	02:50	9.45	12.84	10.07	285.41	0.01	1.99	31.3822	4	5.67596	104.21
AB-G-1	34	54.73107	13.4924	30.05.202	2	02:50	9.29	12.84	10.07	285.24	0.02	1.35	31.5611	9	5.58023	102.49
AB-G-2	0	54.73192	13.50	30.05.202	2	04:00	8.86	11.96	8.82	307.27	0.02	1.30	18.5978	6	5.30816	97.40
AB-G-2	10	54.73192	13.50	30.05.202	2	04:00	9.93	11.92	8.94	303.35	0.02	0.43	22.4962	5	5.95625	108.86
AB-G-2	20	54.73192	13.50	30.05.202	2	04:00	9.11	12.69	9.94	290.78	0.02	1.21	27.4346	8	5.46894	100.74
AB-G-2	30	54.73192	13.50	30.05.202	2	04:00	11.06	12.84	10.07	285.05	0.02	1.08	31.7601	7	6.61534	120.79
AB-G-2	34	54.73192	13.50	30.05.202	2	04:00	12.01	12.83	10.07	285.35	0.02	1.28	7.19249	31.5086	6	131.67
AB-NG	0	54.65603	12.63819	30.05.202	2		10.63	13.45	10.40	304.77	0.01	0.61	7.79272	6	6.37478	116.76
AB-NG	5	54.65603	12.63819	30.05.202	2		11.26	13.10	10.37	240.77	0.01	0.76	72.7030	6	6.75842	124.40
AB-NG	10	54.65603	12.63819	30.05.202	2		10.64	12.95	10.00	240.02	0.01	0.86	75.1619	9	6.39366	117.38
AB-NG	15	54.65603	12.63819	30.05.202	2		10.91	13.04	12.15	285.09	0.01	0.72	26.3830	6	6.58206	122.09
AB-NG	18	54.65603	12.63819	30.05.202	2		11.48	13.02	12.16	278.73	0.01	0.84	32.7340	2	6.92552	128.40